TURUN
YLIOPISTO
UNIVERSITY
OF TURKU

CHARACTERIZATION OF GAMMA-SECRETASE-MEDIATED CLEAVAGE OF RECEPTOR TYROSINE KINASES

Johannes Merilahti

TURUN YLIOPISTON JULKAISUJA – ANNALES UNIVERSITATIS TURKUENSIS
SARJA – SER. D OSA – TOM. 1558 | MEDICA – ODONTOLOGICA | TURKU 2021

TURUN
YLIOPISTO
UNIVERSITY
OF TURKU

CHARACTERIZATION OF GAMMA-SECRETASE-MEDIATED CLEAVAGE OF RECEPTOR TYROSINE KINASES

Johannes Merilahti

TURUN YLIOPISTON JULKAISUJA – ANNALES UNIVERSITATIS TURKUENSIS
SARJA – SER. D OSA – TOM. 1558 | MEDICA – ODONTOLOGICA | TURKU 2021

University of Turku

Faculty of Medicine
Institute of Biomedicine
Medical Biochemistry and Genetics
Turku Doctoral Programme of Molecular Medicine

Supervised by

Professor Klaus Elenius
Institute of Biomedicine and Medicity Research Laboratories, University of Turku, Turku, Finland
Turku Bioscience, University of Turku and Åbo Akademi, Turku, Finland

Reviewed by

Professor Matti Nykter
Faculty of Medicine and Health Technology, Tampere University, Tampere, Finland

Professor Cecilia Sahlgren
Faculty of Science and Engineering
Åbo Akademi, Turku, Finland

Opponent

Professor Kaisa Lehti
Faculty of Natural Sciences, Norwegian University of Science and Technology
Trondheim, Norway

ISBN 978-951-29-8488-6 (PRINT)
ISBN 978-951-29-8489-3 (PDF)
ISSN 0355-9483 (Print)
ISSN 2343-3213 (Online)
Painosalama Oy, Turku, Finland 2021

Always be yourself unless you can be Batman
Then you should be Batman
-Twitter

UNIVERSITY OF TURKU
Faculty of Medicine
Institute of Biomedicine
Medical Biochemistry and Genetics
JOHANNES MERILAHTI: Characterization of Gamma-Secretase-Mediated Cleavage of Receptor Tyrosine Kinases,
Doctoral Dissertation, 165 pp
Turku Doctoral Programme of Molecular Medicine (TuDMM)
June 2021

ABSTRACT

Receptor tyrosine kinases (RTK) are a family of cell surface receptors consisting of 55 members. RTKs regulate intracellular signaling pathways that control fundamental cellular processes including differentiation, proliferation, and survival. The functionality of RTKs is necessary for the development and homeostasis of many tissues. In human pathologies, such as cancer, aberrant RTK signaling is a common feature. Gamma-secretase-mediated regulated intramembrane proteolysis is a proteolytic cleavage of RTKs in two sequential proteolytic events: a sheddase-mediated ectodomain shedding followed by the release of a soluble intracellular domain by a gamma-secretase cleavage.

The aims of my thesis were to characterize the gamma-secretase-mediated cleavage of RTKs, with a focus on identifying the prevalence of cleavage among RTKs and developing novel methods to identify signaling pathways associated with the process. The results of this thesis indicate that at least half of the RTKs are subjected to gamma-secretase cleavage. In total, 12 new gamma-secretase targets were identified. Many of the identified new gamma-secretase target RTKs, for example AXL and TYRO3, presented cleavage-dependent effect on cell growth. My research also demonstrated that the signaling of TYRO3 full-length receptor and soluble intracellular domain of TYRO3 is different as observed with our novel systems biology methods.

Together, these findings represent for a first time an approach to determine the prevalence of gamma-secretase cleavage among RTKs. Moreover, this study presents novel methods and tools for identifying still largely unknown RTK cleavage associated signaling pathways. The RTK processing via proteolytical cleavage has indications for the functionality of RTKs in both normal tissues and cancer. The results of this thesis can provide new insights into the regulation of the functions of RTKs and can be used to develop new strategies to treat cancers.

KEYWORDS: receptor tyrosine kinase, RTK, gamma-secretase, regulated intramembrane proteolysis, intracellular kinase domain, shedding, proteomics

TURUN YLIOPISTO
Lääketieteellinen tiedekunta
Biolääketieteen laitos
Lääketieteellinen biokemia ja genetiikka
JOHANNES MERILAHTI: Reseptorityrosiinikinaasien gamma-sekretaasi-välitteisen katkeamisen karakterisointi
Väitöskirja, 165 s.
Turun yliopiston molekyylilääketieteen tohtoriohjelma (TuDMM)
Kesäkuu 2021

TIIVISTELMÄ

Ihmisen genomi sisältää 55 reseptorityrosiinikinaasia (RTK). RTK:t ovat solukalvolla sijaitsevia signalointiproteiineja. RTK:t signaloivat solunsisäisten signalointireittien välityksellä ja säätelevät elintärkeitä solutapahtumia, kuten solujen lisääntymistä, erilaistumista ja selviytymistä. RTK ovat tärkeitä monien kudosten kehittymisessä, ja niiden epänormaalia toimintaa on todettu monissa sairauksissa, kuten syövissä. Gamma-sekretaasivälitteinen säädelty solukalvonsisäinen proteolyysi on mekanismi, jolla RTK:t katkaistaan proteolyyttisesti. Tämä on kaksivaiheinen tapahtuma. RTK:n solunulkoinen domeeni katkaistaan ensin ADAM-nimisten proteiinien toimesta ja tätä seuraa gamma-sekretaasin tekemä solukalvon sisäisen osan irrottaminen solukalvolta.

Tämän väitöskirjan tavoitteena oli karakterisoida RTK:iden gamma-sekretaasi-katkeamista. RTK:iden katkeamisen yleisyyden selvittäminen, sekä menetelmien kehitys, joilla paremmin pystytään tunnistamaan RTK:iden katkeamiseen liittyvää signalointia, olivat tarkemman tutkimuksen kohteena. Selvitimme, että puolet ihmisen RTK:ista on kohteena gamma-sekretaasi-välitteiselle katkaisulle ja tunnistimme yhteensä 12 uutta kohdetta. TYRO3 ja AXL RTK:iden kohdalla solujen kasvun lisääntyminen liittyi näiden RTK:iden katkeamiseen. Lisäksi väitöskirja-tutkimuksessani pystyimme osoittamaan, että TYRO3 RTK:n katkeamisesta muodostuvan liukoisen osan aikaansaama signalointi eroaa merkittävästi kokopitkän TYRO3:n aikaansaamasta signaloinnista.

Tutkimuksessa tehdyt havainnot osoittavat, että RTK:iden katkeaminen on yleistä ja uudenlaiset analysointimenetelmät auttavat aikaisempaa paremmin tunnistamaan uusia signalointireittejä katkeaville RTK:ille. Tutkimuksen tulokset RTK:iden katkeamisesta sekä sen signaloinnista laajentavat ymmärrystämme RTK:iden signaloinnista ja tulosten antamaa tietoa voidaan käyttää uusien syöpähoitojen kehittämisessä.

AVAINSANAT: reseptorityrosiinikinaasi, RTK, gamma-sekretaasi, säädelty solukalvonsisäinen proteolyysi, solunsisäinen kinaasidomeeni, proteomiikka.

Table of Contents

Abbreviations

ACK1	Activated CDC42 kinase 1
ADAM	A disintegrin and metalloprotease
ALKAL	ALK and LTK ligand
ALLN	N-Acetyl-Leu-Leu-Nle-Cho
ANG	Angiopoietin
APH-1	Anterior pharynx defective-1
APP	Amyloid β-protein precursor
AREG	Amphiregulin
ARTN	Artemin
ATF1	Activating transcription factor 1
ATP	Adenosine triphosphate
BAD	BCL-2-associated agonist of cell death
BDNF	Brain derived neurotrophic factor
BTC	Betaregulin
CANDIS	Conserved adam seventeen dynamic interaction sequence
CREB	cAMP-responsive element-binding protein
CRISPR	Clustered regularly interspaced short palindromic repeats
CSF	Colony stimulating factor
CST	Cell Signaling Technology
CTF	C-terminal fragment
DAG	diacylglycerol
DAPI	4’,6-diamid- ino-2-phenylindole
DTBP	Dimethyl 3,3’-dithiobispropionimidate
EGF	Epidermal growth factor
EGFR	Epidermal growth factor receptor
EMT	Epithelial-to-mesenchymal transition
EPG	Epigen
EREG	Epiregulin
esiRNA	Endoribonuclease-prepared siRNA
ER	Endoplasmic reticulum
FAK1	Focal adhesion kinase 1

FGF	Fibroblast growth factor
FLT3	FMS-like tyrosine kinase 3
FLT3LG	FLT3 ligand
FNIII	Fibronectin type III
GAS6	Growth arrest specific 6
GLA	Gamma-carboxyglutamic
GNDF	Glial cell derived neurotrophic factor
HB-EGF	Heparin-binding EGF-like growth factor
HGF	Hepatocyte growth factor
HIF-1α	Hypoxia-inducible factor 1 alpha
HRP	Horseradish peroxidase
ICD	Intracellular domain
IGF	Insulin like growth factor
IF	Immunofluorescence
Ig	Immunoglobulin
IL	Interleukin
IP	Immunoprecipitation
IP3	Inositol trisphosphate
iRhom	Inactive rhomboid
JAK	Janus kinase
KITLG	KIT ligand
LRP	LDL receptor related protein
MCL1	Myeloid cell leukemia 1
MITF	Microphthalmia-associated transcription factor
MMP9	Matrix metalloproteinase 9
MPD	Membrane proximal domain
MST	Macrophage stimulating
MMP	Matrix metalloprotease
MDSC	Myeloid derived suppressor cells
NF-κB	Nuclear factor-κB
NGF	Nerve growth factor
NMDAR	N-methyl-D-aspartate receptor
NMIIA	Non-muscle myosin IIA
NRG	Neuregulin
NRTN	Neurturin
NLS	Nuclear localization signal
NTF	Neurotrophin; N-terminal fragment
PACS-2	Phosphofurin acidic cluster sorting protein 2
PD-L1	Immune checkpoint molecule programmed death ligand 1
PDGF	Platelet derived growth factor

PEN-2	Presenilin enchancer-2
PGF	Placental growth factor
PIP2	Phosphatidylinositol-2-phosphate
PIP3	Phosphatidylinositol-3-phosphate
PI3K	Phosphatidylinositol 3-kinase
PMA	Phorbol 12-myristate 13-acetate
PUMA	P53 upregulated modulator of apoptosis
PTB	Phosphotyrosine-binding
PSPN	Persephin
RIP	Regulated intramembrane proteolysis
RTK	Receptor tyrosine kinase
SCBT	Santa Cruz Biotechnology
SDF-1	Stromal cell-derived factor 1
SH2	Src-homology 2
SHBG	Sex hormone-binding globulin
shRNA	Short hairpin RNA
SUMO	Small ubiquitin-like modifier
STAT	Signal transducer and activator of transcription
TAM	TYRO3, AXL, MER
TCEP	Tris(2-carboxyethyl)phosphine
TIMP	Tissue inhibitor of metalloproteinases
TFA	Trifluoroacetic acid
VEGF	Vascular endothelial growth factor
WB	Western blot
WNT	Wingless-type MMTV integration site
WWOX	WW domain-containing oxidoreductase

List of Original Publications

This dissertation is based on the following original publications, which are referred to in the text by their Roman numerals:

I Merilahti JAM, Ojala VK, Knittle AM, Pulliainen AT, Elenius K. Genome-wide screen of gamma-secretase–mediated intramembrane cleavage of receptor tyrosine kinases. Molecular Biology of the Cell, 2017; 22: 3123-3131.

II Merilahti JAM*, Vaparanta K*, Ojala VK, Elenius K. Unbiased multi-omics inference of TYRO3 signaling pathways. Manuscript, 2021.
* These authors contributed equally.

1 Introduction

Receptor tyrosine kinases (RTK) are cell surface receptors that mediate extracellular signals into activation of a range of intracellular signaling pathways regulating central cellular processes such as differentiation, proliferation, and survival. RTKs have essential roles in embryonic development and maintaining the homeostasis of adult tissues. In human pathologies, including cancer, aberrant RTK signaling is a common feature.

TYRO3, AXL and MER (TAM) are a subfamily of RTKs that are generally expressed in immune, hematopoietic, reproductive and nerve cells. They mediate phagocytosis of apoptotic cells and viruses and have a role in termination of inflammation. In contrast to many other RTKs, TAMs are not essential for embryonic development but are specialized in maintaining homeostasis in adult tissues that are subject to continuous renewal. Additionally, TAM RTKs regulate the innate immune system, dampening inflammatory responses to prevent chronic inflammation and autoimmunity. Gamma-secretase-mediated regulated intramembrane proteolysis (RIP) is a process where RTKs are cleaved in two sequential proteolytical cleavage events: a sheddase-mediated ectodomain shedding followed by the release of soluble intracellular domain by a gamma-secretase cleavage.

Although many aspects of RTK signaling have been extensively studied, the role of gamma-secretase-mediated RIP in RTK signaling is largely unexplored. The focus of this study was to characterize the prevalence of gamma-secretase cleavage in RTKs as well as cellular signaling generated from TYRO3 cleavage.

2 Review of the Literature

2.1 Receptor tyrosine kinases

Receptor tyrosine kinases (RTK) are cell surface receptors that mediate extracellular growth factor signals from outside of the cell to inside of the cell via phosphorylation-dependent signaling cascades. The phosphorylation of proteins is a post-translational modification that is mediated by protein kinases. Protein kinases catalyze the transfer of a γ-phosphate group from adenosine triphosphate (ATP) to specific amino acid residues of the receiver protein (Figure 1). Amino acids that are phosphorylated include tyrosine, serine, and threonine residues. In the human genome, 55 RTKs are found, which are divided into 19 subfamilies (Figure 2) (Wheeler and Yarden, 2015).

2.1.1 RTK structure and activation

All human RTKs share a roughly similar structure (Figure 1). The N-terminal extracellular domain contains the ligand binding site and is connected to a single pass transmembrane domain anchoring RTKs to the cell membrane. The transmembrane domain in turn is connected to a tyrosine kinase activity containing intracellular domain (ICD), including the activation loop and regulatory element (Lemmon and Schlessinger, 2010).

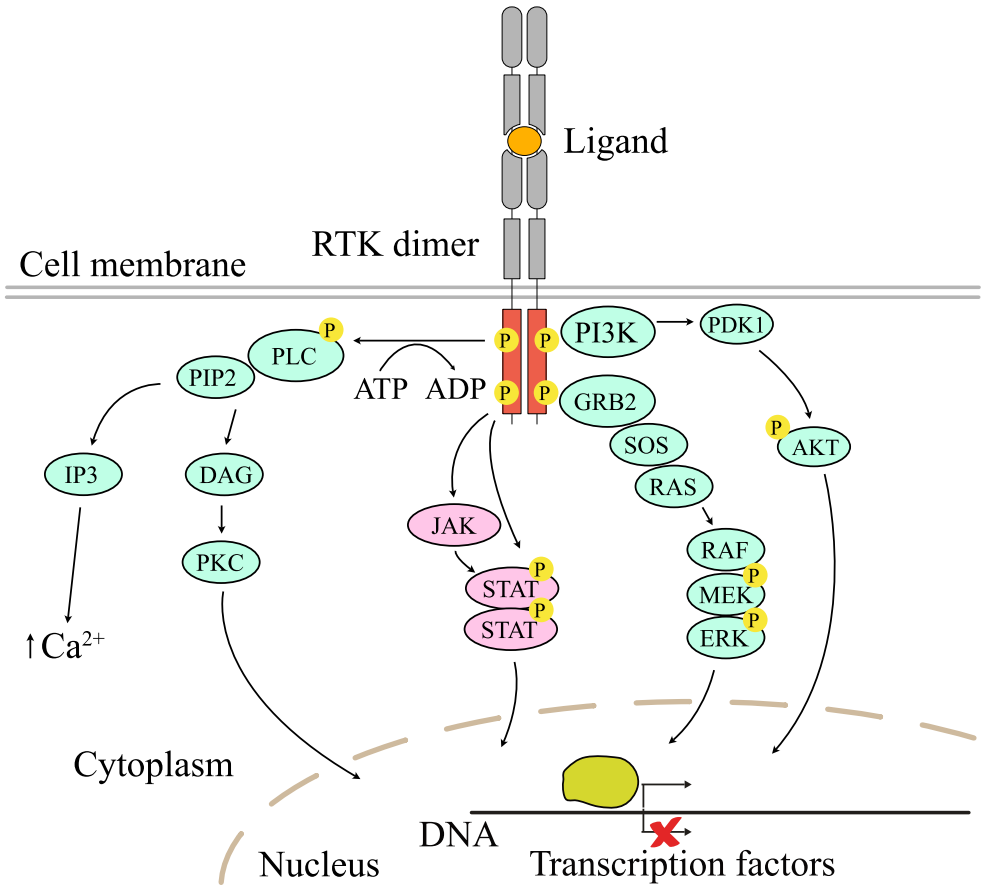

Figure 1. Common signaling pathways activated by RTKs. RTKs are activated by ligand binding followed by receptor dimerization and kinase domain activation. ADP, adenosine diphosphate; ATP, adenosine triphosphate; DAG, diacylglycerol; GRB2, growth factor receptor-bound protein 2; IP3, inositol trisphosphate; JAK, Janus kinase; P, phosphorylated amino acid residue; PI3K, phosphatidylinositol 3-kinase; PIP2, phosphatidylinositol-2-phosphate; PIP3, phosphatidylinositol-3-phosphate; PLC, phospholipase C; SOS, son of sevenless; STAT, signal transducer and activator of transcription.

RTKs mediate signals that control cell differentiation, proliferation, survival, and migration among other cellular processes. Signaling of RTKs is initiated by activation of the intracellular kinase domains of the RTKs by binding of extracellular ligands to RTKs. This induces receptor dimerization. Following the dimerization, the activation loop is either autophosphorylated or phosphorylated by the dimerization partner (Hubbard and Till, 2000). This leads to the phosphorylation of C-terminal tails of RTKs and to the activation of intracellular signaling pathways. Known ligands for RTKs are listed in the Figure 2.

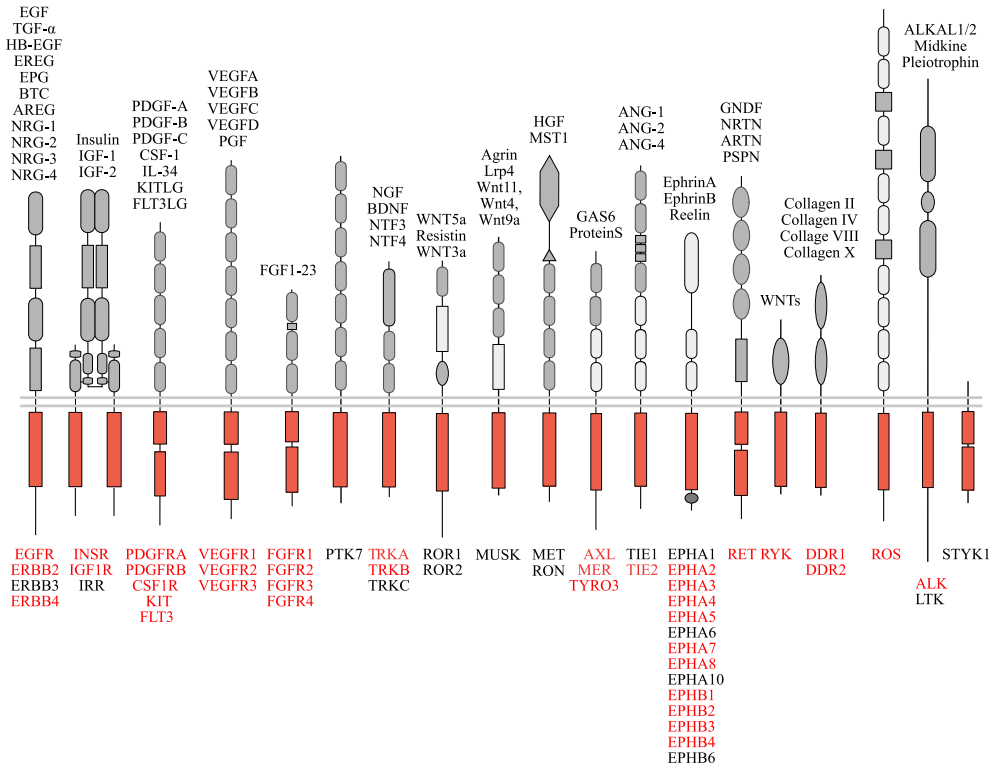

Figure 2. Human RTKs. Top: Known ligands for receptor tyrosine kinases. Middle: Schematic structures of RTKs. Bottom: Names of RTKs. Targets for approved cancer drugs are marked with red. Data have been collected from GeneCa database (FICAN West, 2020) and from a book edited by Wheeler and Yarden 2015. ALKAL, ALK and LTK ligand; ANG, angiopoietin; AREG, amphiregulin; ARTN, artemin; BDNF, brain derived neurotrophic factor; BTC, betaregulin; CSF, colony stimulating factor; GAS, growth arrest specific; EGF, epidermal growth factor; EPG, epigen; EREG, epiregulin; FGF, fibroblast growth factor; GNDF, glial cell derived neurotrophic factor; FLT3LG, FLT3 ligand; HB-EGF, heparin-binding EGF-like growth factor; HGF, hepatocyte growth factor; IGF, insulin like growth factor; IL, interleukin; KITLG, KIT ligand; LRP, LDL receptor related protein; MST, macrophage stimulating; NGF, nerve growth factor; NRG, neuregulin; NRTN, neurturin; NTF, neurotrophin; PDGF, platelet derived growth factor; PGF, placental growth factor; PSPN, persephin; VEGF, vascular endothelial growth factor; WNT, wingless-type MMTV integration site.

2.1.2 RTK signaling pathways

The activation of intracellular, RTK associated, signaling pathways is mediated through the binding of phosphotyrosine-binding (PTB) or Src-homology 2 (SH2) domain containing downstream signaling proteins to the phosphorylated docking sites at the RTK ICDs (Blume-Jensen and Hunter, 2001). Janus kinase/signal transducer and activator of transcription (JAK/STAT) pathway, mitogen-activated protein kinase (MAPK) pathway, phosphatidylinositol 3-kinase (PI3K)/AKT

pathway and phospholipase C gamma (PLC-γ) pathway are the main signaling pathways that RTKs activate (Figure 1).

STAT signaling pathway can be activated by directly activating STATs or by JAK phosphorylation (Blume-Jensen and Hunter, 2001). Phosphorylation activates STATs leading to their dimerization, nuclear translocation, and activity as transcription factors. MAPK pathway is activated by the recruitment of multiple growth factor receptor-bound protein 2 (GRB2) molecules. This leads to activation of RAS by son of sevenless (SOS) (Lemmon and Schlessinger, 2010). PI3K pathway is activated by binding PI3K via its SH2 domains to RTKs. This induces the conversion of phosphatidylinositol-2-phosphate (PIP2) into phosphatidylinositol-3-phosphate (PIP3) (Blume-Jensen and Hunter, 2001). Furthermore, PI3K can be activated directly by RAS binding to PI3K (Blume-Jensen and Hunter, 2001). Following PIP3 formation, AKT is recruited to cell membrane together with its activator kinase PDK1 leading to AKT activation by phosphorylation (Blume-Jensen and Hunter, 2001). The PLC-γ pathway is activated by RTKs phosphorylating PLC-γ and activated PLC-γ converts PIP2 into inositol trisphosphate (IP3) and diacylglycerol (DAG) (Rhee, 2001; Lemmon and Schlessinger, 2010).

2.1.3 RTKs as drug targets

The activity of RTKs is normally tightly controlled in their physiological roles governing embryonic development and maintaining adult tissue homeostasis. Aberrant signaling of RTKs is often observed in carcinogenesis. Cancer cells can become addicted to specific activating alterations in the sequence of RTKs or in RTK copy number (Du and Lovly, 2018). The defective down-regulation of RTK signaling can also participate in the altered RTK signaling (Bache *et al.*, 2004). Hence, multiple cancer drugs that specifically inhibit RTK signaling have been developed and introduced to clinical use (Carvalho *et al.*, 2016; Roskoski, 2019, 2020).

RTKs that currently have approved cancer-treatment drugs against them are shown in red in Figure 2. The drugs are divided in two major classes: Monoclonal antibodies that prevent the binding of ligands, block the dimerization of RTKs, promote endocytosis and degradation or enhance immunological mechanisms that depend on antibodies, and tyrosine kinase inhibitors that prevent kinase-dependent signaling by competing with ATP in binding to the kinase domain of the RTKs (Zwick *et al.*, 2002; Fauvel and Yasri, 2014; Roskoski, 2019, 2020).

The approved cancer-treatment drugs against RTKs have proven to be rather effective but development of resistance is quite often observed in patients (Yamaoka *et al.*, 2018). Additionally, side effects from these drugs occur in most patients with

symptoms from mild to severe and up to a potentially life threatening (Hansel *et al.*, 2010; Vogel *et. al.*, 2016, Yamaoka *et al.*, 2018).

The resistance against the treatments can occur through the acquired genomic mutations that enable bypassing target inhibition through defective binding of the drugs, for example. Additionally, downstream effectors in the same signaling pathway or alternative survival pathways can be activated that will also lead to resistance against treatments (Fauvel and Yasri, 2014; Boumahdi and de Sauvage, 2020). These mechanisms of resistance emerge either because of the selection of rare pre-existing genetic alterations upon drug treatment or through the acquisition of additional mutations during treatment.

In addition to these genetic mechanisms of drug resistance, non-mutational mechanisms in the emergence of resistance have been observed (Ramirez *et al.*, 2016, Luskin *et al.,* 2018, Boumahdi and de Sauvage, 2020). Even with the most effective cancer therapies that lead complete response, small populations of cancer cells often survive (Sharma *et al.*, 2010, Kurppa *et al.*, 2020). These drug-tolerant cells can be the drivers of cancer relapse if treatment is discontinued, for example due to severe adverse effects. These residual cells are also proposed to act as a reservoir of slow-cycling cells that may eventually acquire genetic mutations that lead to drug resistance (Ramirez *et al.*, 2016; Luskin *et al.*, 2018; Boumahdi and de Sauvage*,* 2020).

2.2 TYRO3, AXL, MER family of RTKs

TYRO3, AXL, and MER (TAM) receptors are a subfamily of RTKs. TAMs were among the last RTKs to be identified (Lai and Lemke, 1991; O'Bryan *et al.*, 1991; Graham *et al.*, 1994; Lai *et al.*, 1994). TAM receptors are transmembrane type I protein glycoproteins and share a common structure with other RTKs. The extracellular domain is constructed of two immunoglobulin-like (Ig-like) domains and two fibronectin type III domains (Figure 3). The extracellular domain mediates receptor activation through ligand binding to the Ig-like domains and subsequent receptor dimerization (O'Bryan *et al.*, 1991; Graham *et al.*, 1994; Lai *et al.*, 1994; Heiring *et al.*, 2004; Sasaki *et al.*, 2006; Lemke and Rothlin, 2008; Allen *et al.*, 2010; Lew *et al.*, 2014). The transmembrane domain anchors TAM receptors to the cell membrane and the intracellular domain contains the tyrosine kinase activity. During the evolution of kinases, TAM RTKs appeared among the last RTKs (Manning *et al.*, 2002). For example, no TAM representatives are found in *Drosophila* or *C. Elegans*.

TAM RTKs are expressed in immune, hematopoietic, reproductive and nerve cells. They mediate phagocytosis of apoptotic cells and viruses and have a role in termination of inflammation (Lemke, 2013). In contrast to other RTKs, TAM RTKs

are not essential for embryonic development. TAMs are specialized in maintaining homeostasis in adult tissues that are subject to continuous renewal. The knockout mice of all three TAM RTKs are viable but demonstrate severe autoimmunity and chronic inflammation reflecting the loss of TAM activity in tissues that are subject to regular challenge and renewal. The reason for severe autoimmunity and chronic inflammation has been attributed in part to impaired function of natural killer and dendritic cells (Lu *et al.*, 1999; Lu and Lemke, 2001; Rothlin *et al.*, 2007; Ji *et al.*, 2013).

2.2.1 Ligands of TAM RTKs

TAM receptors have a unique mechanism of activation. Growth arrest-specific protein 6 (GAS6) and protein S (Figure 3), the two TAM ligands, have two structural features important for their activities (Manfioletti *et al.*, 1993; Stitt *et al.*, 1995; Mark *et al.*, 1996). The C-terminus of these two ligands is constructed of a sex hormone binding globulin (SHBG) domain that mediates the binding of ligand to TAM RTK immunoglobulin-like (Ig) domains. This binding induces the dimerization of receptor and the activation kinase domain (Nyberg *et al.*, 1997; Tanabe *et al.*, 1997; Evenas *et al.*, 2000; Sasaki *et al.*, 2002, 2006). The N-terminus harbors the gamma-carboxyglutamic (Gla) domain that is rich in glutamic acid residues that are gamma-carboxylated in a vitamin K-dependent reaction (Huang *et al.*, 2003; Li *et al.*, 2004). Gamma-carboxylation is required for Gla domains to be able to bind to phosphatidylserine in a Ca^{2+}-dependent manner. Phosphatidylserine is normally confined to the cytosol facing side of the plasma membrane. However, in apoptotic cells, as well as in platelets, phosphatidylserine is displayed on the extracellular face of the plasma membrane (Van Meer *et al.*, 2008; Suzuki *et al.*, 2013; Segawa *et al.*, 2014). Interaction with phosphatidylserines by Gla domains is crucial for GAS6 and Protein S in activation of TAM RTKs. Phosphatidylserine on the plasma membrane is also recognized by phagocytes (Ravichandran, 2010).

GAS6 and Protein S dimerization is required for binding to TAM receptors. GAS6 can function as a ligand for all three TAM RTKs (Figure 4) (Ohashi *et al.*, 1995; Stitt *et al.*, 1995; Mark *et al.*, 1996; Nagata *et al.*, 1996). Of the three TAM RTKs, AXL activation is solely dependent on GAS6 as AXL does not bind and is not activated by Protein S (Lew *et al.*, 2014; Tsou *et al.*, 2014). In addition to binding to GAS6, full AXL activation requires binding of GAS6 to exposed phosphatidylserine via Gla domain and presence of extracellular Ca^{2+}, which is required for proper interaction between the Gla domain and phosphatidylserine (Lew *et al.*, 2014). In contrast, without a Gla domain, the activation of TYRO3 and MER by GAS6 is notably weakened while it does not activate AXL at all (Lew *et al.*, 2014).

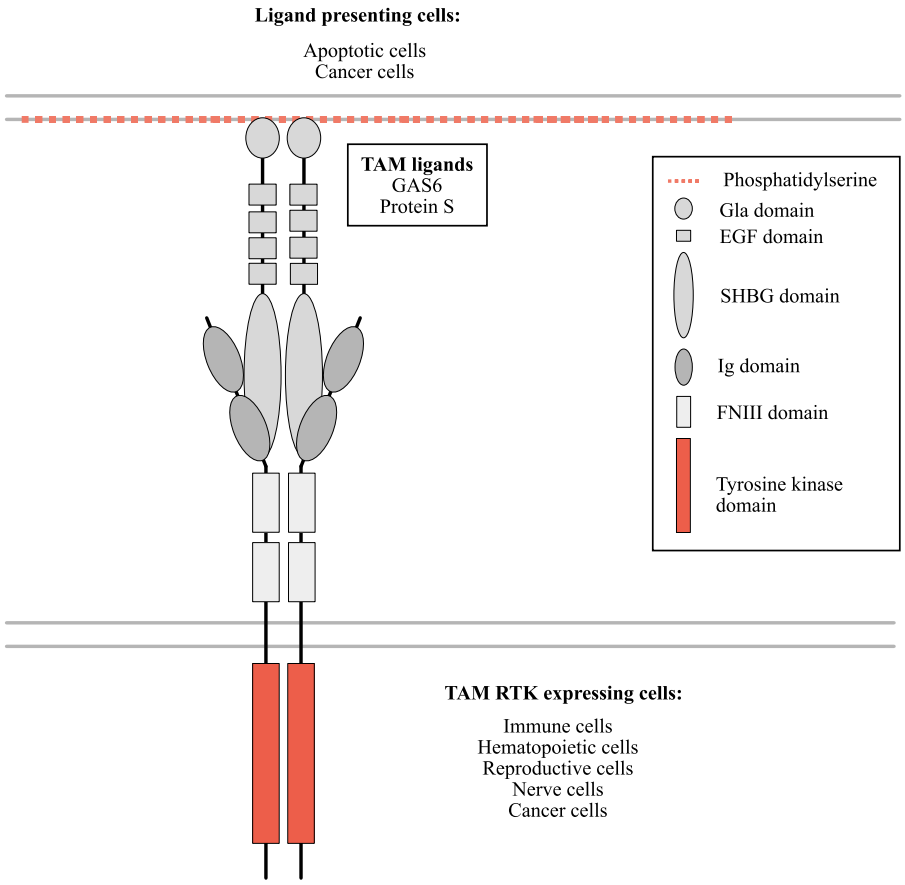

Figure 3. General structures of TAM receptors and their ligands. GAS6 and Protein S bind to immunoglobulin (Ig) domains of TAM RTKs via C-terminal Sex hormone-binding globulin (SHBG) domains. This induces TAM RTK dimerization and activate tyrosine kinases. N-terminal gamma-carboxyglutamic (GLA) domains of dimeric ligands that are gamma-carboxylated by a vitamin-K-dependent reaction, bind to phospholipid phosphatidylserine. Phosphatidylserine is expressed on the surface of apoptotic cells. Phosphatidylserine is normally confined to the inner side of the membrane. (Modified from Lemke and Rothlin 2008). EGF, epidermal growth factor; FNIII, fibronectin type III; GAS6, growth arrest specific; TAM, TYRO3, AXL, MER.

Protein S is a selective TAM RTK ligand. It binds and activates TYRO3 and MER but not AXL (Figure 4) (Stitt *et al.*, 1995; Prasad *et al.*, 2006; Lemke and Rothlin, 2008; Uehara and Shacter, 2008; Zhong *et al.*, 2010; Lew *et al.*, 2014; Tsou *et al.*, 2014). The selectivity of Protein S for TYRO3 and MER over AXL has been observed to be due to the differences in the TYRO3 and MER N-terminal Ig-like domains compared to the Ig-like domains of AXL (Lew *et al.*, 2014).

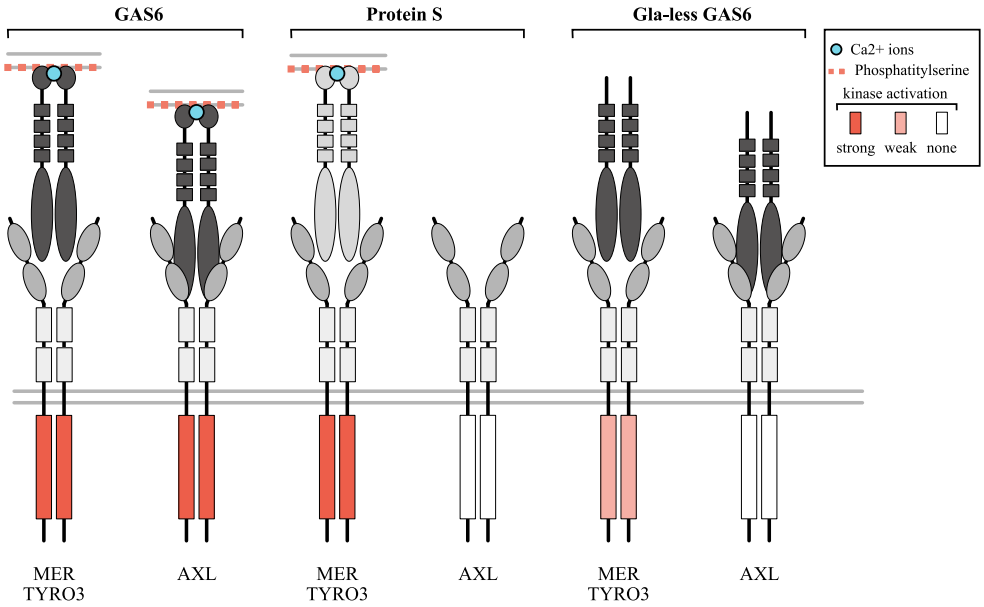

Figure 4. Ligand-mediated activation of TAM receptors. All three TAM RTKs are activated by GAS6. Protein S activates Tyro3 and Mer but not Axl. Simultaneous presence of phosphatidylserine and calcium ions (Ca^{2+}) is required for full activation of any of TAM RTKs by GAS 6 or Protein S. Phosphatidylserine binds to the Gla domain of the ligands. Gla-less GAS6 does not activate AXL while TYRO3 and MER are partially activated. GAS6 can bind to two different domains on distinct AXL molecules, thus resulting in receptor homodimerization and almost complete activation. In TYRO3 and MER, GAS6 can only bind to one GAS6-binding domain. Full TYRO3 and MER receptor activation is achieved by increasing local concentrations of TYRO3 and MER by the presence of phosphatidylserine-presenting membrane. (Adapted from Lew et al. 2014) Gla, gamma-carboxyglutamic.

2.2.2 Signaling of TAM receptors

The signaling pathways associated with TAM RTKs are outlined in Figure 5. The activation and phosphorylation of TAM kinase domains, in majority of cases, leads to activation of PI3K/AKT, Phospholipase C, or MAPK downstream signaling pathways (Figure 5) (Ling *et al.*, 1996; Braunger *et al.*, 1997; Goruppi *et al.*, 1997; Wen *et al.*, 2001; Son *et al.*, 2007; Tibrewal *et al.*, 2008; Weinger *et al.*, 2008; Keating *et al.*, 2010; Lijnen *et al.*, 2011; Ou *et al.*, 2011). The majority of PI3K signaling is mediated through a Grb2 binding site in C-terminal tail of TAM receptors that is autophosphorylated and bound by SH2 domain of Grb2. In contrast, in the sentinel cells of the immune system such as macrophages and dendritic cells, TAM RTK crosstalk with cytokine receptors, like type I interferon receptor, results in preferential activation of JAK/STAT signaling pathway over the activation of PI3K pathway (Zong *et al.*, 1996; Rothlin *et al.*, 2007; Lemke and Rothlin, 2008).

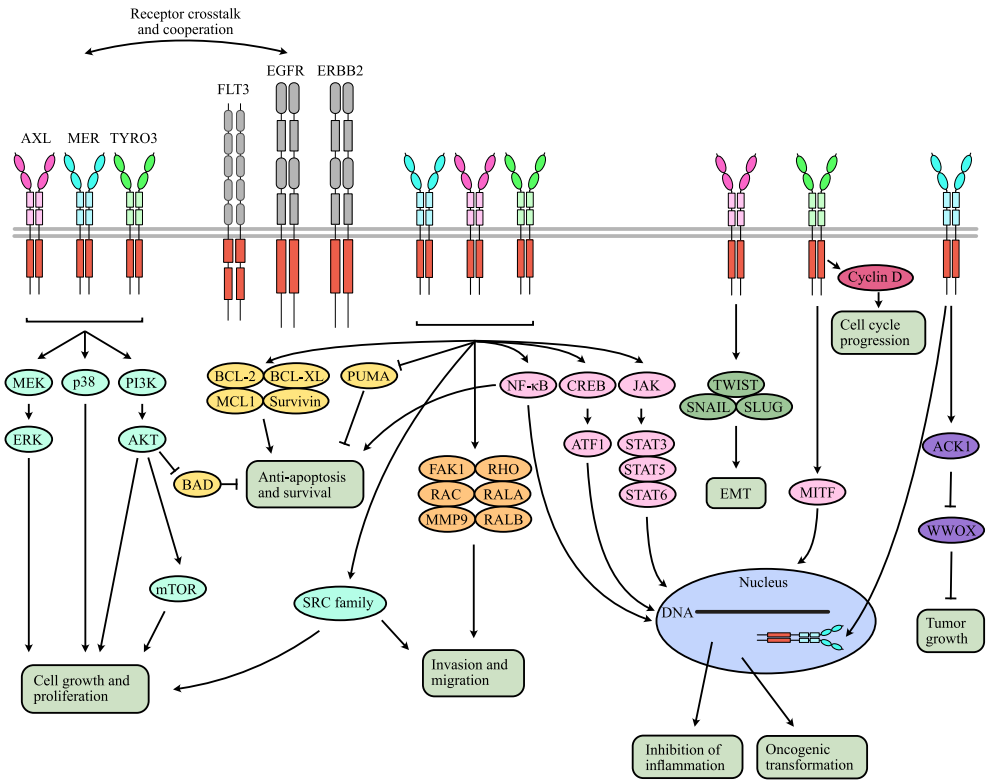

Figure 5. Signaling pathways associated with TAM RTKs in normal and cancer cells. Examples of these pathways are described in the text (Modified from Graham *et al.*, 2014). ACK1, activated Cdc42 kinase 1; ATF1, activating transcription factor 1; BAD, BCL-2-associated agonist of cell death; CREB, cAMP-responsive element-binding protein; EGFR, epidermal growth factor receptor; EMT, epithelial-to-mesenchymal transition; FAK1, focal adhesion kinase 1; FLT3, FMS-like tyrosine kinase 3; JAK, Janus kinase; MCL1, myeloid cell leukemia 1; MITF, microphthalmia-associated transcription factor; MMP9, matrix metalloproteinase 9; NF-κB, nuclear factor-κB; PUMA, p53 upregulated modulator of apoptosis; STAT, signal transducer and activator of transcription; WWOX, WW domain-containing oxidoreductase.

Many of the additional TAM signaling pathways are selectively associated with specific TAMs instead of all TAMs. These include the activation of AXL to regulate the epithelial–mesenchymal transition (EMT), TYRO3 signaling through MITF to bypass senescence in primary melanocytes, and a proposed mechanism to mediate survival signals in cancers cells through activated MER and Cdc42-associated kinase 1 (ACK1), among others (Mahajan *et al.*, 2005; Linger *et al.*, 2008; Zhu *et al.*, 2009; Vuoriluoto *et al.*, 2011; Graham *et al.*, 2014).

The differential activation of separate signaling pathways is thought to be important for differential activation of separate TAM RTK-mediated biological functions. Depending on the context, TAM RTKs can activate various signaling

pathways that regulate cell survival, differentiation, proliferation, and inhibition of pro-inflammatory responses of the immune system. Examples of TAM signaling associated with cancer are discussed in section 2.2.3.1

2.2.3 TAM RTKs in cancer

TAM RTKs have been observed to be overexpressed in various types of cancer (Graham *et al.*, 2014; Burstyn-Cohen and Maimon, 2019) For example, TAM overexpression has been observed in leukemias, gliomas, colorectal cancer, breast cancer, gastrointestinal stromal tumors, melanoma, thyroid cancer, pancreatic cancer, and prostate cancer (Graham *et al.*, 1994, 2006; Craven *et al.*, 1995; Berclaz *et al.*, 2001; Wu *et al.*, 2004; Sainaghi *et al.*, 2005; Mahadevan *et al.*, 2007; Hong *et al.*, 2008; Hutterer *et al.*, 2008; Zhu *et al.*, 2009; Koorstra *et al.*, 2009; Gjerdrum *et al.*, 2010; Keating *et al.*, 2010; Avilla *et al.*, 2011; Song *et al.*, 2011). While TAMs are overexpressed, they are relatively rarely amplified or mutated in cancers. Hence TAM receptors are not viewed as classical oncogenes that would initiate cancer and drive cellular proliferation. TAM RTKs rather seem to have a role in cancer cell maintenance. They may for example prevent apoptosis of cancer cells due to environmental stresses arising within tumors (Lee-Sherick *et al.*, 2013; Linger *et al.*, 2013). It can be implicated that tumors become addicted to TAM receptors and cannot survive without them.

2.2.3.1 Cancer cell-associated cellular functions

Cellular functions associated with TAM RTKs in cancer cells include cell survival, invasion, migration, proliferation, and resistance to treatment (Graham *et al.*, 2014; Nguyen *et al.*, 2014). For example, in melanoma at least one of the TAM receptors is usually overactive (Tworkoski *et al.*, 2011) and in metastatic melanoma patients TAM RTK expression associates with poor prognosis (Zhu *et al.*, 2009; Schlegel *et al.*, 2013; Müller *et al.*, 2014). The general role of TAM RTKs is to mediate survival of melanoma cells (Zhu *et al.*, 2009; Tworkoski *et al.*, 2013; Miller *et al.*, 2016) but specific phenotypes, exhibited by melanoma cells, are associated with different TAM receptors. The invasive and migratory melanoma cell type has been associated with AXL signaling most likely through STAT3 (Tworkoski *et al.*, 2011), while TYRO3 and MER signaling via PI3K/AKT pathway results in a proliferative melanoma cell phenotype (Zhu *et al.*, 2009; Demarest *et al.*, 2013; Tworkoski *et al.*, 2013).

In contrast, in lung cancer cells it has been indicated that AXL promotes a proliferative phenotype while the cell migratory phenotype is governed by MER (Linger *et al.*, 2013). Furthermore, AXL expression in breast cancer, renal cell carcinoma (kidney cancer) and pancreatic cancer associates particularly with the

metastasis of tumor than with the growth of the primary tumor (Gjerdrum *et al.*, 2010; Song *et al.*, 2011; Rankin *et al.*, 2014). Generally, TAM RTKs stimulate MEK/ERK, PI3K/AKT, JAK/STAT, p38, NF-kB and FAK/RAC pathways (Figure 5) (Graham *et al.*, 2014; Nguyen *et al.*, 2014).

2.2.3.2 Modification of the immune response to an immunosuppressive form

The interaction between tumor cells and host cells in the tumor microenvironment has an effect on tumor growth and metastasis (Quail and Joyce, 2013). Especially, the host immune cells are known to interact with tumor and influence tumor growth. In addition to promoting tumor progression directly in cancer cells, TAM RTKs can indirectly promote tumor progression by inhibiting the anti-tumoral effects of the immune cells. The expression of TAM receptors in immune cells can lead to modification of the tumor microenvironment to be immunosuppressive leading to immune evasion of cancer cells by both TAM receptor and cell type -specific mechanisms (Graham *et al.*, 2014; Paolino and Penninger, 2016). Generally, MER expression has been associated with macrophage-mediated functions while TYRO3 and AXL expression is associated with antigen presenting dendritic cells (Seitz *et al.*, 2007). Additionally, cancer cells have been observed to be less immunogenic when they are expressing TAM RTKs, the reason likely being that they are more capable of efferocytosis, a cellular process that leads to destruction of antigens that would normally trigger immune responses (Nguyen *et al.*, 2014; Kasikara *et al.*, 2017).

An example of an immune-modulatory function of TAM RTKs is the upregulation of immune checkpoint molecules, such as programmed death ligands (PD-L), that leads to evasion from immune response (Kasikara *et al.*, 2017; Skinner *et al.*, 2017; Lee-Sherick *et al.*, 2018; Tsukita *et al.*, 2019). The TAM-mediated upregulation of PD-L expression has been observed in leukemia, lung adenocarcinoma and head and neck carcinoma and regulates T cells and CD11b+ monocytes/macrophages contributing to immunosuppressive tumor microenvironment (Skinner *et al.*, 2017; Lee-Sherick *et al.*, 2018; Tsukita *et al.*, 2019). The suppression of T cells has been indicated to be additionally regulated by TAM receptors through immunosuppressive myeloid derived suppressor cells (MDSC) (Holtzhausen *et al.*, 2019).

The activity of MER within the immune cells of the tumor microenvironment is proposed to quench the activity of the immune cells and generate a tumor-supportive environment (Cook *et al.*, 2013). In contrast, AXL and MER activity in CD11b+ lamina propria macrophages is reported to lead to decreased inflammation in lamina propria and inhibition of colorectal cancer progression in an *in vivo* mouse model (Bosurgi *et al.*, 2013). All TAM receptors have been observed to be required for anti-

metastatic activity manifested by natural killer cells (Paolino *et al.*, 2014). The activity of natural killer cells is suppressed by TAM expression in tumors by signaling through Cbl-b, which can be abolished by inhibition of TAM or Cbl-b in *in vivo* mouse models (Paolino *et al.*, 2014).

The examples of opposing outcomes of TAM RTKs illustrate the complexity of TAM signaling in different cancer models. Partnering with different signaling molecules can in part explain the divergent outcomes in cancers. Other possible reasons could be the diverse impact the immune cells have on various cancer models or distinct ligand-receptor interactions and differential TAM expression.

2.2.3.3 The role of TAM ligands

Ligand activation of TAM RTKs has been observed in tumor cells in multiple studies. GAS6 and Protein S have been observed to be expressed in cancer cells, which can lead to autocrine activation of receptors and promote oncogenic properties (Sun *et al.*, 2003, 2004; Hutterer *et al.*, 2008; Che Mat *et al.*, 2016; Abboud-Jarrous *et al.*, 2017; Sadahiro *et al.*, 2018; Wu *et al.*, 2018). Another source for ligand-mediated TAM activation in cancer cells are the immune cells, such as tumor-infiltrating leucocytes (Loges *et al.*, 2010). Interestingly AXL expression levels have been observed to be upregulated by Protein S, leading to increased proliferation and migration of cancer cells, although AXL has not been observed to be activated by this ligand (Lew *et al.*, 2014; Tsou *et al.*, 2014; Abboud-Jarrous *et al.*, 2017). The mechanism of this Protein S -mediated regulation of AXL expression is still unknown.

Besides activating the TAM RTKs of cancer cells, GAS6 and Protein S can have an effect on the immune suppressive nature of the tumor microenvironment. For example, TYRO3 and MER have been observed to promote polarization of host macrophages towards anti-inflammatory M2-phenotype that is induced by secretion of Protein S by melanoma cells (Ubil *et al.*, 2018; Myers *et al.*, 2019). In contrast, the activation of human CD8+ T cells results in upregulation of Protein S and MER expression in these cells and results in induction of T cell proliferation and activation of cytotoxicity (Peeters *et al.*, 2019). This phenomenon has been shown to lead to expansion of tumor infiltrating lymphocytes and an anti-tumor effect. This T cell activation is reduced in the context of high TAM expression in tumor cells that results in high consumption of Protein S (Peeters *et al.*, 2019).

In addition to GAS6 and Protein S, phosphatidylserine in tumor microenvironments can enhance the tumor-supportive environment. As tumors often exhibit multiple apoptosis-inducing conditions such as hypoxia, and chemotherapeutic stress, apoptotic cells are abundant within tumors. These cells contribute to high levels of phosphatidylserine and increased inflammatory tumor microenvironment (Ran *et al.*, 2002; Kasikara *et al.*, 2017). The combined effect of TAM ligands and the

phosphatidylserine can lead to full autocrine and paracrine activation of TAM RTKs in tumor cells. This can result in increased aggressiveness of the tumor due to observed effects that TAM RTKs mediate in cancer cells (Hutterer *et al.*, 2008; Graham *et al.*, 2014). It can be speculated that phosphatidylserine enhanced TAM receptor activation supports the survival of cancer cells that express TAM RTKs. This results in selection of these TAM expressing cells with promoted oncogenic properties. Therefore, it is likely that the ligand/phosphatidylserine-mediated TAM receptor signaling in tumors can provide a mechanism to connect apoptosis with cell proliferation leading to more aggressive form of cancer.

2.2.3.4 TAM RTKs as cancer drug targets

In cancer, the dual role of TAMs makes these RTKs interesting targets for treatment. For example, metastatic melanoma is treated by kinase inhibition of the overly active RAS/RAF/MEK pathway, in cases with mutations in *BRAF* or *NRAS,* or immune checkpoint inhibition by antibodies. Rapidly developing resistance against the kinase inhibitors of BRAF and MEK is regularly observed, even when BRAF and MEK inhibitors are used as combination (Miller *et al.*, 2016). Immune checkpoint inhibitors such as CTLA-4, PD-1 and PD-L1 antibodies, although approved for clinical use, manifest toxicity, and lack of response in some patients (Boutros *et al.*, 2016; Botticelli *et al.*, 2017). The pharmacological inhibition of TAM receptors could combine the advantages of both treatments on one by removing the immunosuppressive characteristics of TAM expressing immune cells and inhibit the pro-tumorigenic effects manifested by TAM expression on the tumor cells. On the same time the inhibition of TAM RTKs could possibly reduce the adverse effects associated with current treatments. Indeed, it has been shown in multiple preclinical cancer models that TAM inhibition inhibits tumor growth both by a direct effect on cancer cells, as well as by releasing the suppressing effect of the innate immune cells on the attack of adaptive immune cells against cancer cells (Holtzhausen *et al.*, 2019; Myers *et al.*, 2019). Additionally in the *in vivo* mouse models, pharmacological inhibition of TAM receptors has been shown to be beneficial when combined with both current treatments: the kinase inhibitors or immunotherapies, such as anti-PD-1 antibodies (Miller *et al.*, 2016; Holtzhausen *et al.*, 2019; Kasikara *et al.*, 2019; Yokoyama *et al.*, 2019).

2.3 Regulated intramembrane proteolysis by gamma-secretase

Besides the canonical signaling executed by RTKs through signaling pathways, fragments of RTKs are detected in the cellular compartments like mitochondria and

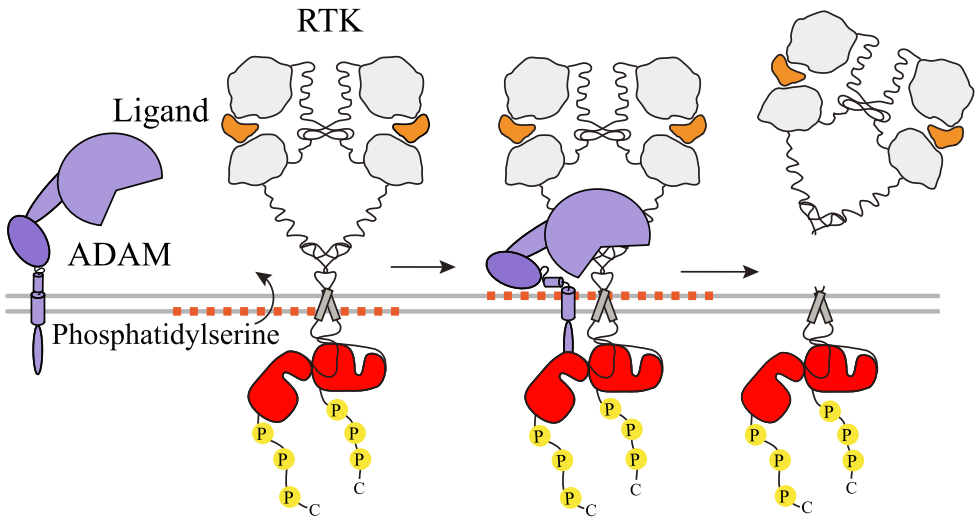

Figure 6. Ectodomain shedding of RTKs. The cleavage at the extracellular juxtamembrane domain results in the release of the ectodomains of RTKs. ADAM10 or ADAM17 are sheddases that mediate the cleavage. The exposure of phosphatidylserine on the cell surface can result from the activation of RTKs by ligands. This results in a conformational change in ADAM17 that facilitates the access to the cleavage site in RTKs. (Adapted from Merilahti and Elenius 2019). ADAM, a disintegrin and metalloproteinase; RTK, receptor tyrosine kinase.

nucleus. These fragments of RTKs can be produced by proteolytic cleavage resulting in the release of the fragments from the membrane. These soluble ICDs of RTKs can be generated from full-length membrane receptors by two sequential proteolytical cleavages. This process is called gamma-secretase-mediated regulated intramembrane proteolysis (RIP) (Brown *et al.*, 2000). RIP best known for its role in the cleavage of amyloid β-protein precursor (APP) in Alzheimer's disease, and the dependency of Notch signaling on the cleavage of Notch (De Strooper *et al.*, 1998, 1999; Wolfe, 2020). The cleavage of Notch is followed by the translocation of Notch ICD to nucleus to activate transcription factors that express genes critical to development of all metazoans and to the maintenance of adult tissues homeostasis (Kopan and Ilagan, 2009).

The cleavage of the extracellular domain of RTKs and its release into extracellular space, is the first step in RIP. Alpha-secretases, such as matrix metalloproteinases, beta-secretases and the disintegrin and metalloproteinase (ADAM) family of proteases are proteases responsible for shedding of the ectodomain. This proteolytic cleavage takes place near the cell membrane in the extracellular juxtamembrane domain of the RTK (Figure 6). Secondary cleavage event follows the ectodomain shedding. Gamma-secretase complex cleaves RTKs at the transmembrane domain and results in the release of an ICD fragment from the membrane (Figure 7).

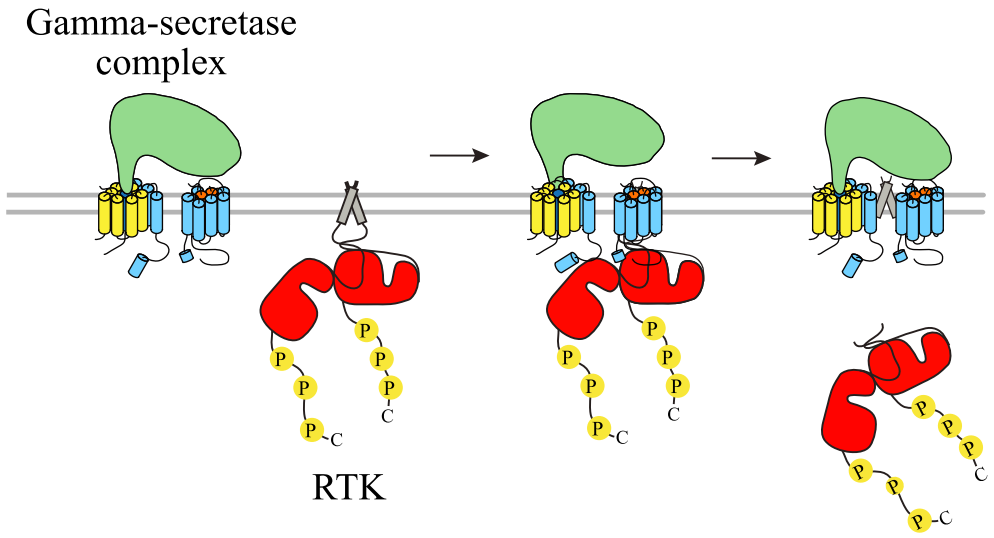

Figure 7. Gamma-secretase-mediated cleavage of RTKs. Gamma-secretase complex gains access to the RTK after the shedding of the ectodomain. Conformational changes are induced in the subunits of gamma-secretase following the binding of the RTK to the gamma-secretase complex. This results in translocation of substrate to the active site of gamma-secretase. Soluble ICD is released into the cytoplasm following the cleavage of the RTK substrate at the transmembrane domain (Adapted from Merilahti and Elenius 2019). RTK, receptor tyrosine kinase.

2.3.1 The family of ADAM proteases

In humans a disintegrin and metalloproteinase (ADAM) family of membrane proteases consists of 22 members with 12 having proteolytical activity (Weber and Saftig, 2012; Lichtenthaler *et al.*, 2018). ADAM10 and ADAM17 are the principal ADAM sheddases in humans. They cleave multiple substrates with diverse functions. In contrast, other ADAMs have more limited substrate repertoire and are less well studied (Reiss and Saftig, 2009; Dreymueller *et al.*, 2015).

The ADAM protease family has a general conserved domain structure and ADAM10 and ADAM17 share a most related structure (Figure 8A). The N-terminal domain is followed by a metalloproteinase domain containing the active site. The disintegrin-like domain and the membrane proximal domain (MPD) are located before a short stalk region and the transmembrane domain (Maskos *et al.*, 1998; Düsterhöft *et al.*, 2013; Seegar *et al.*, 2017). In ADAM 17 the stalk region contains a conserved motif (CANDIS; conserved adam seventeen dynamic interaction sequence), which has a role in the regulation of ADAM17 activity (Düsterhöft *et al.*, 2014). The C-terminus contains the phosphorylation sites. In other ADAMs, MPD is replaced by a cysteine rich domain and an EGF-like domain.

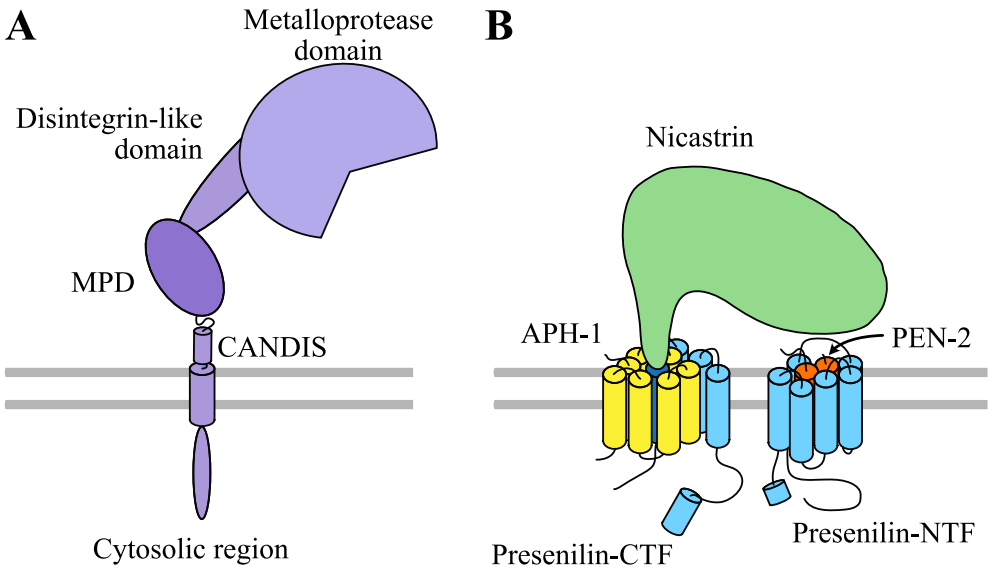

Figure 8. Schematic presentation of **A)** ADAM17 and **B)** gamma-secretase complex. CANDIS, conserved adam seventeen dynamic interaction sequence; MPD, membrane proximal domain; APH-1, anterior pharynx defective-1; PEN-2, presenilin enchancer-2; CTF, C-terminal fragment; NTF, N-terminal fragment.

2.3.2 Gamma-secretase complex

Presenilin, nicastrin, anterior pharynx defective-1 (APH-1) and presenilin enchancer-2 (PEN-2), generate the functional gamma-secretase complex (De Strooper, 2003). Presenilin is proteolytically cleaved to N- and C- terminal fragments to achieve a catalytically active gamma-secretase (Figure 8B). Two isoforms for presenilin and three for APH-1 are found in human proteome resulting in multiple combinations for gamma-secretase complex (De Strooper, 2003).

Nicastrin is responsible for binding to substrates in their free N-termini. It acts as a size limiting step excluding substrates with too large N-termini (Bai *et al.*, 2015; Sun *et al.*, 2015; Bolduc *et al.*, 2016; Fukumori and Steiner, 2016). The requirement for the prior ectodomain cleavage by sheddases is explained by this interaction between nicastrin and gamma-secretase substrate that controls the correct binding of gamma-secretase on substrates.

Presenilin is responsible for enzymatic activity of gamma-secretase. It cleaves type I transmembrane proteins as substrates (Merilahti and Elenius, 2019; Güner and Lichtenthaler, 2020). During the substrate binding step and during the cleavage, substantial conformational changes have been observed in gamma-secretase complex (Fukumori and Steiner, 2016). The binding of substrates to gamma-secretase complex is mediated through a substrate binding site. Following the

binding, substrates are relocated to a docking site near or partially overlapping with the catalytic site. The movement of the substrate from the binding site to the catalytic site is required for a successful cleavage to take place (Fukumori and Steiner, 2016).

2.3.3 Substrate recognition by gamma-secretase

Over 150 substrates have been identified for gamma-secretase (Hemming *et al.*, 2008; Javier-Torrent *et al.*, 2019; Merilahti and Elenius, 2019; Güner and Lichtenthaler, 2020; Liu *et al.*, 2020). Human proteome contains about 2500 single span membrane proteins (Bernhofer *et al.*, 2016; Lomize *et al.*, 2017) indicating that potential substrates greatly exceed the so far identified ones. RIP cleavage requires identification of substrates, scissile bond cleavage at the protease active site and release of the proteolytic product (Langosch *et al.*, 2015).

If compared to cleavage functionality of soluble enzymes, gamma-secretase cleavage is a quite slow process (Kamp *et al.*, 2015). The overall reaction rate can be regulated by the strength of the interaction between gamma-secretase and its substrate, while substrate binding and processing affect the rate of proteolysis.

A structural motif that is conserved in the transmembrane domain is a probable requirement for the recognition of substrates by gamma-secretase. For substrate recognition, or for substrate cleavage site, no conserved amino acid sequence has been identified (Beel and Sanders, 2008). Substrate recognition is assumed to be based on a combination of the interactions, the strength of interactions between gamma-secretase and substrate transmembrane domain, the ectodomain length following the shedding, and relative subcellular localization between gamma-secretase and substrate (Hemming *et al.*, 2008; Funamoto *et al.*, 2013; Bolduc *et al.*, 2016; Meckler and Checler, 2016; Sannerud *et al.*, 2016).

Transmembrane proteins with ectodomain lengths from 12 to 35 amino acids can serve as substrates for gamma-secretase complex (Funamoto *et al.*, 2013). Additionally, gamma-secretase can directly cleave some substrates without prior shedding. The ectodomains of these substrates are required to be naturally short enough to bypass the size exclusion step manifested by the nicastrin (Laurent *et al.*, 2015; Schauenburg *et al.*, 2018).

Most of the interactions between the substrate and the gamma-secretase complex are associated to the N- and C-termini of presenilin. In PEN-2 and nicastrin, additional interactions have been detected as well (Fukumori and Steiner, 2016). Amino acids in the N-terminus of the substrate are subject for the interactions with nicastrin and PEN-2, leading to a proposition that an interaction between nicastrin and PEN-2 takes place as substrates enter gamma-secretase complex (Fukumori and Steiner, 2016; Zhou *et al.*, 2019). Nicastrin has been shown to act as a gatekeeper. It obstructs the entrance of substrates with too large ectodomains into gamma-secretase (Bai *et al.*, 2015; Sun *et*

al., 2015). Despite these advances, the complete picture of mechanisms, on how gamma-secretase recognizes substrates, remains to be elucidated.

2.3.4 Regulation of substrate RIP

Ectodomain shedding and following cleavage by gamma-secretase complex are irreversible events. This is in contrast to many other signaling mechanisms in cells that are transient and reversible. Tight regulation for gamma-secretase cleavage is therefore needed.

Main factors regulating RIP include

- Initial selection of substrates by ectodomain shedding before gamma-secretase cleavage
- Subcellular localization of sheddases, substrates and gamma-secretase complex

Not all the potential membrane proteins that have been reported to be subjected to ectodomain shedding undergo gamma-secretase cleavage. For example, TIE2 has been identified to shed its ectodomain but no gamma-secretase cleavage had been reported (Reusch *et al.*, 2001). The explanation for this could be that specific subcellular location or molecular context are required for further cleavage by gamma-secretase (Bolduc *et al.*, 2016; Fukumori and Steiner, 2016; Meckler and Checler, 2016; Sannerud *et al.*, 2016). In addition, the half-life of the soluble ICD could be so brief that it would prevent the observations of ICD without the usage of reagents that induce the gamma-secretase cleavage or inhibit the degradation of ICDs (Määttä *et al.*, 2006). ERBB2 has been recently identified as a gamma-secretase substrate with cleavage requiring activation of beta2-adenergic receptors with catecholamines, and shedding by ADAM10 (Liu *et al.*, 2020). This identification of ERBB2 as a gamma-secretase substrate can be seen as an example of a requirement for a specific molecular context.

2.3.4.1 Regulation by ADAM10 and ADAM17

As the shedding of ectodomains is a prerequisite for gamma-secretase cleavage, all circumstances affecting the activity or the expression of sheddases can in principle control the overall gamma-secretase cleavage process. In many cancers, the expression of ADAMs is upregulated. Many effectors affecting *ADAM* expression have been identified, such as cytokines and growth factors (Murphy, 2008, 2009). For example, higher amounts of the ectodomain of ERBB4 is identified from the serum of the breast cancer patients than from the serum of the healthy individuals (Hollmén *et al.*, 2012). Additionally, it has been reported that in breast cancer tissue,

more ADAM17 is present than in paired samples of adjacent, histologically normal breast tissue (Määttä *et al.*, 2006).

It has been observed that ADAM17 in its mature form is mainly localized intracellularly. Only a small fraction of ADAM17 resides on the cell surface due to constitutive internalization (Lorenzen *et al.*, 2016). In addition, the majority of the intracellular ADAM17 resides in the endoplasmic reticulum (ER) in an inactive precursor form. ADAM17 maturation takes place in the Golgi apparatus. Inactive Rhomboids 1 and 2 (iRhom) mediate the ADAM 17 trafficking from ER to Golgi (Maretzky *et al.*, 2013; Li *et al.*, 2015; Grieve *et al.*, 2017). The iRhoms have also been linked to regulation of substrate selectivity and shedding activity of ADAM17, in addition to cell surface stability of ADAM17. Phosphofurin acidic cluster sorting protein 2 (PACS-2) also participates with trafficking and sustaining cell surface presence of ADAM17 (Dombernowsky *et al.*, 2015). At the cell surface, tissue inhibitor of metalloproteinases 3 (TIMP3) regulate ADAM17. TIMP3 binds to the catalytic domain of ADAM17 (Xu *et al.*, 2012). In contrast, TIMP1 and TIMP3 can regulate ADAM10 (Murphy, 2011). In addition, integrin beta1 has been reported to interact with ADAM17. This interaction results in inhibition of the activity of cell surface ADAM17 (Bax *et al.*, 2004; Gooz *et al.*, 2012).

One aspect of the regulation of shedding is the requirement of phosphatidylserine exposure at the outer layer of the plasma membrane. The ADAM17 membrane-proximal domain interacts with phosphatidylserine and leads to change in the conformation of ectodomain of ADAM17 (Figure 6). Following the conformational change, the catalytic site of ADAM17 is able to interact with substrate cleavage sites (Düsterhöft *et al.*, 2015; Sommer *et al.*, 2016). As a general rule, it has been proposed that ADAM10 is operating constitutively, while ADAM17 needs to be activated (Grötzinger *et al.*, 2017).

ADAM10 has been shown to reside in a same multiprotease complex with gamma-secretase (Chen *et al.*, 2015). It is plausible that other multiprotease complexes exist where other sheddases reside with gamma-secretase as well. Indeed, ADAM17 has not been found to immunoprecipitate with ADAM10 (Chen *et al.*, 2015). If gamma-secretase and sheddases reside in the same complex, it can result in more optimal processivity of the total cleavage event. The shed substrates could efficiently bind to gamma-secretase complex for a more efficient ICD release than if gamma-secretase and sheddases did not reside in the same complex. However, research in this area is still limited and further studies are needed.

2.3.4.2 Regulation of shedding by post-translational modification of substrates

A form of post-translational modification, O-glycosylation, of substrates, may take part in regulation of shedding of membrane proteins (Goth *et al.*, 2015). Substrates are cleaved at the membrane-proximal extracellular juxtamembrane domain, and O-glycosylation takes frequently place in the same place. As an example, in many ADAM17 substrates, glycosylation of the extracellular juxtamembrane domain reduces ADAM17-mediated shedding. Glycosylation has also been shown to alter the location of the ADAM17 cleavage sites in some cases, by making original cleavage sites uncleavable (Goth *et al.*, 2015). It can be speculated that shedding is regulated to some extent by selective GalNac transferase isoform expression as only one or few GalNac transferase isoforms control the specific sites of O-glycosylation (Bennett *et al.*, 2012; Kong *et al.*, 2015).

2.3.4.3 Subcellular localization in regulation of RIP

Differently composed gamma-secretase complexes by different presenilins have been shown to be directed to distinct subcellular localizations (Meckler and Checler, 2016; Sannerud *et al.*, 2016). Gamma-secretase complexes with presenilin-2 are found in late endosomes or lysosomes while gamma-secretase complexes with presenilin-1 are distributed more diffusely at the cell membranes (Sannerud *et al.*, 2016). The lipid composition of the membrane has been observed to affect the activity and localization of gamma-secretase. Gamma-secretase complexes with presenilin-1 have been shown to reside in the membrane areas called lipid rafts and the activity of gamma-secretase to be dependent on the composition of lipids (Vetrivel *et al.*, 2004; Urano *et al.*, 2005; Osenkowski *et al.*, 2008; Wakabayashi *et al.*, 2009). All in all, for a successful RIP cleavage, proper compartmentalization, and spatial distribution of gamma-secretase along with its substrates are required.

2.4 Cleavage of receptor tyrosine kinases

ADAM10 and ADAM17 are mostly responsible for the ectodomain shedding of RTKs (Table 1). In total 11 out the 20 RTKs with identified sheddase have been reported to be shed by ADAM10 or ADAM17. It is noteworthy that six out of these 20 RTKs have been reported, in general terms, to be shed by metalloproteinases. It is therefore possible that these RTKs can also be shed by ADAM10 or ADAM17. In total 29 out of 55 human RTKs have been indicated to be substrates for gamma-secretase (Table 1).

Table 1. Gamma-secretase-mediated cleavage in RTKs. Proteases responsible for ectodomain cleavage are also listed.

RTK	SHEDDASE	REFERENCE FOR SHEDDASE	REFERENCE FOR GAMMA-SECRETASE CLEAVAGE
AXL	ADAM10/ADAM17	(Miller *et al.*, 2016)	(Bae *et al.*, 2015)
CSF1R	ADAM17	(Rovida *et al.*, 2001)	(Wilhelmsen and van der Geer, 2004)
EPHA2	MT-MMP	(Sugiyama *et al.*, 2013)	(Merilahti *et al.*, 2017)
EPHA3	Metalloprotease	(Javier-Torrent *et al.*, 2019)	(Javier-Torrent *et al.*, 2019)
EPHA4	ADAM19	(Yumoto *et al.*, 2008)	(Inoue *et al.*, 2009)
EPHA5			(Merilahti *et al.*, 2017)
EPHA7			(Merilahti *et al.*, 2017)
EPHB2	ADAM10	(Litterst *et al.*, 2007)	(Litterst *et al.*, 2007)
EPHB3			(Merilahti *et al.*, 2017)
EPHB4	ADAM8	(Guaiquil *et al.*, 2010)	(Merilahti *et al.*, 2017)
EPHB6			(Merilahti *et al.*, 2017)
ERBB2	ADAM10	(Liu *et al.*, 2020)	(Liu *et al.*, 2020)
ERBB4	ADAM17	(Rio *et al.*, 2000)	(Ni *et al.*, 2001)
FGFR3	Metalloprotease	(Degnin *et al.*, 2011)	(Degnin *et al.*, 2011)
FGFR4			(Merilahti *et al.*, 2017)
IGF1R			(McElroy et al. 2007)
INSR	ADAM17	(Kasuga *et al.*, 2007)	(Kasuga *et al.*, 2007)
MER	ADAM17	(Thorp *et al.*, 2011)	(Merilahti *et al.*, 2017)
MET	ADAM10/ADAM17	(Foveau *et al.*, 2009; Schelter *et al.*, 2010)	(Foveau *et al.*, 2009)
MUSK			(Merilahti *et al.*, 2017)
PTK7	ADAM17	(Na *et al.*, 2012)	(Na *et al.*, 2012)
RYK	Metalloprotease	(Halford *et al.*, 2013)	(Lyu *et al.*, 2008)
TIE1	Metalloprotease	(Marron *et al.*, 2007)	(Marron *et al.*, 2007)
TRKA	Metalloprotease	(Pandiella, 1999)	(Merilahti *et al.*, 2017)
TRKB	Metalloprotease	(Tejeda *et al.*, 2016)	(Tejeda *et al.*, 2016)
TYRO3			(Merilahti *et al.*, 2017)
VEGFR1	ADAM8/ADAM10/ ADAM17	(Guaiquil *et al.*, 2010; Raikwar *et al.*, 2014)	(Cai *et al.*, 2006)
VEGFR2	ADAM17	(Swendeman *et al.*, 2008)	(Ablonczy *et al.*, 2009)
VEGFR3			(Merilahti *et al.*, 2017)

In many cases, RTK activation by ligand binding has been reported to be a prerequisite for these transmembrane proteins to be cleaved by gamma-secretase. In addition, basal gamma-secretase cleavage is also observed. With CSF1R, EPHB2, ERBB4, FGFR3, RYK, VEGFR1 and VEGFR2, ligand-induced cleavage has been detected (Ni *et al.*, 2001; Glenn and van der Geer, 2007; Litterst *et al.*, 2007; Lyu *et*

al., 2008; Rahimi *et al.*, 2009; Cai *et al.*, 2011; Degnin *et al.*, 2011). The activation of downstream signaling kinases is the likely explanation for cleavage of the RTKs following the ligand activation. Downstream signaling kinases, in turn, activate shedding by phosphorylating the cytoplasmic tail of ADAM10 or ADAM17. The kinases that have been observed to phosphorylate ADAM10 or ADAM17 include PLK2, MAPKs and PKC (Grötzinger *et al.*, 2017; Miller *et al.*, 2017).

Changes of ion concentrations across the cellular membranes and activation of other membrane receptors, that are not gamma-secretase substrates, have been observed to activate gamma-secretase cleavage as well. For CSF1R, EPHB2 and ERBB4 these types of cleavage activation mechanisms have been observed (Litterst *et al.*, 2007; Glenn and van der Geer, 2008; Hollmén *et al.*, 2012).

2.4.1 Subcellular trafficking of the cleaved RTK ICD

The ICDs released by gamma-secretase cleavage have been found in multiple subcellular compartments. The ICDs have been observed to localize to nucleus, mitochondria or remain in the cytosol. For the most studied cleavable RTK, ERBB4, nuclear localization has been detected by multiple *in vitro* and *in vivo* methods and models (Ni *et al.*, 2001; Määttä *et al.*, 2006; Muraoka-Cook *et al.*, 2006; Sardi *et al.*, 2006; Hoeing *et al.*, 2011). Cells naturally trafficking ERBB4 ICD to their nuclei include mammary epithelial cells and different breast cancer cell types. In breast cancer tissue increased ERBB4 nuclear localization has been observed compared to normal breast tissue and nuclear localization of ERBB4 is associated with worse prognosis than cell surface localization (Srinivasan *et al.*, 2000; Junttila *et al.*, 2005). RTK ICDs or C-terminal epitopes of RTKs, whose subcellular localization has been determined are listed in Table 2. Subcellular localizations of RTK ICDs have been observed with both endogenous and overexpression models. However, observations on the localization of INSR and PTK7 ICDs have been done with overexpression of ICD constructs, which may have an effect on interpretation of these findings. (Kasuga *et al.*, 2007; Na *et al.*, 2012).

Mechanisms governing the ICD translocation to various cellular compartments are largely unknown, but for ERBB4 ICD, the nuclear localization has been observed to be promoted by modification by small ubiquitin-like modifier (SUMO). The increased nuclear localization is likely due to inhibition of nuclear export of ERBB4 ICD back to the cytosol and increased activity of the kinase domain of ERBB4 following the sumoylation of ERBB4 (Sundvall et al. 2012; Knittle et al. 2017).

Additionally, RTK ICDs can be translocated to proteasome for swift degradation after the cleavage. This downregulation of RTKs is further discussed in section 2.4.3.

Table 2. Reported subcellular localizations of RTK ICDs. IF, immunofluorescence; IHC, immunohistochemistry; SCF, subcellular fractionation.

RTK	SUBCELLULAR LOCALIZATION	DETECTED *IN VITRO*/ *IN VIVO*	DETECTION METHOD	CELLULAR EXPRESSION	REFERENCES
AXL	Nucleus	*In vitro*	IF	Endogenous	(Lu *et al.*, 2017; Merilahti *et al.*, 2017)
EPHB2	Cytosol	*In vitro*	SCF	Endogenous	(Xu *et al.*, 2009)
EPHA3	Cytosol	*In vitro*	IF	Endogenous	(Javier-Torrent *et al.*, 2019)
EPHA4	Nucleus	*In vitro, in vivo*	IF	Endogenous	(Inoue *et al.*, 2009)
ERBB2	Nucleus	*In vitro, in vivo*	IF	Endogenous	(Liu *et al.*, 2020)
ERBB4	Mitochondria, nucleus	*In vitro, in vivo*	IF, IHC, SCF	Endogenous	(Ni *et al.*, 2001; Vidal *et al.*, 2005; Naresh *et al.*, 2006; Hoeing *et al.*, 2011)
FGFR3	Nucleus	*In vitro*	IF	Overexpression	(Degnin *et al.*, 2011)
INSR	Nucleus	*In vitro*	IF	Overexpression	(Kasuga *et al.*, 2007)
PTK7	Nucleus	*In vitro*	IF	Overexpression	(Na *et al.*, 2012)
RYK	Nucleus	*In vivo*	IF, SCF	Endogenous	(Lyu *et al.*, 2008)
TRKA	Nucleus	*In vivo*	IHC	Endogenous	(Bonacchi *et al.*, 2008)
VEGFR1	Cytosol	*In vitro*	IF, SCF	Endogenous	(Cai *et al.*, 2006)

2.4.2 Cellular functions actively regulated by RTK ICDs

Following the release from the cell membrane, ICDs of RTKs can function as signaling molecules with multiple observed activities (Figure 9). The functions depicted in the Figure 9 are mostly collected from research on ERBB4 and examples are discussed below.

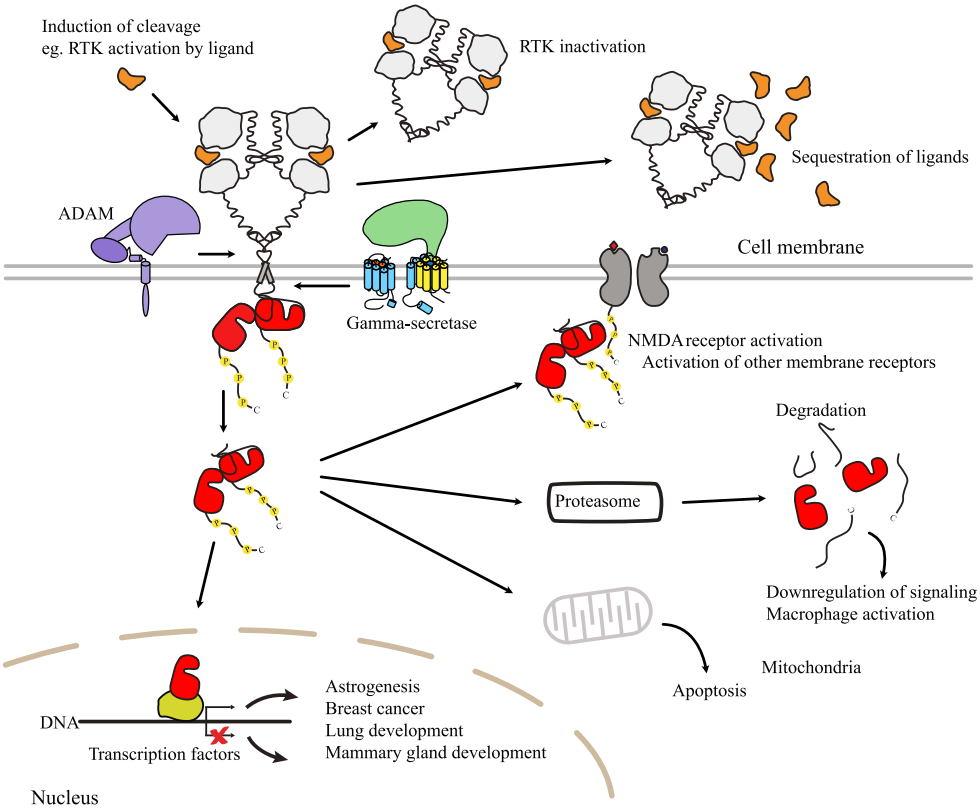

Figure 9. Cellular functions regulated by gamma-secretase-mediated cleavage of RTKs. (Adapted from Merilahti and Elenius 2019). ADAM, a disintegrin and metalloproteinase; NMDA, N-methyl-D-aspartate; RTK, receptor tyrosine kinase.

2.4.2.1 Development and growth regulated by ERBB4 ICD signaling

Multiple developmental processes and organ differentiations have been suggested to be regulated by ERBB4 ICD localizing into the nucleus. The nuclear localization of ERBB4 ICD has been observed to induce the differentiation of mouse mammary gland as well as maturation of fetal lungs (Muraoka-Cook *et al.*, 2006; Thor *et al.*, 2009; Hoeing *et al.*, 2011; Zscheppang *et al.*, 2011b, 2011a; Paatero *et al.*, 2014). These processes may require ERBB4 ICD interaction with the transcription factor STAT5 leading to activation of beta-casein promoter or ERBB4 ICD interaction with the transcription factor YAP and estrogen receptor beta (Williams *et al.*, 2004; Hoeing *et al.*, 2011; Zscheppang *et al.*, 2011a, 2011b). ERBB4 ICD – hypoxia-inducible factor 1 alpha (HIF-1α) interaction has been shown to result in stabilization of HIF-1α and increase transcription mediated by HIF (Paatero *et al.*,

2012). In addition, HIF-1α has been found to regulate ERBB4 endocytosis and ERBB4-mediated differentiation of mammary epithelial cells (Paatero *et al.*, 2014), implying a complementary regulation by these two proteins.

ERBB4 ICD has been associated with estrogen-responsive gene expression. Estrogen receptor alpha and ERBB4 ICD together localize to estrogen-inducible gene promoters. For example, the expression of stromal cell-derived factor 1 (SDF-1) and the expression of progesterone receptor are regulated by this ERBB4 ICD localization (Zhu *et al.*, 2006). In addition, *ERBB4* is expressed in estrogen receptor-positive breast cancers (Junttila *et al.*, 2005). The survival or proliferation of estrogen receptor-positive breast cancer cells may be promoted by ERBB4 ICD as overexpression of the isoform of cleavable ERBB4 increases the growth of breast cancer cells both in *in vitro* and *in vivo* (Junttila *et al.*, 2005; Sundvall *et al.*, 2010, 2012; Paatero *et al.*, 2014; Wali *et al.*, 2014). This increase in growth can be suppressed with an antibody blocking the ERBB4 cleavage (Hollmén *et al.*, 2009).

2.4.2.2 Neural development and neural functions regulated by RTK ICDs

The soluble ICDs of EPHA3, EPHA4, EPHB2, ERBB4 and RYK have been observed to participate in the regulation of neural development and neural functions. ERBB4 ICD formation is essential for governing the astrogenic differentiation during the development in mouse (Sardi *et al.*, 2006). In this context, ERBB4 ICD interacts with N-COR and TAB2 (a co-repressor and an adaptor protein). The ICD escorts these proteins to the nucleus. In the nucleus, the repression of astrocytic-associated gene expression is induced *in vitro* and *in vivo* (Sardi *et al.*, 2006). In addition to regulation of astrogenesis, inhibition of ligand induced gamma-secretase cleavage of ERBB4 has been shown to hinder the maturation of oligodendrocytes *in vitro* (Lai and Feng, 2004).

Wnt3-dependent neuronal differentiation has been indicated to be dependent on gamma-secretase cleavage of RYK RTK and in neural progenitor cells, Wnt activation is required for nuclear localization of RYK ICD, *in vitro* (Lyu *et al.*, 2008). RYK ICD accumulates to nuclei throughout the cortical development promoting differentiation of undifferentiated cells to neurons (Lyu *et al.*, 2008). This nuclear localization of RYK ICD is reported to be dependent on SMEK1 and SMEK2 proteins (Chang *et al.*, 2017). The proposed mechanism includes that RYK ICD is escorted to the nucleus by SMEK1 and SMEK2. RYK ICD and both SMEKs associate with *DLX1/2* intergenic regulation element in chromatin. This interaction regulates the *DLX1/2* transcription and in mouse primary cortical neural stem cells leads to neuronal differentiation (Chang *et al.*, 2017).

The ICDs of EPHA3, EPHA4 and EPHB2 are associated with the regulation of neural functions. The functions associated with EPHA3 and EPHA4 ICD suggest of the existence of an interesting dual-regulatory role of the same RTK that manifests opposing effects dependent on the source of activation. The gamma-secretase-mediated cleavage of EPHA3 has been proposed to manifest ligand independent signaling of EPHA3 ICD leading to axon growth in cultured mouse hippocampal neurons, while EPHA4 ICD increases the number of dendritic spines in cultured rat primary neurons (Inoue *et al.*, 2009; Javier-Torrent *et al.*, 2019). This is in contrast with proposed ligand induced retraction of axons and dendritic spines mediated by EPHA3 and EPHA4, respectively (Inoue *et al.*, 2009; Javier-Torrent *et al.*, 2019).

The gamma-secretase-mediated cleavage of EPHB2 has been observed to generate an ICD that phosphorylates N-methyl-D-aspartate receptor (NMDAR). The phosphorylation increases the cell surface expression of NMDAR in cultured rat primary neurons (Xu *et al.*, 2009). It can be speculated that EPHB2 ICD has an effect on learning and memory through NMDAR as NMDAR is an ionotropic glutamate receptor expressed in the mammalian central nervous system. The regulation of NMDAR by Src kinase family-mediated phosphorylation plays crucial roles in cellular signaling, learning and memory. (Salter and Kalia, 2004; Paoletti *et al.*, 2013).

2.4.2.3 Regulation of apoptosis by ERBB4 ICD

In breast cancer cells, ERBB4 has been shown to induce apoptosis. ERBB4 ICD localizes to mitochondria in SKBr3 cells where it may act as a proapoptotic protein (Naresh *et al.*, 2006). A BH3 domain is found in the ERBB4 ICD that is similar to BH3-only type BCL2 (prototype antiapoptotic protein) protein family. In accordance, when ERBB4 transmembrane domain is mutated to prevent gamma-secretase cleavage, mitochondrial ICD translocation and apoptosis are down-regulated (Vidal *et al.*, 2005; Naresh *et al.*, 2006). ERBB4 ICD interacts with BCL2 and overexpression of BCL2 leads to reduction of apoptosis induced by ERBB4 ICD (Naresh *et al.*, 2006). Moreover, p53 repressor MDM2 has been observed to be phosphorylated by ERBB4 ICD promoting the ubiquitination of MDM2 and leading to increase in the levels of p53 and its transcriptional target Cyclin-dependent kinase inhibitor 1 *in vitro* (Arasada and Carpenter, 2005). These results indicate that there are multiple mechanisms by which ERBB4 ICD can regulate apoptosis.

2.4.2.4 Regulation of angiogenesis and vascular and cellular permeability by VEGFR ICDs

The gamma-secretase cleavage of two VEGFR RTKs provide an interesting example of how the cellular context affects the regulation of gamma-secretase cleavage.

Gamma-secretase-mediated cleavage of VEGFR1 has been observed to be increased by pigment epithelium-derived factor (PEDF) that results in inhibition of VEGF-induced endothelial cell permeability and endothelial tube generation (Cai *et al.*, 2006, 2011). In retinal microvascular endothelial cells, the VEGFR1 ICD formation is associated with decreased VEGFR1 phosphorylation (Cai *et al.*, 2011). While VEGFR1 is considered to be a negative regulator of angiogenesis (Roberts *et al.*, 2004), the shedding of the ectodomain of the VEGFR1, prior to gamma-secretase cleavage, could also explain the results above. The shed ectodomain of VEGFR1 could sequester ligands that activate pro-angiogenic VEGFR2 such as VEGFA. This mechanism is further discussed in section 2.4.3. These speculations are supported by observations of gamma-secretase cleavage of VEGFR1 in leukemic cells, a rare example of non-endothelial cell type naturally expressing VEGFR1 (Rahimi *et al.*, 2009).

In retinal pigment epithelium cells, VEGFR2 has also been identified to be cleaved by gamma-secretase (Ablonczy *et al.*, 2009). The cleavage has been shown to be induced by a VEGFR1 agonist, PEDF, and leads to reduced cellular permeability, induced by VEGF-E, a VEGFR2 agonist. This PEDF-dependent effect is achieved only by indirect processing of VEGFR2 by a gamma-secretase cleavage but not of VEGFR1.

2.4.3 Downregulation of RTK functions by RIP

While gamma-secretase cleavage creates active signaling fragments that add diversity to cell signaling, cleavage also represents a putative mechanism for RTK turn-over and degradation. The ectodomain generated from shedding and ICD generated from gamma-secretase cleavage can participate in downregulation of RTK signaling. This is manifested by releasing the ligand-binding capacity containing extracellular domain from the membrane and by the degradation of the active kinase domain. Overall, it can be expected that the kinetics of ICD inactivation by dephosphorylation and the kinetics of ICD degradation have a central role in determining the functional outcome of ICD generation.

For CSF1R, IGF1R, MET and TIE1, rapid degradation after gamma-secretase cleavage have been observed (Wilhelmsen and van der Geer, 2004; Marron *et al.*, 2007; McElroy *et al.*, 2007; Foveau *et al.*, 2009). MET RTK is constitutively shed and cleaved by gamma-secretase. Interestingly, a non-cleavable, mutant version of MET accumulates to the cell membrane and manifests invasive growth of the cells through ligand-independent signaling (Foveau *et al.*, 2009).

The fate of the extracellular fragments generated by shedding are largely unknown apart from some examples of TYRO3, AXL, MER and TRKB with

indicated roles in neutralizing respective ligands (Sather *et al.*, 2007; Miller *et al.*, 2016; Orme *et al.*, 2016; Tejeda *et al.*, 2016; Xu *et al.*, 2018).

2.4.4 Implications of RTK cleavage in cancer

Alteration of RTK-mediated signaling by gamma-secretase cleavage can have an effect on processes relevant to tumor growth. Thus, in principle tumor formation can be regulated by any possible defects in RIP or in the regulation of the cleavage process.

In humans, most RTKs are classified as targets for one or several currently approved cancer drugs as described in section 2.1.3 (Figure 2). RTKs that are targets for cancer drugs are often targets for gamma-secretase cleavage as well (Table 1). It is conceivable that the modulators of gamma-secretase, by regulating the RTK cleavage, could affect the tumor promoting effects of RTKs. It has been shown that gamma-secretase inhibitors may have an anti-tumor effect in tumor models (Golde *et al.*, 2013).

Many clinical trials have also been executed with gamma-secretase inhibitors (ClinicalTrials.gov, 2020; McCaw *et al.*, 2020) Although the role of RTKs is uncertain, as most effects of these inhibitors have been connected to their capability to block the signaling of Notch (Rahimi *et al.*, 2009; Golde *et al.*, 2013; McCaw *et al.*, 2020). The tested first-generation gamma-secretase inhibitors have proven to be anti-tumorigenic, but adverse effects of these inhibitors have not been bearable. The vast amount of already identified gamma-secretase substrates makes it difficult to develop inhibitors that would be selective only for the desired target. Another cause for the observed adverse effects can be that other membrane proteases such as rhomboids are induced to cleave gamma-secretase substrates as a result of gamma-secretase inhibition (Urban and Moin, 2014).

The relevance of RTK cleavage as a mechanism for resistance to RTK-targeted therapies has not been extensively studied. In principle, several possible mechanisms exist on how the sensitivity of cancer cells to current therapies targeting RTKs can be affected by RTK processing. Not only are the structures that can mediate interactions with therapeutic antibodies depleted by the ectodomain shedding but shedding also creates decoy receptors that can bind the antibodies in the extracellular space. This binding neutralizes the antibody-mediated therapeutic effect from cells still expressing intact RTKs. The other class of RTK targeted drugs, tyrosine kinase inhibitors, could still be functional despite the release of the ICD from the membrane. Targeting the shedding of gamma-secretase substrates could be an additional target for cancer treatment (Miller *et al.*, 2017). On the other hand, recent evidence indicates that this may not be achievable as the inhibition of shedding also reduces the production of decoy receptors and stabilize the cell surface localized active RTKs

(Miller *et al.*, 2016). It has been shown that the resistance to MEK inhibitors in melanoma patients is associated to reduced shedding of RTKs such as AXL, MET and ERBB4 (Miller *et al.*, 2016). This reduction in shedding was observed to be due to the inhibition of ADAM10 by increased amount of TIMP-1 on cell surface. Furthermore, in *KRAS* mutant colorectal cancer, the reduced ADAM17-mediated MET shedding mediates resistance to MEK inhibitors (Van Schaeybroeck *et al.*, 2014).

3 Aims

The specific aims of this study were following:

1. Determining the prevalence of gamma-secretase-mediated RIP among RTKs.
2. Identification of biological functions and signaling pathways associated with gamma-secretase cleavage of RTKs.

4 Materials and Methods

4.1 Expression plasmids (I-II)

Plasmids used in this study are listed in Table 3. All the plasmids were cloned with Gateway cloning method from pDONR221, pDONR223 or pENTR223 plasmids to the expression plasmids described in the Table 3 or by using common molecular cloning methods.

Gamma-secretase cleavage mutants (ΔGS), and nuclear localization signal mutants (ΔNLS) for AXL and TYRO3, and ADAM cleavage mutant (ΔADAM) for TYRO3 were generated using synthetic DNA fragments (Integrated DNA technologies). Synthetic DNA fragments contained the mutations as indicated below. NEBuilder Hifi DNA Assembly Master Mix (New England Biolabs) was used to ligate synthetic DNA fragments to plasmids according to the manufacturer's instructions.

The AXL ΔGS mutant (amino acids 453YVLLGAVV459 replaced by 453IIIGPLIF459) and ΔNLS mutant (R474A/R475A) have been previously described (Lu *et al.*, 2017). To generate a plasmid encoding TYRO3 ΔGS mutant, an I449A mutation was introduced. To generate a plasmid encoding TYRO3 ΔNLS mutant, a R452A/K453A double mutation to the putative NLS site that closely resembles that of AXL (Migdall-Wilson *et al.*, 2012), was introduced. To generate a plasmid encoding TYRO3 ΔADAM mutant, predicted cleavage sites with highest predicted cleavage site probabilities for both ADAM10 and ADAM17 cleavage (4.2) were selected and P408A/L409P and G419P mutations were introduced.

Table 3. Expression plasmids used in this study.

INSERT	BACKBONE	PURPOSE	USED IN
ALK	pDEST-eGFP-N1	Mammalian expression	I
AXL	pDEST-eGFP-N1	Mammalian expression	I
AXL	pLX302, pDEST-eGFP-N1	Mammalian expression	I
AXL ΔGS	pDEST-eGFP-N1	Mammalian expression	I
AXL ΔNLS	pDEST-eGFP-N1	Mammalian expression	I
CSF1R	pDEST-eGFP-N1	Mammalian expression	I
DDR1	pLX302	Mammalian expression	I
DDR2	pDEST-eGFP-N1	Mammalian expression	I
EGFR	pcDNA3.1-HA	Mammalian expression	I

EPHA1	pLX302	Mammalian expression	I
EPHA2	pDEST-eGFP-N1	Mammalian expression	I
EPHA3	pDEST-eGFP-N1	Mammalian expression	I
EPHA4	pDEST-eGFP-N1	Mammalian expression	I
EPHA5	pDEST-eGFP-N1	Mammalian expression	I
EPHA7	pDEST-eGFP-N1	Mammalian expression	I
EPHA8	pMAX-DEST	Mammalian expression	I
EPHB1	pDEST-eGFP-N1	Mammalian expression	I
EPHB2	pDEST-eGFP-N1	Mammalian expression	I
EPHB3	pDEST-eGFP-N1	Mammalian expression	I
EPHB4	pDEST-eGFP-N1	Mammalian expression	I
EPHB6	pLX302	Mammalian expression	I
ERBB2	pcDNA3.1-HA	Mammalian expression	I
ERBB3	pcDNA3.1-HA	Mammalian expression	I
ERBB4	pcDNA3.1-HA	Mammalian expression	I
FGFR1	pLX302	Mammalian expression	I
FGFR2	pLX302	Mammalian expression	I
FGFR3	pDEST-eGFP-N1	Mammalian expression	I
FGFR4	pDEST-eGFP-N1	Mammalian expression	I
FLT3	pLX302	Mammalian expression	I
INSR	pDEST-eGFP-N1	Mammalian expression	I
IRR	pDEST-eGFP-N1	Mammalian expression	I
LTK	pDEST-eGFP-N1	Mammalian expression	I
MER	pMAX-DEST	Mammalian expression	I
MUSK	pcDNA3.1-HA	Mammalian expression	I
PDGFRA	pDEST-eGFP-N1	Mammalian expression	I
PDGFRB	pDEST-eGFP-N1	Mammalian expression	I
PTK7	pDEST-eGFP-N1	Mammalian expression	I
RET	pDEST-eGFP-N1	Mammalian expression	I
RON	pDEST-eGFP-N1	Mammalian expression	I
ROR1	pDEST-eGFP-N1	Mammalian expression	I
ROR2	pDEST-eGFP-N1	Mammalian expression	I
ROS	pDEST-eGFP-N1	Mammalian expression	I
TIE1	pLX302	Mammalian expression	I
TIE2	pMAX-DEST	Mammalian expression	I
TRKA	pDEST-eGFP-N1	Mammalian expression	I
TRKC	pDEST-eGFP-N1	Mammalian expression	I
TYRO3	pDEST-eGFP-N1, pMAX-DEST, pEZY-Myc-His	Mammalian expression	I, II
TYRO3 ΔADAM	pEZY-Myc-His, pMAX-DEST	Mammalian expression	II
TYRO3 ΔGS	pDEST-eGFP-N1, pEZY-Myc-His, pMAX-DEST	Mammalian expression	I, II
TYRO3 NLS	pDEST-eGFP-N1	Mammalian expression	I
TYRO3 shRNA	pLKO.1-puromycin	Gene silencing	II
VEGFR3	pLX302	Mammalian expression	I
REV	pRSV-Rev	Lentiviral packaging	II
HIV-1 GAG/POL	pMD	Lentiviral packaging	II
VSV G	pMD2.G	Lentiviral packaging	II

The expression plasmid encoding ERBB4-HA has been previously described (Määttä et al. 2006).

4.2 ADAM10 and ADAM17 cleavage site prediction (II)

The prediction of ADAM10 and ADAM17 was done using a method based on Lähdesmäki *et al.*, 2008. Published cleavage sites for ADAM10 and ADAM17 were collected from literature (Caescu et al, 2009; Tucher et al., 2014). Possible cleavage sites were predicted with a sliding window analysis calculating the probability of a sequence window of 10 residues having an ADAM cleavage based on the positional relative frequencies of amino acid residues collected from the literature with a 0th order Markov chain. The probability for not having an ADAM cleavage site was calculated from the same sequence windows with 0th order Markov chain using the relative frequencies of amino acid residues in proteins as determined by Uniprot (Bateman et al, 2021) as positional frequencies. The sequence windows with at least 2 times higher probability for having an ADAM cleavage site than not having an ADAM cleavage site and cleavage sites residing within 35 amino acids from the transmembrane were considered as probable cleavage sites.

4.3 Cell culture and transfections (I-II)

Cells used in this study are listed in Table 4. Growth media were supplemented with 10% (wt/vol) fetal calf serum (FCS) (Promocell), 50 U/ml penicillin and 50 µg/ml streptomycin (Sigma-Aldrich), MCF-7 cell medium was additionally supplemented with 1 nM 17-β-estradiol (Sigma-Aldrich), and 1 µg/ml insulin (Sigma-Aldrich).

Cell transfections were done using HilyMAX (Dojindo), jetPRIME (Polyplus-transfection) or FuGENE 6 (Promega) transfection reagents according to the manufacturer's instructions.

Table 4. Cell lines used in the study.

CELL LINE	TYPE	SPECIES	MEDIUM	USED IN
A431	Epidermoid carcinoma cell line	Human	DMEM	I
HEK293 and HEK293T	Embryonic kidney cell line	Human	DMEM	I
MCF-7	Mammary adenocarcinoma cell line	Human	RPMI 1640	I
MDA-MB-231	Mammary adenocarcinoma cell line	Human	DMEM	I
NIH-3T3	Fibroblast cell line	Mouse	DMEM	I
PC-3	Prostate cancer cell line	Human	RPMI 1640	I
WM-266-4	Melanoma cell line	Human	DMEM	II

4.3.1 Generation of stable TYRO3 knock-down cell lines by lentiviral transduction (II)

PLKO.1-puromycin plasmid (containing the shRNA described below in detail) (Sigma-Aldrich), pMDLg/pRRE (Addgene plasmid #12251), pMD2.G (Addgene plasmid #12259) and pRSV-Rev (Addgene plasmid #12253) (gifts from Didier Trono) were used to produce lentiviral vectors.

For stable downregulation of TYRO3, TYRO3 targeted shRNA TRCN0000231528 (CCGGTTGGTATCTCAGGTCTGAATCCTCGAGGATTCAGACCTGAGATACCAATTTTTG) (MISSION, Sigma-Aldrich) was used. Control shRNA (Addgene plasmid #1864) was a gift from David Sabatini (Sarbassov *et al.*, 2005). HEK293T cells were used to produce shRNA-carrying lentiviruses. Third generation lentiviral packaging system (Addgene) was used with pRSV-Rev, pMDLg/pRRE, pMD2.G plasmids in addition to the shRNA encoding plasmid. For every 24 h, post-transfection the growth medium was changed. Virus-containing medium was collected after 48 h and 72 h, filtered and titered. Viruses were used to infect WM-266-4 cells at a multiplicity of infection of 2 in the presence of 8 μg/ml polybrene (Sigma-Aldrich). Cells were maintained in the presence of 1 μg/ml puromycin (Sigma-Aldrich) to select the cells that stably express the plasmid containing shRNA and puromycin resistance gene.

4.4 Screening of novel gamma-secretase substrates (I)

HEK293 or MCF-7 cells were transfected with RTK expression plasmids. On the next day, cells were treated with or without 5 μM GSI IX (Calbiochem) for 4 h. The gamma-secretase cleavage was induced with 100 ng/ml phorbol 12-myristate 13-acetate (PMA) (Sigma-Aldrich) for 20 min. Western analysis was used to observe the GSI-stimulated accumulation of C-terminal fragments.

4.5 Primary Antibodies (I-II)

Primary antibodies used in this study are listed in Table 5. Antibodies were used to detect the indicated proteins or their epitope tags by Western blotting, immunoprecipitation, or immunofluorescence.

Table 5. Primary antibodies used in this study. IF immunofluorescence; IP, immunoprecipitation; WB, Western blotting; CST, Cell Signaling Technology; SCBT, Santa Cruz Biotechnology.

ANTIGEN	CAT#	COMPANY	TYPE	APPLICATION	USED IN
Actin	Sc-1616	SCBT	Goat polyclonal	WB	I
Actin	MA1-744	Thermo Fisher Scientific	Mouse monoclonal	WB	II
AXL	8661	CST	Rabbit monoclonal	IF, WB	I
GFP	Sc-9996	SCBT	Mouse monoclonal	WB	I
HA	2367	CST	Mouse monoclonal	WB	I
HSP90	Ab13495	Abcam	Rabbit polyclonal	WB	I
MEK1/2	4694	CST	Mouse monoclonal	WB	I
Na/K ATPase	Ab76020	Abcam	Rabbit monoclonal	WB	I
Phosphotyrosine (4G10)	Mab3090	Upstate	Mouse monoclonal	WB	II
TYRO3	5585	CST	Rabbit monoclonal	IF, WB	I, II
Phospho-AXL/MER/TYRO3	44463	CST	Rabbit monoclonal	WB	II
Tubulin	T7816	Sigma-Aldrich	Mouse monoclonal	WB	
V5	Sc-81594	SCBT	Mouse monoclonal	WB	I
V5	800076	CST	Mouse monoclonal	IF	II
V5	13202	CST	Rabbit monoclonal	IF, IP, WB	II

4.6 Inhibitors (I-II)

The inhibitors used in the study are listed in Table 6.

Table 6. Inhibitors used in the study.

REAGENT	APPLICATION	COMPANY	USED IN
GSI IX	Inhibition of gamma-secretase	Calbiochem	I, II
ALLN (N-Acetyl-Leu-Leu-Nle-Cho)	Inhibition of proteasomes	Calbiochem	I
TAPI-0	Inhibition of ADAM17, ADAM10	Calbiochem	I
PMA (Phorbol 12-myristate 13-acetate)	Stimulation of gamma-secretase cleavage	Calbiochem	I, II

4.7 Immunofluorescence and confocal microscopy (I-II)

Endogenous AXL was detected from A431 cells. The cells were grown on coverslips and treated for 4 h with or without 5 µM GSI IX. Methanol was used to fix the cells.

Cells were stained with anti-AXL (8661; Cell Signaling Technologies) and AlexaFluor 488 goat anti-rabbit (Molecular Probes). Ectopically expressed AXL or TYRO3 were detected from NIH- 3T3 cells that were transfected with GFP-tagged constructs. Cells were cultured on coverslips and 3% paraformaldehyde was used to fix the cells. Cells were permeabilized with 0.1% Triton X-100.

WM-266-4 TYRO3 knock-down cells with ectopic V5-tagged TYRO3 wild-type or TYRO3 cleavage mutant expression were cultured on coverslips and starved without serum overnight. Cells were fixed with 3% paraformaldehyde, and permeabilized with 0.1% Triton X-100. Cells were stained with anti-V5 (13202; Cell Signaling Technologies) and AlexaFluor 555 goat anti-rabbit (Molecular Probes).

The nuclei of the cells were stained with 4',6-diamidino-2-phenylindole (DAPI) (Sigma-Aldrich). Mowiol 40-88 (Sigma-Aldrich) was used to mount the cells on glass slides.

Images were acquired with Zeiss LSM 780 (I) or with Zeiss LSM 880 (II) confocal microscope and Zen software (Zeiss). ImageJ software version 1.51 (I) or version 1.53c (II) was used to analyzed microscopy images. Coloc2 plugin (I) or EzColocalization plugin (II) (Stauffer *et al.*, 2018) was used to analyze colocalization. Nuclear localization of AXL or TYRO3 was estimated by measuring the percentage of AXL- or GFP-specific pixels colocalizing with DAPI of all AXL- or GFP-specific pixels within the cells (I). Nuclear localization of TYRO3 was calculated using Pearson correlation coefficient (Manders *et al.*, 1992) by measuring the V5-specific pixels colocalizing with DAPI (II).

4.8 Gene silencing (I)

Endoribonuclease-prepared siRNA (esiRNA) was used to downregulate the expression of ADAM10, ADAM17, AXL and PSEN1. The esiRNA nucleotides used are listed in Table 7.

Table 7. siRNA and esiRNA oligonucleotides.

TARGET	CAT#	COMPANY	SPECIES	USED IN
Control (e*GFP*)	EHUEGFP	Sigma Aldrich	-	I
ADAM10	EHU129311	Sigma Aldrich	Human	I
ADAM17	EHU075381	Sigma Aldrich	Human	I
AXL	EHU081461	Sigma Aldrich	Human	I
PSEN1	EHU073361	Sigma Aldrich	Human	I

4.9 Cell lysis (I, II)

For Western blotting and immunoprecipitation experiments, cells were lysed using lysis buffer (0.1% Triton X-100, 10 mM Tris-Cl pH 7.4, 1 mM EDTA, 5 mM NaF, 10 µg/ml aprotinin, 10 µg/ml leupeptin, 1 mM Na3VO4, 2 mM phenylmethane sulfonyl fluoride, and 10 mM Na4P2O7). After the lysis, lysates were centrifuged, and the supernatants were used for analyses. Bradford protein assay (Bio-Rad) was used to measure protein concentration of the supernatants.

For mass spectrometry samples, cells were lysed using phosphoproteomics lysis buffer (6 M Guanidine hydrochloride, 100 mM Tris-HCl pH 8.5, 5 mM Tris(2-carboxyethyl)phosphine (TCEP), 10 mM chloroacetamide) or affinity enrichment lysis buffer (70 mM Octyl-β-D-glucopyranoside, 25 mM Tris-HCl pH 7.5, 150 mM NaCl, Pierce protease and phosphatase inhibitor mini tablet according to manufacturer's instructions). After the lysis, lysates were centrifuged, and the supernatants used for analyses. Bradford protein assay (Bio-Rad) was used to measure protein concentration of the supernatants.

4.10 Immunoprecipitation and Western blotting (I-II)

Immunoprecipitation was used in analyses of interaction or post-translational modification (5.5-5.6). Protein G agarose (GE Healthcare) was used to pre-clear cell lysates at 4 °C for 1 hour. Antibodies recognizing the protein of interest and 50 µl protein G agarose were used for immunoprecipitation from pre-cleared cell lysates at 4 °C overnight. To remove non-specific binding, protein G agarose beads were washed with lysis buffer for five times. To elute and denature the precipitated proteins samples were heated at 95 °C for 5 minutes in Laemmli loading buffer.

Western blotting was used to analyze the presence and abundance as well as the phosphorylation of endogenous and ectopically expressed proteins in cell lysates. Immunoprecipitates were analyzed by Western blotting as well. Cell lysate proteins were denatured by heating samples to 95 °C for 5 minutes in Laemmli loading buffer. SDS-PAGE was used to separate equal amounts of samples. After SDS-PAGE, samples were transferred to nitrocellulose membranes. Primary antibodies, as indicated in Table 5, were incubated with the membranes, followed by incubation with either horseradish peroxidase (HRP)-conjugated (Santa Cruz Biotechnology) or IRDye-conjugated (LI-COR) anti-goat, anti-mouse and anti-rabbit secondary antibodies. Actin, HSP90, MEK1/2, RNA polymerase II or tubulin recognizing antibodies were used to control loading. Signals were visualized using the Odyssey CLx imaging system (LI-COR) or enhanced chemiluminescence with SuperSignal West Pico chemiluminescent substrate (Thermo Fischer Scientific).

4.11 Subcellular fractionation (I)

MDA-MB-231 cells were treated with or without 5 μM GSI IX. WM-266-4 TYRO3 knock-down cells with ectopic TYRO3 wild-type or TYRO3 cleavage mutant expression were starved overnight without serum. Subcellular fractionation kit (Cell Signaling Technologies) was used to perform subcellular fractionation according to the manufacturer's instructions. Samples were analyzed by Western blotting.

4.12 Cell proliferation assay (I)

NIH-3T3 cells transfected with RTKs, as indicated in original publication, were plated on 96-well plates at a density of 3000 cells per well in 12 replicates. Cells were grown for 72 h with or without the presence of 5 μM GSI IX in DMEM + 1% FCS. For every 24 h, growth medium was replaced with fresh medium with or without GSI IX. WST-8 reagent (Nippon Genetic) and measurement of absorbance at 450 nm (Thermo Scientific Multiskan FC Microplate Photometer) was used to estimate the number of viable cells.

4.13 Real-time RT-PCR and RNA-sequencing (II)

WM-266-4 TYRO3 knock-down cells were transiently transfected with pEZY-Myc-His plasmids encoding TYRO3 wild-type, TYRO3 ΔGS mutant or TYRO3 ΔADAM mutant. pEZY-Myc-His plasmid encoding GFP was used as a control. In all analyses, WM-266-4 transfectants were starved without serum overnight before cell lysis and total RNA extraction. Total RNA was extracted using NucleoSpin Triprep kit or NucleoSpin RNA Plus kit (Macherey-Nagel) for Real-time RT-PCR and RNA-sequencing, respectively, according to manufacturer's instructions.

The quality of the RNA samples was ensured using Advanced Analytical Fragment Analyzer. The sequencing library was created with 300ng of sample with TruSeq Stranded mRNA HT Kit (Illumina) and indexed with IDT for Illumina TruSeq RNA UD Indices according to manufacturer's protocol. Genome-wide strand specific RNA-sequencing (RNA-seq) was performed at Turku Bioscience center sequencing core with Illumina HiSeq3000 using 75 bp paired-end reading.

For generation of cDNA libraries, reverse transcription was performed using SensiFAST cDNA Synthesis Kit (Bioline) for 1000 ng of total RNA. For the real-time reverse-transcriptase polymerase chain reaction (RT-PCR) analysis of WM-266-4 transfectant samples, qPCR Assay Design tool (Eurofins Genomics) was used to design primers and probes. The primers and probes used are listed in Table 8. *B2M, PPIA, GADPH, GUSB* were used as reference genes from PrimeTime Std qPCR Assays (Integrated DNA Technologies). TaqMan Universal Master Mix II (Thermo Fisher Scientific) was used in the reactions with primers and probes.

Reactions were performed with A QuantStudio 12 K Flex Real-Time PCR System thermal cycler (Thermo Fisher Scientific). Technical triplicates per each biological sample were performed in all reactions.

Table 8. Primers and probes used in RT-PCR reactions

TARGET	SPECIES	LEFT PRIMER	RIGHT PRIMER	PROBE
DLG1	Human	ACCAACTCTTCT TCTCAGCC	GAGGAGAAGATG GAGAAGGAA	CCAGACACCAGCATCTCC AGCCAGATAC
NOL3	Human	GTTGAAGAAAG CGGAGAGTC	CTTGGGACACTTA GGCATTG	TCACGGTACACAGAAGAA GGAACCACCA
MTOR	Human	TGCCTTTGTCAT GCCTTTC	GGAAATGAGGAA ATGGGTTGA	TGAAACTGAAAGATCCAG ACCCTGATCCAAACCC
CMTM7	Human	AATCCCTTCTAC TTCACTCCTC	GTGCATGTGTTTG TGTGTTT	CTTGTGTCTCCTCTCCATC TCTGCCTTTGTT

4.14 Preparation of mass spectrometry samples (II)

WM-266-4 TYRO3 knock-down cells were transiently transfected with pEZY-Myc-His plasmids encoding TYRO3 wild-type, TYRO3 GS mutant or TYRO3 ADAM mutant. pEZY-Myc-His plasmid encoding GFP was used as a control. In all analyses, WM-266-4 transfectants were starved without serum for overnight before cell lysis and proceeding to affinity enrichment or to protein digestion to peptides.

4.14.1 Affinity enrichment

WM-266-4 transfectants were subjected to protein crosslinking with 2 mM dimethyl 3,3'-dithiobispropionimidate (DTBP) for 10 minutes. Crosslinking reaction was quenched with 50 mM Tris-HCl pH 7.5 before cell lysis. Equal amounts of WM-266-4 cell lysates were pre-cleared with Pierce protein G magnetic beads (Thermo Fisher Scientific) at 4 °C for 1 hour and subjected to affinity enrichment with Pierce anti-c-myc magnetic beads (Thermo Fisher Scientific) at 4 °C overnight. Proteins bound to beads were washed five times with 5×TBS-T buffer (125 mM Tris, 750 mM NaCl, 0.25% Tween-20) and one time with water. Proteins were heated at 95 °C for 10 minutes in elution buffer (6 M guanidine hydrochloride, 100 mM Tris-HCl pH 8.5, 10 mM Tris(2-carboxyethyl)phosphine (TCEP), 10 mM chloroacetamide) to elute, denature and alkylate the enriched proteins.

4.14.2 Protein digestion to peptides

Proteins enriched in affinity enrichment or lysed WM-266-4 transfectants were digested with lys-C (New England BioLabs) (enzyme/protein ratio 1:100) for 1 hour

at 37 °C before diluting samples with 50 mM NH_4HCO_3 to ten-fold followed by digestion with trypsin (Thermo Fisher Scientific) (enzyme/protein ratio 1:100) at 37 °C overnight.

4.14.3 Sample desalting

Digested peptides were acidified to a pH 3 with trifluoroacetic acid (TFA) and desalted using Sep-Pak tC18 96-well plate (Waters). Plate was activated with 100% methanol and conditioned with 0.1% TFA, 80% acetonitrile (Thermo Fisher Scientific) before sample binding to the plate. Samples were washed with 0.1% TFA and eluted with 0.1% formic acid, 50% acetonitrile. For total protein analysis, 10% of peptide samples of WM-266-4 transfectants were taken as separate samples. All samples were dried in Hetovac vacuum centrifuge (Heto Lab Equipment) and stored dry in -20 °C until analysis with mass spectrometer.

4.14.4 Phosphopeptide enrichment

Phosphopetides were enriched from desalted and dried peptides using Pierce High-Select TiO_2 phosphopeptide enrichment kit (Thermo Fisher Scientific) according to the manufacturer's instructions. After elution, phosphopeptides were dried with Hetovac vacuum centrifuge and stored as dry in -20 °C until analysis with mass spectrometer.

4.15 Mass spectrometry (II)

Dried peptide samples were resuspended in 0.1% formic acid and sample concentrations were measured using Nanodrop 1000 (Thermo Fisher Scientific). Equal amounts of samples were analyzed on an Easy-nLC 1000 coupled to an Orbitrap Fusion Lumos instrument (Thermo Fisher Scientific). Peptides were loaded on in-house packed 100 µm × 2 cm precolumn packed with ReproSil-Pur 5 µm 200 Å C18-AQ beads (Dr. Maisch Gmbh) using 0.1% formic acid in water (buffer A) and separated by reverse phase chromatography on a 75 µm × 15 cm analytical column packed with ReproSil-Pur 5 µm 200 Å C18-AQ beads (Dr. Maisch). All separations were performed using a 60 min gradient ranging from 8% buffer B (80% acetonitrile in 0.1% formic acid) to 21% in buffer B in 28 min and to 36% buffer B in 22 min and ramped to 100% buffer B in 5 min at flow rate of 300 nl/min. The washout followed at 100% buffer B for 5 min.

All MS spectra were acquired on the orbitrap mass analyzer and stored in centroid mode. For data-dependent acquisition experiments full MS scans were acquired from 300 to 1600 m/z at 120,000 resolution with fill target of 7×10^5 ions

and maximum injection time of 50 ms. The most abundant ions on the full MS scan were selected for fragmentation using 1.6 m/z precursor isolation window and beam-type collisional-activation dissociation (HCD) with 30% normalized collision energy for a cycle time of 3 seconds. MS/MS spectra were collected at 15,000 resolution with fill target of 5×10^4 ions and maximum injection time of 100 ms. Fragmented precursors were dynamically excluded from selection for 35 seconds.

4.16 Protein identification and data analysis (II)

MS/MS spectra were searched with Metamorpheus (version 0.0.304) (Solntsev *et al.*, 2018) against human proteome containing known post-translational modifications (downloaded from Uniprot at 19.2.2019). Mass spectrometry files were calibrated, possible post-translational modifications were searched, and peptides and proteins were identified and quantified using FlashLFQ algorithm (Millikin *et al.*, 2018). Constant modification of cysteine carbamidomethylation was set as constant modification and methionine oxidation was set as variable modification. All other possible modifications were set using G-DPM search in Metamorpheus. Search results were filtered to a 1% FDR at PSM level. Peptides were accepted with search engine score above 5 and with identifications in at least three samples.

4.17 Statistics (I-II)

Cell proliferation data analyses, colocalization data analyses and RT-PCR data analyses were done using R and RStudio (I) or GraphPad Prism (II). ComBat algorithm was used to process the data from cell proliferation assays to remove the batch effect between repeated samples (Johnson *et al.*, 2007). Nonparametric Mann-Whitney U-test (two-group comparisons) or Kruskal-Wallis test (multiple comparisons) were used to calculate P-values and P-values were adjusted using false discovery rate correction, when needed. Results with P-values lower than 0.05 were considered significant. Heatmaps were generated with Morpheus (https://software.broadinstitute.org/morpheus)

4.18 RNAseq and mass spectrometry data analysis (II)

Quality check of the RNAseq reads was done with FastQC (Babraham Bioinformatics). PRINSEQ (Schmieder & Edwards, 2011) and Trimmomatic (Bolger *et al,* 2014) were used for quality and adapter trimming. Pseudoalignment was done with kallisto (v 0.46.0; Bray *et al,* 2016) to human transcriptome (Ensembl

v96; Yates *et al,* 2020) to retrieve TPM (transcripts per million) values. Batchelor package (Haghverdi *et al,* 2018) was used to correct the batch effect between experiment 1 and experiments 2 and 3 and the library size was used to normalize TPM values. DeSeq2 (Love *et al.* 2014) was used for differential expression between the control treatment and different variants of TYRO3.

The sum of intensities of all detected proteins in the sample was used to normalize the interactome, phosphoproteome and proteome data. To estimate the P-value for differential expression from the cumulative density function, a probability density function was fitted with Epanechnikov kernel to median normalized intensities of different treatments.

For further analyses, transcripts, and proteins from proteome and phosphoproteome data with fold change over 1.5 or under -1.5 and FDR adjusted P-value lower or equal than 0.05 were chosen. For interactome data, only proteins with fold change over 1.5 was chosen for further analyses as interactome data contains only positively enriched proteins. The transcripts and proteins significantly different from the control treatment in all TYRO3 variants were considered as full-length TYRO3-mediated signaling. The transcripts and proteins significantly different from the control treatment in the wild-type TYRO3, but not in the non-cleavable variants of TYRO3 were considered as TYRO3 ICD-mediated signaling.

4.19 The inference of regulatory complexes and the combination of them (II)

A combination score was used to determine the pair-wise association between two proteins, phosphosites or transcripts. The combined score is derived from the multiplication of the correlation and the stoichiometry score of the mathematical formulations (II, Figure 1A). Spearman correlation was used calculate the correlation score for all the possible protein, phosphosite or transcript combinations and ranked to derive scores from 1 to 0 in equal increments. The stoichiometry score for all the possible protein, phosphosite or transcript combinations was calculated by dividing the third quartile value (Q_3) of relative abundances with the first quartile (Q_1) value and ranked to derive scores from 1 to 0 in equal increments, similarly. For non-zero-inflated and zero-inflated data, two versions of the stoichiometry score were devised. In the non-zero-inflated version of the stoichiometry score, the relative abundance in the samples where proteins, phosphosites and transcripts are present are only considered. In the zero-inflated version of the stoichiometry score, missing values in the same sample of only one of the protein, phosphosite or transcript is punished by inflating the stoichiometry score and missing values in the same sample of both proteins, phosphosites or transcripts is rewarded by deflating the stoichiometry score.

The regulatory complex inference analysis utilizes the nearest neighbor concept to find the highest scoring (sum of the combined score between all three members) three-member networks for all proteins, phosphosites or transcripts in the list. Next, the regulatory complex inference analysis combines and trims the networks based on common network members and combined scores in the following order:

1. Networks with two common members are combined until additional two complexes with two common members cannot be found.
2. Networks with only one common member are combined if the size of both networks is under than or equal to 4 and the network score is higher than or equal to 2.
3. Networks with two common members are again combined until additional two complexes with two common members cannot be found.
4. If two out of three members are already present in another complex, two out of the three members of the remaining three-member networks are removed.
5. If the remaining three-member networks still have a common member, these three-member networks are joined. A protein, phosphosite or a transcript is allowed to be a member for more than one regulatory complex.

For the combination of the regulatory complexes into larger modules, the same strategy that was used for the derivation of the regulatory complexes in the first place, was used with a few modifications. Regulatory complexed were combined by using the median value of all complex members in each sample. Absolute value of the Spearman correlation was used to allow equal combination of upregulated and downregulated regulatory complexes.

4.20 Validation of regulatory complexes and their combination (II)

STRING, PhosphoSitePlus and ChEA3 databases (Lachmann *et al.*, 2018; Hornbeck *et al.*, 2019; Szklarczyk *et al.*, 2019) were used to acquire data on known protein-protein interactions, kinase substrate phosphosite relationships and transcription factor target gene relationships, respectively. Interactome, phosphoproteome and transcription data acquired from the publications of Batth et al, Karayel et al and ArchS4 database (Batth *et al.*, 2018; Lachmann *et al.*, 2018; Karayel *et al.*, 2020), were used for validations. For the validation score, the sum of all protein-protein interactions, kinase substrate phosphosite relationships or transcription factor target gene relationships in the modelled regulatory complexes was used. The validation

score was compared to the sum of all protein-protein interactions, kinase substrate phosphosite relationships or transcription factor target gene relationships in randomly modelled regulatory complexes of same size as in the modelled data to derive an empirical probability density function from 1000 rounds of simulation. To fit the simulated data into the empirical probability density function, an Epanechnikov kernel was used. The corresponding P-values were drawn from the empirical cumulative distribution function. The complexes were modelled with either correlation score, stoichiometry score or the combined score to assess the effect of different scores on the accuracy of the modelled regulatory complexes. Additionally, the median score of the modelled complexes in different datasets from the one used for the initial modelling was derived to assess the conservation of the different scores in each data type.

Data on annotated signaling pathways was acquired from PathwayCommons (Cerami *et al.*, 2011). The validation data for the combination was acquired from the LinkedOmics database (Vasaikar *et al.*, 2018). A combination of either proteomics, transcriptomics, methylomics, phosphoproteomics, protein array or acetylation data from the same samples were modelled and combined. The sum of co-occurrences of two complex members from two different combined complexes in the same pathway annotation for all the combined complexes was used as a validation score. The validation score was compared to the sum of co-occurrences of two complex members from two different randomly combined complexes in the same pathway annotation for all the combined complexes to derive an empirical probability density function from 10000 rounds of simulation. An Epanechnikov kernel was used to fit the simulated data into the empirical probability density function. The empirical cumulative distribution function was used to draw the corresponding P-values. The conservation of the different scores in regulatory complexes modelled with different scores and combined with different scores was assessed by modelling and combining a dataset and assessing the median score for the combination of the modelled complexes in another dataset.

4.21 Transcription factor prediction (II)

An enrichment analysis to specifically find a transcription factor for each transcriptome regulatory complex was prepared. Annotations from the ChEA3 data resource (Keenan *et al,* 2019) were used. The target gene annotations for the transcription factors present in the dataset with at least 5 transcripts were only considered. The enrichment analysis was created to follow the three steps:

1. The annotation of most enriched in all the members of all the complexes is given to the complexes with highest enrichment score from the annotation (the number of transcripts found in the annotation divided by

the number of transcripts in the complex). The annotation and complexes are removed. The same process is repeated for the remaining dataset until no complex remains. If more than one annotation provides the same overall and complex specific enrichment, all annotations are attached to every complex with equal probability. A P-value for the category fitness of the enrichment is calculated by randomly assigning the same number of transcripts as the size of the complex to the annotation and calculating their respective enrichment. For 10000 rounds of analyzed enrichment from simulated random complexes a probability density function is fitted with an Epanechnikov kernel and the corresponding P-values are drawn from the empirical cumulative distribution function.

2. Secondary transcription factor predictions are made by assessing if the transcription factor assigned to different complexes in the modelled datasets also fit additional regulatory complexes other than the ones to what they have been assigned to, in the first step with the highest enrichment score. If the P-value for the transcription factor assigned during the first step is more than 0.05, the secondary transcription factor is given as the primary transcription factor for that complex. P-values are acquired similarly for the secondary transcription factors. If more than one annotation provides the same complex specific enrichment with a P-value lower than 0.05, all annotations are given with equal probability to the complex.
3. For the remaining unannotated complexes, all annotations are re-searched to find the first one with the highest enrichment score and P-value lower than 0.05 for that complex. If more than one annotation provides the same complex specific enrichment with a P-value lower than 0.05, all annotations are given with equal probability to the complex.

4.22 Subcellular location and function prediction (II)

For the prediction of subcellular location, the annotations of subcellular locations were acquired from the knowledge, experiments and text mining channels of COMPARTMENTS database (Binder *et al,* 2014). The enrichment score (relative frequency) of each annotation for each interactome complex was calculated. To derive a P-value for the enrichment of each annotation in each regulatory complex, 1000 random sets of equal size from all possible proteins identified in the interactome data was drawn. The respective enrichment of each of these randomized sets was derived and an Epanechnikov kernel was used to fit a probability density function to the enrichment scores. The P-values for the enrichment were drawn from

the corresponding empirical cumulative distribution function. Annotations with a P-value lower or equal to 0.05 were considered significant. The subcellular location annotation with a highest enrichment score and lowest P-value were selected.

For the prediction of the biological process involved with the inferred pathway, the Gene Ontology resource (Ashburner *et al,* 2000) annotations for biological processes were acquired from the MSigDB v7.3 (Liberzon *et al*, 2011). The enrichment score (relative frequency) of each annotation for each pathway was calculated. To derive a P-value for the enrichment of each annotation in each pathway, 10000 random sets of equal size from all possible proteins, transcripts and phosphorylated proteins identified as significantly altered in the condition were drawn. The respective enrichment of each of these randomized sets was derived and an Epanechnikov kernel was used to fit a probability density function to the enrichment scores. The P-values for the enrichment were drawn from the corresponding empirical cumulative distribution function. Annotations with a P-value lower or equal to 0.05 were considered significant. The function annotation with a highest enrichment score and lowest P-value were selected. Contextually irrelevant annotations, such as specific functions of certain non-skin tissues or non-melanoma cell types, were ignored.

5 Results

5.1 Screen to identify gamma-secretase cleaved RTKs (I)

RTKs have been reported to undergo gamma-secretase-mediated cleavage (Merilahti and Elenius, 2019). For most of the human RTKs there is no published information on whether they are susceptible to gamma-secretase cleavage.

To identify human RTKs that are subjected to gamma-secretase-mediated cleavage, a human kinome-wide RTK screen was established. The screening was based on the accumulation of membrane bound C-terminal fragments (CTF) of RTKs as a response to gamma-secretase inhibitor (GSI IX) (I, Figure 1B). PMA was used to induce the cleavage as PMA is a known stimulator of shedding (Huovila *et al.*, 2005). Accumulation of CTFs was observed by Western analysis on cells that were transiently transfected with plasmids encoding human C-terminally epitope tagged RTKs. The CTFs with sizes consistent with the expected size of the CTFs were regarded as positive identifications. The screen was successfully validated by analyzing the ERBB family of RTKs (I, Figure 1C). ERBB4 has been documented as the only gamma-secretase substrate among ERBB RTKs (Ni *et al.*, 2001). Consistently, only ERBB4 demonstrated accumulation of CTF in Western analysis.

5.2 Novel gamma-secretase substrates identified (I)

The screen to identify novel gamma-secretase substrates covered 45 out of the 55 human RTKs. Nine RTKs were excluded due to not being adequately expressed in the experimental setup. STYK1 was excluded because our approach was not efficient in detecting cleavage of membrane proteins with very short ectodomains.

In total, 21 RTKs out of the 45 analyzed RTKs were shown to react to GSI treatment with accumulation of CTF (I, Figure 1C, D, Figure 2). Additionally, six RTKs not included in the screen have been previously identified as gamma-secretase substrates (Cai *et al.*, 2006; McElroy *et al.*, 2007; Lyu *et al.*, 2008; Ablonczy *et al.*, 2009; Foveau *et al.*, 2009; Tejeda *et al.*, 2016). All in all, 27 out of 55 human RTKs were identified as gamma-secretase substrates (RTK names in red; I, Figure 2). Our

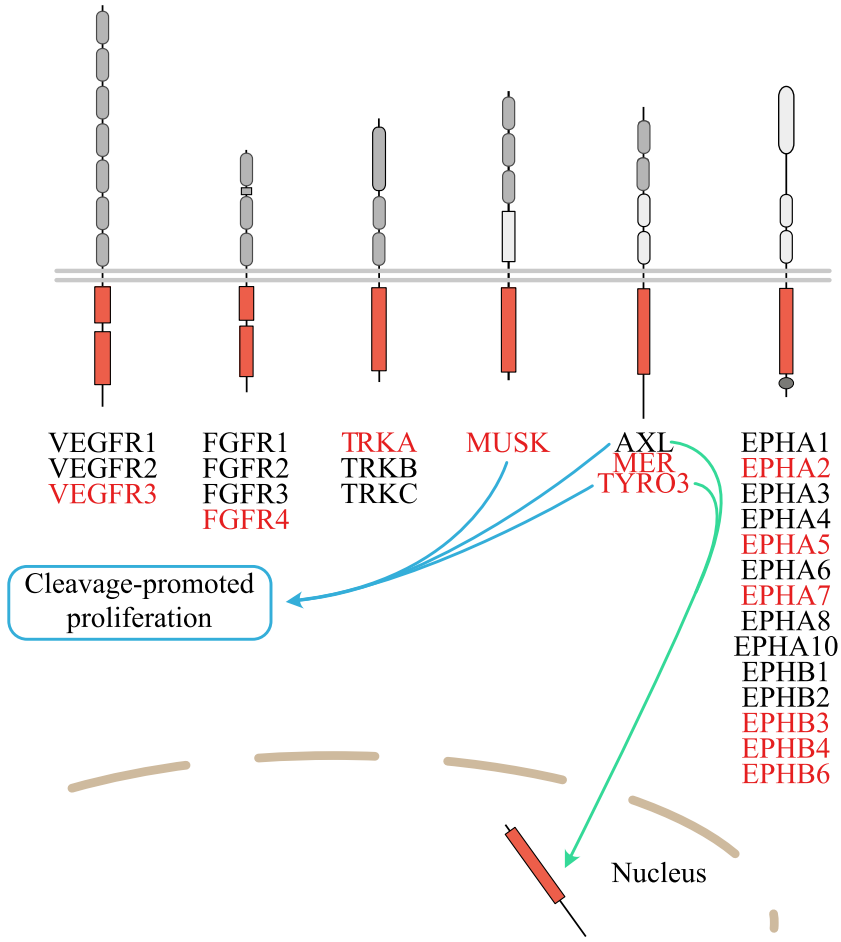

Figure 10. Schematic presentation of RTK families with 12 novel cleavable RTKs. RTKs that were identified as gamma-secretase substrates are indicated in red. Gamma-secretase cleavage-promoted increased cell proliferation was observed with AXL, MER and MUSK. The ICDs of AXL and TYRO3 were observed to localize to cell nucleus.

results identified 12 new gamma-secretase substrates (Figure 10; I, Figure2; RTK names with asterisks) including the whole TAM subfamily (Figure 10). Supporting the validity of the findings, all nine RTKs that had been previously reported to be gamma-secretase substrates, were also identified in the screen (Ni *et al.*, 2001; Wilhelmsen and van der Geer, 2004; Kasuga *et al.*, 2007; Litterst *et al.*, 2007; Marron *et al.*, 2007; Inoue *et al.*, 2009; Degnin *et al.*, 2011; Na *et al.*, 2012; Bae *et al.*, 2015).

5.3 AXL is shed by ADAM10 and cleaved by gamma-secretase (I)

The findings of the gamma-secretase substrate screen were further characterized by experimentation with endogenously expressed AXL in A431, MDA-MB-231 and PC-3 cells. Endogenous AXL was observed to react to treatments with GSI IX or PMA by enhanced CTF accumulation (I, Figure 3A, D). Inhibition of ADAM-mediated shedding by TAPI-0, a chemical ADAM inhibitor, (I, Figure 3A) and by RNA interference of ADAM10 was shown to suppress the cleavage of endogenous AXL, while RNA interference of ADAM17 did not (I, Figure 3B). Additionally, RNA interference targeting presenilin-1 promoted accumulation of CTF similarly to the effect acquired with GSI IX (I, Figure 3C).

Gamma-secretase-cleaved RTK ICDs have been observed to form soluble intracellular signaling units or become degraded in the proteasomes. To characterize the fate of endogenous AXL ICD, MDA-MB231 cells were subjected to proteasome inhibition and to subcellular fractionation to membrane and cytosolic fractions. Inhibition of proteasomal activity resulted in the accumulation of AXL ICD (I, Figure 3D). AXL ICD was observed to be present in the cytosolic fraction and the presence in the cytosol was dependent on gamma-secretase inhibitor GSI IX (I, Figure 3E). The cytosolic ICD fragment was slightly smaller than similarly sized AXL fragment in the membrane fractions. The soluble ICDs are expected to have smaller molecular weight than the membrane-anchored CTF generated by shedding of the ectodomain as the ICDs released as a result of gamma-secretase cleavage lack the transmembrane domain and the extracellular juxtamembrane domain of CTF (I, Figure 1A).

5.4 Growth promoted by the RTKs can be dependent on gamma-secretase-cleavage (I)

In NIH-3T3 fibroblasts, AXL overexpression has been shown to enhance the growth of the cells (O'Bryan *et al.*, 1991; Burchert *et al.*, 1998). The functional significance of cleavage for the novel gamma-secretase substrates identified in our screen was characterized in NIH-3T3 cells. Cells were transfected with plasmids encoding each of the 12 novel gamma-secretase substrates. Cells were cultured in the presence or absence of GSI IX for 72 hours. Growth was analyzed by measuring the number of viable cells using a cell proliferation assay (I, Figure 4A). Ectopic expression of AXL, EPHB6, MUSK, TYRO3 or VEGFR3 significantly promoted growth. Gamma-secretase inhibition suppressed the enhanced growth in the case of TYRO3, AXL and MUSK (Figure 10; I, Figure 4A). The growth of the control cells, or cells expressing other cleavable RTKs was not significantly affected by the gamma-secretase inhibition.

Constructs encoding gamma-secretase cleavage resistant TYRO3 or AXL mutants (TYRO3 ΔGS and AXL ΔGS) were used to validate the functional data acquired from analyses with the chemical inhibitor GSI IX. Expression of a ΔGS mutant of either receptor reduced the growth of transfected NIH-3T3 cells as compared to control cells expressing respective wild-type receptors (I, Figure 4D, Supplemental Figure 2D).

5.5 TYRO3 cleavage mutants and their validation (II)

To further characterize the cleavage-dependent signaling promoted by TYRO3 in a more natural cellular context, WM-266-4 human melanoma cells naturally expressing TYRO3 (II, Supplemental Figure 3) were chosen. To replace the endogenous TYRO3 with cleavage-resistant ectopic mutant receptors, the endogenous TYRO3 was knocked down by TYRO3 targeted shRNA followed by overexpression of different TYRO3 constructs by transfection. In addition to TYRO3 ΔGS construct, an ADAM cleavage-resistant TYRO3 ΔADAM construct was generated. The sites for TYRO3 ΔADAM mutations were designed based on the predicted ADAM10 and ADAM17 cleavage sites (II, Figure 4B).

To validate the functionality of cleavage mutants, WM-266-4 TYRO3 knock-down cells transfected with constructs encoding the TYRO3 ΔGS or TYRO3 ΔADAM mutants were starved overnight in a medium with 0% FCS. Cells were subjected to subcellular fractionation, TYRO3 immunoprecipitation or direct Western analyses. Ectopic expression of TYRO3 wild-type receptor in the background with knocked down endogenous TYRO3 was used as a control. TYRO3 cleavage mutants were tyrosine phosphorylated in a similar manner as wild-type TYRO3 (II, Figure 5B). The phosphorylation of ΔADAM mutant was observed to be slightly higher compared to others.

TYRO3 cleavage mutants were also observed to be localized to cell membrane in subcellular fractionation (II, Supplemental figure 3). As a downstream signaling target, TYRO3 has been shown to activate STAT3 by phosphorylation (Tsai *et al.*, 2020). STAT3 activation via phosphorylation was observed with TYRO3 cleavage mutants and with wild-type TYRO3, indicating similar downstream signaling (II, Figure 5B). Together these results indicated that TYRO3 cleavage mutants were functionally similar to wild-type TYRO3 except for the resistance to ADAM- or gamma-secretase-mediated cleavage.

5.6 Subcellular localization of the ICDs of TYRO3 and AXL (I-II)

Cellular functions linked to gamma-secretase cleavage of RTKs are often associated with the localization of the RTK ICD into the nucleus and its interaction with effectors such as transcription factors (Williams *et al.*, 2004; Paatero *et al.*, 2012). To study whether the gamma-secretase-dependent, cell growth-inducing effects displayed by TYRO3 and AXL were due to nuclear localization of ICDs, NIH-3T3 cells were transfected with constructs encoding TYRO3 and AXL with mutated nuclear localization signals (TYRO3 ΔNLS and AXL ΔNLS) in addition to the respective ΔGS constructs.

NIH-3T3 cells with ectopic expression of ΔGS and ΔNLS mutants of AXL and TYRO3 were imaged with confocal microscopy. Indeed, nuclear localization was observed with wild-type AXL (Figure 10; I, Figure 4B, C). The nuclear localization of AXL was greatly decreased with ΔGS and ΔNLS mutants (I, Figure 4B, C). Similar effect was observed with GSI IX on endogenously expressed AXL in A431 cells (I, Figure 3F, G). In contrast, no significant nuclear localization was observed with wild-type TYRO3, or with its ΔGS and ΔNLS mutants (I, Supplemental Figure 2B, C). AXL and TYRO3 ΔNLS mutants also demonstrated no difference in reduction of growth of transfected NIH-3T3 cells as compared to respective wild-type controls. This indicates that in contrast to gamma-secretase-dependent generation of soluble ICDs, the translocation of the ICD to the nucleus is not necessary for TYRO3- or AXL-promoted growth in NIH-3T3 cells.

Interestingly a C-terminal epitope of TYRO3 was also observed to localize into the cell nucleus in WM-266-4 cells with rescued TYRO3 expression in the background of knocked down endogenous TYRO3 (Figure 10; II, Figure 5C, D). The nuclear localization was observed to be dependent on gamma-secretase cleavage as mutations disrupting ADAM cleavage or gamma-secretase cleavage abolished nuclear localization.

5.7 Comparing signaling by full-length TYRO3 and TYRO3 ICD using cleavage-resistant receptor constructs (II)

In melanoma, at least one of the TAM receptors is usually overactive (Tworkoski *et al.*, 2011). TYRO3 signaling via PI3K/AKT pathway has also been shown to result in increased proliferation of melanoma cells (Zhu *et al.*, 2009; Demarest *et al.*, 2013). In our analyses, TYRO3 was identified as a gamma-secretase substrate and TYRO3-mediated increased proliferation of NIH-3T3 cells was dependent on gamma-secretase cleavage (I). However, the cellular signaling and cellular functions dependent on the RIP-produced soluble TYRO3 ICD are not known.

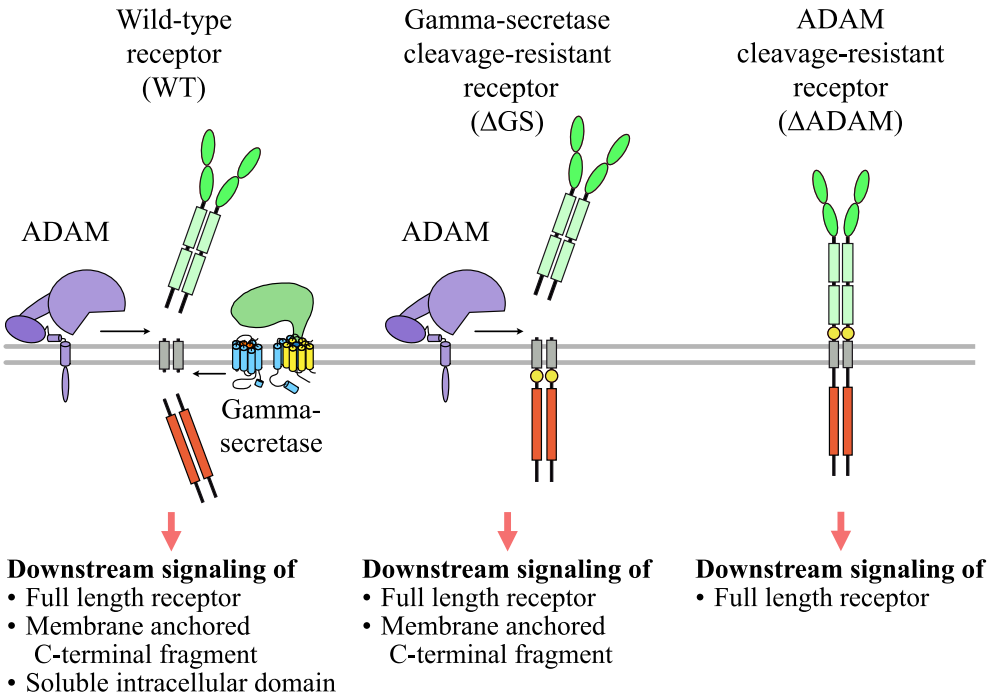

Figure 11. Schematic presentation of the signaling mediated by TYRO3 wild-type and different TYRO3 cleavage mutants. ADAM, a disintegrin and metalloproteinase.

To be able to compare molecular signaling events induced by full-length TYRO3 to signaling promoted by the soluble TYRO3 ICD in the melanoma cell context, the different TYRO3 constructs were expressed in the WM-266-4 cells with knocked-down endogenous TYRO3 expression. Cellular signaling portrayed by wild-type TYRO3 and by both TYRO3 cleavage mutants was considered as signaling mediated by full-length TYRO3 and to contain canonical TYRO3 associated signaling cascades of RTKs. The ΔADAM mutant can only signal by this manner. Cellular signaling portrayed only by wild-type TYRO3 was considered as signaling mediated by TYRO3 ICD (Figure 11).

5.8 Soluble TYRO3 ICD manifests differential TYRO3 phosphorylation as compared to full-length receptor (II)

RTKs are activated by phosphorylation of the kinase domain at specific tyrosine residues (Hubbard and Till, 2000; Lemmon and Schlessinger, 2010). To characterize the phosphorylation status and phosphorylation levels of TYRO3 amino acids, WM-266-4 TYRO3 knock-down cells transiently expressing TYRO3 cleavage mutants

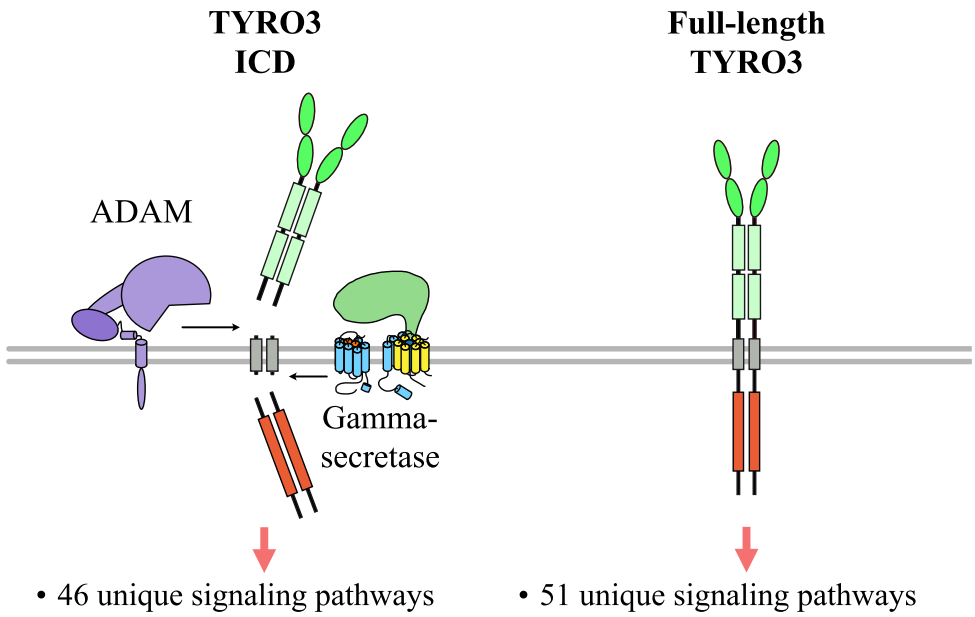

Figure 12. Summary of the differential downstream signaling stimulated by TYRO3 ICD and full-length TYRO3. ADAM, a disintegrin and metalloproteinase; ICD, intracellular domain.

were starved overnight, and phosphorylation status of cellular peptides were identified and quantified using mass spectrometry. Wild-type WM-266-4 cells with endogenous TYRO3 expression were used as a control. Multiple phosphorylation sites were identified including two novel phosphosites (Y742 and Y849) (II, Supplemental Figure 4).

By comparing the data obtained with the different TYRO3 constructs (Figure 11), it was observed that phosphorylation of full-length TYRO3 was relatively increased at the amino acid Y681 while phosphorylation of the soluble TYRO3 ICD was increased at Y742 and Y849 (II, Supplemental Figure 4). Interestingly, differential serine phosphorylation was observed as well. Phosphorylation of full-length TYRO3 was observed to be elevated at amino acid S869 located at the C-terminal tail of TYRO3 and phosphorylation of soluble TYRO3 ICD was observed to be elevated at S472 located at the intracellular juxtamembrane area.

5.9 Differential downstream signaling stimulated by TYRO3 ICD and full-length TYRO3 (II)

To identify downstream signaling events dependent on TYRO3 cleavage, WM-266-4 TYRO3 knock-down cells transiently expressing the TYRO3 cleavage mutants were starved in 0% FCS overnight and subjected to interactome, phosphoproteome, total proteome, and transcriptome analyses (II, Figure 6). The collected different omics datasets were subjected to our novel unbiased analysis method to identify gamma-secretase cleavage-dependent TYRO3 signaling pathways (II, Figure 1B).

Different signaling pathways were observed to be activated by TYRO3 ICD or full-length TYRO3 (Figure 11) In total, 46 pathways were significantly associated with TYRO3 ICD and 51 pathways with the signaling of the full-length TYRO3 (Figure 12; II, Supplemental Table 1, 2). Pathways involving various cellular processes including processes associated with the pathogenesis of cancer were identified (II, Figure 7).

Interestingly, given the role TYRO3 in melanoma by being overly active and mediating suppression of immune responses in cancers (Zhu *et al.*, 2009; Demarest *et al.*, 2013; Graham *et al.*, 2014; Paolino and Penninger, 2016), a notable difference was observed in the number of pathways related to cell growth, cell cycle, cell motility and immune response between the cells expressing the TYRO3 ICD and full-length TYRO3 (Figure 12; II, Figure 7). For example, TYRO3 ICD was observed to regulate a pathway that contained proteins, transcripts and phosphorylation of proteins known to associated with cell motility or cell migration (II, Figure 8A).

The results suggesting that TYRO3 ICD regulates signaling pathways predicted to functionally associate with immune responses (II, Figure 7, Supplemental Figure 6A) were further examined by measuring mRNA expression levels of the separate members of the transcriptional complexes from visualized signaling pathways (II, Supplemental Figure 6A). The mRNA expression levels of *NOL3*, *DLG1, CMTM7* and *mTOR* were measured with real-time RT-PCR from the WM-266-4 cells expressing the different TYRO3 constructs (II, Supplemental Figure 6B). The results indicated that transcription of *NOL3* and *DLG1* was upregulated and transcription of *CMTM7* and *mTOR* was downregulated as a response to TYRO3 ICD signaling as compared to full-length TYRO3 (II, Supplemental Figure 6B). All other differences except the difference in the expression of *mTOR* were statistically significant. These observations are consistent with the results obtained with our analysis method from the collected omics datasets as well as with observations that interferon signaling is often downregulated in melanoma (Alavi *et al.*, 2018).

Full-length TYRO3-associated signaling, but not TYRO3 ICD-associated signaling, was also indicated to upregulate tyrosine phosphorylation of MER at Y682 as well as Rab1B at Y5, Rab11A/B at Y8 and Rab14 at Y8 (II, Figure 8B). In addition

to tyrosine phosphorylation, Rab11B was contained as a part of proteome complex included in the same pathway indicating that the expression of Rab11B is connected to its own phosphorylation (II, Figure 8B). Similarly, in the same pathway proteins and phosphorylation of proteins known to associate with cytoskeleton organization were identified in almost all regulatory complexes (II, Figure 8B). For the most part of these molecules in regulating cell motility or cytoskeleton organization, no interplay has been described, indicating that our unbiased pathway analysis provides identifications of novel signaling modules. Taken together, these results suggested that TYRO3 ICD and full-length TYRO3 activate overlapping as well as unique signaling pathways.

6 Discussion

6.1 Over half of the RTKs are gamma-secretase substrates

Our screen of gamma-secretase-mediated cleavage of RTKs represented the first comprehensive analysis about the prevalence of cleavage among RTKs. In total, 45 out of 55 human RTKs were examined for gamma-secretase-mediated cleavage and 12 RTKs were identified as novel gamma-secretase targets. Moreover, all tested RTKs that had been previously published as gamma-secretase substrates, were also identified to be cleavable. Together with previously published data, the results from the screen indicated that 27 out of the 55 RTKs are cleavable by gamma-secretase. Recently, EPHA3 and ERBB2 have also been identified as gamma-secretase substrates (Javier-Torrent *et al.*, 2019; Liu *et al.*, 2020). In total, over half of the RTKs can be targets for gamma-secretase cleavage. These results indicate that the occurrence of this event is common but not a feature that is universally exploited by every human RTK.

Interestingly neither of the most recently reported gamma-secretase substrates, EPHA3 and ERBB2, were observed as cleavable RTKs in our screen. While positive identifications of gamma-secretase substrates could be gathered from our screen, a screen cannot exclude the non-targets as absolutely non-cleavable. Consistently, there has not been published identifications of proteins that are not substrates for gamma-secretase, besides the exception of integrin beta 1 (Hemming *et al.*, 2008). Additional gamma-secretase substrate identifications are still possible. It is likely that for the novel substrates to be cleaved by gamma-secretase, it would require specific subcellular location or molecular context (Bolduc *et al.*, 2016; Fukumori and Steiner, 2016; Meckler and Checler, 2016; Sannerud *et al.*, 2016). In accordance, both additional gamma-secretase substrate identifications following our screen required specific cellular conditions and specific cells to be subjected to gamma-secretase-mediated RIP (Javier-Torrent *et al.*, 2019; Liu *et al.*, 2020).

No consensus sequence for gamma-secretase cleavage could be identified from additional new substrates identified in our screen. This was in agreement with the previous findings (Beel and Sanders, 2008). The current view is that instead of substrates harboring any specific consensus sequence, the recognition of substrates

is based on a combination of the number of interactions and the strength of interactions between the gamma-secretase and substrate, the length of the remaining receptor following ectodomain shedding, and the relative subcellular localization between gamma-secretase and substrate (Hemming *et al.*, 2008; Funamoto *et al.*, 2013; Bolduc *et al.*, 2016; Meckler and Checler, 2016; Sannerud *et al.*, 2016).

6.2 Inhibition of cleavage as an approach to study gamma-secretase cleavage of substrates

The identified gamma-secretase substrates and functions associated with RTK ICDs have been observed with multiple endogenous and overexpression models *in vitro* and *in vivo.* (Güner and Lichtenthaler, 2020). The majority of experiments regarding RTK ICDs have been done with the aid of inhibitors of gamma-secretase and/or sheddases. We analyzed the effect of gamma-secretase cleavage of 12 novel RTKs identified in our screen for the growth of cells. The transfected cells were cultured with or without the presence of gamma-secretase inhibitor GSI IX. The growth inducing effect of ectopic expression of multiple RTKs was associated with the gamma-secretase cleavage in the cases of MUSK, TYRO3 and AXL.

Although the inhibitors themselves can be specific in inhibition, it is conceivable that some off-target effects might be observed due to gamma-secretase and sheddases having multiple other substrates. Over 150 substrates have been identified for gamma-secretase (Güner and Lichtenthaler, 2020) and over 100 substrates just for ADAM10 and ADAM17 together (Lichtenthaler *et al.*, 2018). Our results did not show any apparent off-target effects of gamma-secretase inhibition as the growth of NIH-3T3 cells without the ectopic expression of cleavable RTKs was not affected by the presence of GSI IX. However, it cannot be overruled that functional consequences observed by the inhibition of components associated with RTK cleavage can be, at least partially, due to combination of the inhibition of the cleavage of other substrates as well.

6.3 Gamma-secretase cleavage mutants as tools for research on cleavage

Some of the experiments regarding subcellular localization of soluble ICDs and functionality of ICDs have been done, in addition to inhibitors of cleavage, with overexpression of ICD constructs containing just the intracellular domain part of the whole RTK (Kasuga *et al.*, 2007; Na *et al.*, 2012; Lu *et al.*, 2017). In principle, overexpression of an ICD construct generates an ectopic protein that is not under the same regulation as endogenously emerging ICDs. Only minute amounts of ICDs are normally generated when compared to the levels of full-length receptors, while

expression from the ICD constructs can be comparable to the expression of full-length RTKs. Thus, it is possible that inaccurate interpretations emerge for the ICD signaling and functionality.

A more advantageous approach to the research of the functionality and localization of soluble ICD, is the usage of mutants against gamma-secretase cleavage. Cleavage-resistant substrates can circumvent the complications associated with other methods by specifically affecting only the cleavage of one substrate and avoiding the creation of additional proteins to cells.

In addition to our work, only few studies exist where cleavage-resistant mutant constructs of RTKs have been used (Vidal *et al.*, 2005; Na *et al.*, 2012; Lu *et al.*, 2017). The likely reason is that no apparent strategy for designing cleavage mutants has been available, as no conserved recognition sequences or conserved cleavage sites have been identified for the gamma-secretase complex. Also, actual identifications of cleavage sites are rare (Litterst *et al.*, 2007; Na *et al.*, 2012; Javier-Torrent *et al.*, 2019). Although cleavage sites are mentioned in publications, often they are only the approximations of the cleavage area (Degnin *et al.*, 2011; Lu *et al.*, 2017), or the proposed cleavage sites are based on the sequence similarities of transmembrane domains to substrates with published, documented cleavage sites. (Vidal *et al.*, 2005; McElroy *et al.*, 2007).

Mutation of sites where gamma-secretase complex is interacting with the substrate (Fukumori and Steiner, 2016; Fukumori *et al.*, 2020) could be a viable strategy for efficient generation of gamma-secretase cleavage-resistant mutants. With our gamma-secretase cleavage mutant of TYRO3 (I449A), the mutation site near the cytoplasmic end of the transmembrane domain is indeed in the area of most prominent interactions with presenilin-1 C-terminal fragment (Fukumori and Steiner, 2016; Fukumori *et al.*, 2020). It can be speculated that although this mutation is not likely at the actual site for gamma-secretase cleavage of TYRO3, this TYRO3 mutant is cleavage-resistant due to attenuation of interactions between the substrate and presenilin. Further possible sites for mutations are located in the extracellular end of the transmembrane domain and in the extracellular juxtamembrane area near the transmembrane domain, where interactions with nicastrin and presenilin N-terminal fragment, and with PEN-2 are observed, respectively (Fukumori and Steiner, 2016; Fukumori *et al.*, 2020).

6.4 Shedding mutants as tools to study soluble ICD signaling

The significance of the first cleavage in the process of generation soluble ICDs, the shedding, is often overlooked when addressing the prevention of cleavage by mutations. Previously only some ADAM cleavage mutants have been generated

(Houri *et al.*, 2013; Chen *et al.*, 2014; Riethmueller *et al.*, 2016; Feuerbach *et al.*, 2017) with none in the context of research on RTK cleavage.

In the context of studying the signaling of soluble ICDs, the prevention of shedding could be more appropriate than the prevention of gamma-secretase cleavage. Shedding is the prequisite for the whole RIP process to proceed and averting the cleavage at the level of shedding essentially locks the RTK in a state of full-length receptor signaling. Hindering the cleavage at the level of gamma-secretase cleavage can lead, in principle, to unwanted non-specific signaling mediated by membrane bound CTFs generated from shedding. These CTFs remain at the membrane longer than normal CTFs as they are not down-regulated by further gamma-secretase cleavage. Normally these constructs are transient intermediate products of RIP with half-life expected to be short.

In contrast to the gamma-secretase complex, both ADAM10 and ADAM17 recognize conserved cleavage site sequences (Tucher *et al.*, 2014). For the substrates with still unknown cleavage sites, ADAM10 and ADAM17 cleavage sites can be predicted abolishing the need to experimentally identify the sites of shedding. In this study, shedding mutants, based on prediction of possible cleavage sites in TYRO3, were generated and were functionally verified to be cleavage resistant.

The most advanced approach and closest to preserving the endogenous functionality and regulation of the target protein, would be to use the ADAM cleavage mutants in combination with the CRISPR (clustered regularly interspaced short palindromic repeats) technique (Cong *et al.*, 2013). This would enable the creation of RIP resistant endogenous version of the respective receptor.

6.5 Variability in the nuclear localization of TYRO3 ICD

Nuclear localization of soluble ICDs have been observed for multiple RTKs. Additionally, biological functions associated with soluble RTK ICDs are often associated with the nuclear localization of the ICD (Muraoka-Cook *et al.*, 2006; Sardi *et al.*, 2006; Lyu *et al.*, 2008; Hoeing *et al.*, 2011). Our results indicated that TYRO3 ICD translocates to the nucleus following the gamma-secretase cleavage in WM-266-4 cells. This localization was not observed with ectopic expression in NIH-3T3 cells, although nuclear localization was observed with another TAM RTK, AXL. Endogenous expression of TYRO3 is very low in NIH-3T3 cells (Yanagihashi *et al.*, 2017) while AXL is expressed at high level. It is plausible that factors governing nuclear localization depend on the context of the cellular background. Nuclear translocation could require specific conditions tailored for each molecule. Similarly, specific conditions or specific cell types have been observed to be a

requirement the cleavage of some RTKs (Javier-Torrent *et al.*, 2019; Liu *et al.*, 2020).

6.6 Differences in phosphorylation between the full-length TYRO3 and TYRO3 ICD

Tyrosine phosphorylation has been identified as an absolute requirement for functionality and activation of RTKs (Hubbard and Till, 2000; Lemmon and Schlessinger, 2010). In our phosphoproteomic analyses, full-length TYRO3 and soluble TYRO3 ICD were observed to be differentially phosphorylated mainly at the phosphosites of tyrosine residues. Tyrosine phosphorylation of full-length TYRO3 was observed to be elevated at amino acid Y681, while tyrosine phosphorylation of soluble TYRO3 ICD was elevated at amino acids Y742 and Y849. The Y681 is the proposed conserved TYRO3 autophosphorylation site located in the activation loop of kinase domain. However, this site has only been identified through sequence similarity with other TAM RTKs (Ling *et al.*, 1996; Linger *et al.*, 2008; Onken *et al.*, 2017). The phosphorylation of this site is required for full kinase activation. This indicates that full-length TYRO3 signals through canonical RTK signaling, as was to be expected. The novel phosphorylation site Y742 lies in the area harboring additional autophosphorylation sites indicating similar functionality in the activation of TYRO3 (Shao *et al.*, 2017). Y849 is located in the C-terminal tail of TYRO3 that contains the interactions sites for SH2 containing downstream signaling proteins, such as Grb2 or p85, that have shown to be phosphorylated by TAM RTKs (Braunger *et al.*, 1997; Goruppi *et al.*, 1997; Georgescu *et al.*, 1999; Weinger *et al.*, 2008).

The knowledge on the functionality of serine and threonine residues that are also subject to modification by phosphorylation, is quite limited for RTKs. Serine phosphorylation of RTKs have been implicated to be connected to downregulation of RTK activity. Especially, elevated phosphorylation of serine residues at the intracellular juxtamembrane area and C-terminal tail of RTKs are associated with a decrease in the kinase activity of EGFR, ERBB4, IGF1R, INSR, MET and PDGRB RTKs (Gandino *et al.*, 1994; Lewis *et al.*, 1994; Barbier *et al.*, 1999; Bioukar *et al.*, 1999; Feinmesser *et al.*, 1999; Kelly *et al.*, 2012; Haryuni *et al.*, 2019). Our phosphoproteomic results indicated that serine phosphorylation of full-length TYRO3 was elevated at amino acid S869 located at the C-terminal tail and serine phosphorylation of soluble TYRO3 ICD was elevated at S472 located at the intracellular juxtamembrane area. Whether the phosphorylation of these residues contribute to the downregulation of TYRO3 kinase activity is not known and requires further experimentation.

6.7 Unbiased identification of gamma-secretase cleavage-dependent TYRO3 signaling cascades using multiomics data

Gamma-secretase-mediated cleavage of RTKs creates an additional layer of signaling for RTKs. In contrast to canonical RTK signaling cascades, soluble ICDs themselves can translocate to various cellular compartments such as the nucleus and mediate signaling (Merilahti and Elenius, 2019; Güner and Lichtenthaler, 2020). Gamma-secretase mediated cleavage of RTKs was identified 20 years ago by identification of ERBB4 cleavage and nuclear localization of its ICD (Ni *et al.*, 2001). To date, 29 RTKs have been identified as gamma-secretase substrates but very little is still known about the biological functions associated with the RIP of RTKs. Most of the functions for RTK ICDs have been identified by experiments considering ERBB4.

The research on cell signaling pathways using different omics methods has created the need for accurate modeling of the large amount of data that has been acquired to gain better understanding of cellular signaling events. Here we created a novel unbiased method to interpret signaling pathways from one-time-point multiomics data (II, Figure 1, 2, 3). Gamma-secretase cleavage-associated signaling of TYRO3 was used as an example for such data analysis approach.

Most analysis methods are based on the previous knowledge and include the gene set enrichment analysis (Subramanian *et al.*, 2005) and multiple topology-based methods that use previous data to infer pathway networks (Ma *et al.*, 2019).

Modeling that is based on previous knowledge has some major caveats:

1. Previous knowledge is often incomplete so that available databases do not contain all the observed genes, proteins, transcripts, or post-translational modifications.
2. The uneven acquirement of previous knowledge leads to skewed results that favor already discovered and extensively researched relationships.
3. Molecular associations are often context-dependent indicating that the associations found in a different context may not universally apply.

Robust methods that are independent on previous knowledge have been mainly based on the correlation between different genes, proteins, transcripts, and post-translational modifications (Langfelder and Horvath, 2008; Care *et al.*, 2019). More sophisticated methods that utilize machine learning such as regressions, Bayesian networks and ODE models only solve single molecular association problems such as gene regulatory networks (Chen and Mar, 2018; Pratapa *et al.*, 2020). Most accurate interpretations of the cellular signaling have been acquired with methods

that are tracking the changes in time-course data (Chen and Mar, 2018; Köksal *et al.*, 2018), but the availability of this kind of data is often limited.

The results acquired from our multiomics analyses indicate that without prior knowledge about the signaling of soluble TYRO3 ICD, relevant biological associations can be identified. Moreover, cellular signaling known to be mediated by the full-length TYRO3, such as activation of STAT signaling (Lemke and Rothlin, 2008; Mirea *et al.*, 2020), was observed in these analyses, indicating the validity of the acquired TYRO3 results. The advantages of our analysis method include its independence on previous knowledge, robustness, making it easily scalable to other omics data types and low computational demand.

Since the unbiased multi-omics pathway analysis is based on the inherent variation between samples in the omics data, the quality of the omics data is a limiting factor to the analysis. If the data contains a lot of technical variation, missing values and lacks repetitions, it will lead to loss of model accuracy. The nonparametric formulation and a zero inflated version of the stoichiometry score were devised to aid solving two of these limitations. Additionally, the choice of cut-offs for the data to be modelled will affect the final modelled pathways as the correlation, stoichiometry and combined scores are ranked and hence dependent on the choice of the signaling molecules included in the dataset. Moreover, including or omitting proteins, phosphosites or transcripts from the data used for the analysis will have an influence on the interpreted final pathways. For accurate interpretation of the multiomics pathways, the multiomics data should be acquired from the same samples.

6.8 Differential signaling of TYRO3 ICD and full-length TYRO3

Signaling pathways observed to be differentially regulated by TYRO3 ICD and full-length TYRO3 contained pathways with predicted functions in cell growth, cell cycle, cell motility and adhesion, immune response, chromosome organization, cell death and cell differentiation. Many of these functions are connected to the progression and therapeutic response of melanoma or are regulated by TYRO3-mediated signaling. For example, TYRO3 has been indicated to have a role in the proliferation, tumorigenesis, and invasion of melanoma cells (Zhu *et al.*, 2009; Tworkoski *et al.*, 2011; Demarest *et al.*, 2013; Shao *et al.*, 2018).

The *NOL3, DLG1* and *CMTM7* genes that were identified to be transcriptionally regulated by TYRO3 ICD have not been previously identified to have a role in melanoma. Nevertheless, it can be mentioned that high expression of NOL3 (https://www.proteinatlas.org/ENSG00000140939-NOL3/pathology/melanoma) and DLG1 (https://www.proteinatlas.org/ENSG00000075711-DLG1/pathology/melanoma)

in addition to low expression of CMTM7 (https://www.proteinatlas.org/ENSG00000153551-CMTM7/pathology/melanoma) associate with poor survival in melanoma (Uhlen *et al.*, 2017). These results indicate that the formation of TYRO3 ICD and the effects the ICD manifests on gene expression might affect the aggressiveness of melanoma.

Interestingly, full-length TYRO3-associated tyrosine phosphorylation was observed with the MER RTK and the Rab proteins 1B, 11A/B, and 14. The MER tyrosine phosphorylation site is conserved among RTKs and is linked to activation of MERTK (Schulze *et al.*, 2005; Sugiyama *et al.*, 2019), suggesting that MER is activated by TYRO3. Tyrosine phosphorylation is rarely observed with Rab proteins (Waschbüsch and Khan, 2020). Only Rab7, Rab24 and Rab34 have been indicated to be subjects for tyrosine phosphorylation, These Rab proteins have suggested roles in regulation of membrane protein recycling (Ding *et al.*, 2003; Lin *et al.*, 2017; Sun *et al.*, 2018). The Rab proteins Rab1, Rab14 and Rab11 are involved in trafficking from ER to Golgi, Golgi to endosome and recycling endosome to plasma membrane, respectively (Hutagalung & Novick, 2011). These results indicate that full-length TYRO3 signaling could take part in receptor crosstalk, by activation of other TAMs and in membrane trafficking of TYRO3 itself.

This research represents the first study on the gamma-secretase cleavage-dependent signaling of TYRO3 ICD and provides an important first step for studying the gamma-secretase cleavage associated RTK signaling on a systemic level. Future experimentation should involve the validation of the acquired results. In addition, the systemic level approach, as presented in this study, should be expanded to other cleavable RTKs. This would allow the identification of possible common signaling themes and further advance the knowledge on gamma-secretase cleavage-mediated signaling of RTKs.

6.9 Biological relevance of the findings

The majority of the cleavable RTKs have no identified cellular function for their soluble ICDs. Additional research is also needed for the expansion of our current understanding of RTK ICD signaling that is largely based on studies on one RTK, ERBB4 (Carpenter and Liao, 2013; Merilahti and Elenius, 2019). Furthermore, the knowledge about the biological relevance of gamma-secretase-mediated cleavage of RTKs is mostly based on *in vitro* observations (Merilahti and Elenius, 2019; Güner and Lichtenthaler, 2020). Therefore, comprehensive *in vivo* validations of the *in vitro* findings are needed. Additional identifications of regulatory mechanisms critical for the cleavage could greatly advance this objective, as specific genetic and molecular interferences with the cleavage event would be more achievable.

In addition, our understanding of the regulation of substrate identification and functionality of gamma-secretase complex is almost solely based on the research focused on APP and Notch cleavage (Wolfe, 2020). Verification of these findings among RTKs could provide a better selection of tools for the development of treatments that specifically target the gamma-secretase-mediated cleavage of RTKs. A better understanding of the mechanisms on how gamma-secretase substrates are identified and distinguished from nonsubstrates, is also needed for the development of more specific inhibitors against RTK cleavage (Golde *et al.*, 2013; McCaw *et al.*, 2020).

7 Conclusions

This thesis aimed to characterize an additional signaling mechanism for RTKs: the gamma-secretase-mediated cleavage of RTKs. The focus was on finding the prevalence of this cleavage process among RTKs and on characterizing molecular signaling events specifically stimulated by the gamma-secretase-mediated cleavage. TAM receptors, in particular TYRO3, were used as examples of RTKs with previously unknown roles as targets for gamma-secretase cleavage.

Based on the results of this study, following conclusions can be made:

1. Gamma-secretase cleavage is common for RTKs. Over half of the RTKs are currently identified as gamma-secretase substrates.
2. Soluble RTK ICDs, generated from gamma-secretase cleavage, exert biological functionality such as regulation of cellular growth.
3. The signaling that is associated with the soluble RTK ICDs after gamma-secretase cleavage is different from signaling associated with the full-length receptors. Indications for this were observed by studying TYRO3 signaling in melanoma cells.

Together these results provide new insights into gamma-secretase-mediated cleavage of RTKs. The findings of this thesis, the identified molecular mechanisms, and the prevalence of cleavage among RTKs, can provide new understanding on the processes that regulate biological functions of RTKs in both healthy tissues and cancer.

Acknowledgements

The work for this study was performed in the MediCity Research Laboratories at the Institute of Biomedicine of the University of Turku. I thank the director of MediCity Research Laboratories, Professor Sirpa Jalkanen for providing the excellent facilities and environment for research.

I wish to express my deepest gratitude to my supervisor, Professor Klaus Elenius for his invaluable guidance, support, and encouragement throughout the PhD process. I highly appreciate your expertise and commitment to this work, and I have enjoyed working under your supervision through these years.

I am deeply grateful for Professors Jyrki Heino, Mark Johnson, and docent Arto Pulliainen, members of my thesis follow-up committee, for their interest and insight provided for my projects over the years. Professors Cecilia Sahlgren and Matti Nykter are warmly thanked for the thorough review of my thesis manuscript and providing valuable feedback.

I would like to express my gratefulness to Turku Doctoral Programme of Molecular Medicine (TuDMM) for providing educational support during my doctoral training. I want to thank the director of doctoral programme Professor Kati Elima as well as coordinator Eeva Valve and former doctoral programme secretary Nina Widberg for their valuable work at running the doctoral programme. Additionally, I would like to thank the doctoral programme for providing many delightful social events, and fellow PhD students in the doctoral programme for an important source of peer support during my PhD project.

The Finnish Cultural Foundation, Jenny and Antti Wihuri Foundation, the K. Albin Johanssons stiftelse, the Southwest Finland Cancer Association, Cancer Society of Finland, the Orion Research Foundation, and Turku University Foundation are specially acknowledged for financial support and travel grants, which allowed me to focus full-time on my thesis work and enabled me to connect with fellow researchers around the world.

I am truly thankful for all my co-authors Anna Knittle, Veera Ojala, Arto Pulliainen and Katri Vaparanta for successful and effective collaboration. Without your contribution, this work could not have been possible.

I want to express my gratitude to present and former members of the Elenius lab, Kaisa Aalto, Deepankar Chakroborty, Juho Heliste, Maria Helkkula, Anne Jokilammi, Peppi Kirjalainen, Anna Knittle, Marika Koivu, Maarit Kortesoja, Kari Kurppa, Matias Mäenpää, Elli Narvi, Janne Nordberg, Veera Ojala, Ilkka Paatero, Arto Pulliainen, Fred Saarinen, Minna Santanen, Mika Savisalo, Jori Torkkila, Maria Tuominen, Katri Vaparanta, and Ville Veikkolainen. I also want to thank the present and former Heino lab members in Medicity, Abbi, Camilla, Elina, Johanna, Kalle, Maria S., Marjaana O., Marjaana P., Noora and Salli, and other fellow PhD colleagues as well. We have shared countless coffee breaks, scientific and non-scientific discussions, and social events during the past years. It has been such a joy working with you and to get to know you as a person.

Maria Tuominen and Turku Bioscience staff of Turku Proteomics Facility Anne Rokka, Arttu Heinonen, Mirva Pääkkönen and Pekka Haapaniemi are thanked for excellent technical assistance.

My sincerest thanks go to my family and friends, for always believing in me and supporting me in my choises and for contributing greatly to the quality of life during my PhD journey. I want to thank my parents Juha and Paula for encouraging me to pursuit my interest. I want to thank my parents and my brother Tuomas and his family for all support and love you have shown throughout the years.

Finally, I thank my wife Pirjo for always supporting and loving and encouraging me in everything I do. I also especially want to thank you for keeping me stocked with the best pulla. I also want to thank our daughters Aada and Aino: you provide me with love, comfort, and joy for the life beyond the work.

June 2021

Johannes Merilahti

References

Abboud-Jarrous, G, Priya, S, Maimon, A, Fischman, S, Cohen-Elisha, M, Czerninski, R, and Burstyn-Cohen, T (2017). Protein S drives oral squamous cell carcinoma tumorigenicity through regulation of AXL. Oncotarget 8, 13986–14002.

Ablonczy, Z, Prakasam, A, Fant, J, Fauq, A, Crosson, C, and Sambamurti, K (2009). Pigment epithelium-derived factor maintains retinal pigment epithelium function by inhibiting vascular endothelial growth factor-R2 signaling through gamma-secretase. J Biol Chem 284, 30177–30186.

Ashburner M, Ball CA, Blake JA, Botstein D, Butler H, Cherry JM, Davis AP, Dolinski K, Dwight SS, Eppig JT, et al (2000) Gene ontology: Tool for the unification of biology. Nat Genet 25: 25–29.

Alavi, S, Stewart, AJ, Kefford, RF, Lim, SY, Shklovskaya, E, and Rizos, H (2018). Interferon signaling is frequently downregulated in melanoma. Front Immunol 9.

Allen, HL et al. (2010). Hundreds of variants clustered in genomic loci and biological pathways affect human height. Nature 467, 832–838.

Arasada, RR, and Carpenter, G (2005). Secretase-dependent Tyrosine Phosphorylation of Mdm2 by the ErbB-4 Intracellular Domain Fragment. J Biol Chem 280, 30783–30787.

Avilla, E, Guarino, V, Visciano, C, Liotti, F, Svelto, M, Krishnamoorthy, GP, Franco, R, and Melillo, RM (2011). Activation of TYRO3/AXL tyrosine kinase receptors in thyroid cancer. Cancer Res 71, 1792–1804.

Bache, KG, Slagsvold, T, and Stenmark, H (2004). Defective downregulation of receptor tyrosine kinases in cancer. EMBO J 23, 2707–2712.

Bae, SY, Hong, J-Y, Lee, H-J, Park, HJ, and Lee, SK (2015). Targeting the degradation of AXL receptor tyrosine kinase to overcome resistance in gefitinib-resistant non-small cell lung cancer. Oncotarget 6, 10146–10160.

Bai, XC, Yan, C, Yang, G, Lu, P, Ma, D, Sun, L, Zhou, R, Scheres, SHW, and Shi, Y (2015). An atomic structure of human γ-secretase. Nature 525, 212–217.

Barbier, AJ, Poppleton, HM, Yigzaw, Y, Mullenix, JB, Wiepz, GJ, Bertics, PJ, and Patel, TB (1999). Transmodulation of epidermal growth factor receptor function by cyclic AMP-dependent protein kinase. J Biol Chem 274, 14067–14073.

Bateman A, Martin MJ, Orchard S, Magrane M, Agivetova R, Ahmad S, Alpi E, Bowler-Barnett EH, Britto R, Bursteinas B, et al (2021) UniProt: The universal protein knowledgebase in 2021. Nucleic Acids Res 49: D480–D489

Batth, TS, Papetti, M, Pfeiffer, A, Tollenaere, MAX, Francavilla, C, and Olsen, J V. (2018). Large-Scale Phosphoproteomics Reveals Shp-2 Phosphatase-Dependent Regulators of Pdgf Receptor Signaling. Cell Rep 22, 2784–2796.

Bax, D V., Messent, AJ, Tart, J, Van Hoang, M, Kott, J, Maciewicz, RA, and Humphries, MJ (2004). Integrin α5β1 and ADAM-17 interact in vitro and co-localize in migrating HeLa cells. J Biol Chem 279, 22377–22386.

Beel, a J, and Sanders, CR (2008). Substrate specificity of gamma-secretase and other intramembrane proteases. Cell Mol Life Sci 65, 1311–1334.

Bennett, EP, Mandel, U, Clausen, H, Gerken, TA, Fritz, TA, and Tabak, LA (2012). Control of mucin-type O-glycosylation: A classification of the polypeptide GalNAc-transferase gene family. Glycobiology 22, 736–756.

Berclaz, G, Altermatt, HJ, Rohrbach, V, Kieffer, I, Dreher, E, and Andres, A-C (2001). Estrogen dependent expression of the receptor tyrosine kinase axl in normal and malignant human breast. Ann Oncol 12, 819–824.

Bernhofer, M, Kloppmann, E, Reeb, J, and Rost, B (2016). TMSEG: Novel prediction of transmembrane helices. Proteins Struct Funct Bioinforma 84, 1706–1716.

Binder JX, Pletscher-Frankild S, Tsafou K, Stolte C, O'Donoghue SI, Schneider R & Jensen LJ (2014) COMPARTMENTS: unification and visualization of protein subcellular localization evidence. Database 2014: bau012–bau012

Bioukar, EB, Marricco, NC, Zuo, D, and Larose, L (1999). Serine phosphorylation of the ligand-activated β-platelet-derived growth factor receptor by casein kinase I-γ2 inhibits the receptor's autophosphorylating activity. J Biol Chem 274, 21457–21463.

Blume-Jensen, P, and Hunter, T (2001). Oncogenic kinase signalling. Nature 411, 355–365.

Bolduc, DM, Montagna, DR, Gu, Y, Selkoe, DJ, and Wolfe, MS (2016). Nicastrin functions to sterically hinder γ-secretase–substrate interactions driven by substrate transmembrane domain. Proc Natl Acad Sci 113, E509–E518.

Bolger AM, Lohse M & Usadel B (2014) Trimmomatic: A flexible trimmer for Illumina sequence data. Bioinformatics 30: 2114–2120

Bonacchi, A et al. (2008). Nuclear localization of TRK-A in liver cells. Histol Histopathol 23, 327–340.

Boregowda, RK et al. (2016). The transcription factor RUNX2 regulates receptor tyrosine kinase expression in melanoma. Oncotarget 7, 29689–29707.

Bosurgi, L, Bernink, JH, Cuevas, VD, Gagliani, N, Joannas, L, Schmid, ET, Booth, CJ, Ghosh, S, and Rothlin, C V. (2013). Paradoxical role of the proto-oncogene Axl and Mer receptor tyrosine kinases in colon cancer. Proc Natl Acad Sci U S A 110, 13091–13096.

Botticelli, A, Zizzari, I, Mazzuca, F, Ascierto, PA, Putignani, L, Marchetti, L, Napoletano, C, Nuti, M, and Marchetti, P (2017). Cross-talk between microbiota and immune fitness to steer and control response to anti PD-1/PDl-1 treatment. Oncotarget 8, 8890–8899.

Boumahdi, S, and de Sauvage, FJ (2020). The great escape: tumour cell plasticity in resistance to targeted therapy. Nat Rev Drug Discov 19, 39–56.

Boutros, C et al. (2016). Safety profiles of anti-CTLA-4 and anti-PD-1 antibodies alone and in combination. Nat Rev Clin Oncol 13, 473–486.

Braunger, J, Schleithoff, L, Schulz, AS, Kessler, H, Lammers, R, Ullrich, A, Bartram, CR, and Janssen, JWG (1997). Intracellular signaling of the Ufo/Axl receptor tyrosine kinase is mediated mainly by a multi-substrate docking-site. Oncogene 14, 2619–2631.

Bray NL, Pimentel H, Melsted P & Pachter L (2016) Near-optimal probabilistic RNA-seq quantification. Nat Biotechnol 34: 525–527.

Brown, MS, Ye, J, Rawson, RB, and Goldstein, JL (2000). Regulated intramembrane proteolysis: a control mechanism conserved from bacteria to humans. Cell 100, 391–398.

Brown JE, Krodel M, Pazos M, Lai C & Prieto AL (2012) Cross-phosphorylation, signaling and proliferative functions of the Tyro3 and Axl receptors in Rat2 cells. PLoS One 7: 1–11

Burchert, a, Attar, EC, McCloskey, P, Fridell, YW, and Liu, ET (1998). Determinants for transformation induced by the Axl receptor tyrosine kinase. Oncogene 16, 3177–3187.

Burstyn-Cohen, T, and Maimon, A (2019). TAM receptors, Phosphatidylserine, inflammation, and Cancer. Cell Commun Signal 17, 156.

Caescu CI, Jeschke GR & Turk BE (2009) Active-site determinants of substrate recognition by the metalloproteinases TACE and ADAM10. Biochem J 424: 79–88.

Cai, J, Jiang, WG, Grant, MB, and Boulton, M (2006). Pigment epithelium-derived factor inhibits angiogenesis via regulated intracellular proteolysis of vascular endothelial growth factor receptor 1. J Biol Chem 281, 3604–3613.

Cai, J, Wu, L, Qi, X, Li Calzi, S, Caballero, S, Shaw, L, Ruan, Q, Grant, MB, and Boulton, ME (2011). PEDF regulates vascular permeability by a γ-secretase-mediated pathway. PLoS One 6, e21164.

Care, MA, Westhead, DR, and Tooze, RM (2019). Parsimonious Gene Correlation Network Analysis (PGCNA): a tool to define modular gene co-expression for refined molecular stratification in cancer. Npj Syst Biol Appl 5, 1–17.

Carpenter, G, and Liao, HJ (2013). Receptor tyrosine kinases in the nucleus. Cold Spring HarbPerspectBiol 5, a008979.

Carvalho, S, Levi-Schaffer, F, Sela, M, and Yarden, Y (2016). Immunotherapy of cancer: From monoclonal to oligoclonal cocktails of anti-cancer antibodies: IUPHAR Review 18. Br J Pharmacol 173, 1407–1424.

Cerami, EG, Gross, BE, Demir, E, Rodchenkov, I, Babur, Ö, Anwar, N, Schultz, N, Bader, GD, and Sander, C (2011). Pathway Commons, a web resource for biological pathway data. Nucleic Acids Res 39, 685–690.

Chang, W-H et al. (2017). Smek1/2 is a nuclear chaperone and cofactor for cleaved Wnt receptor Ryk, regulating cortical neurogenesis. Proc Natl Acad Sci, 201715772.

Che Mat, MF, Murad, NAA, Ibrahim, K, Mokhtar, NM, Ngah, WZW, Harun, R, and Jamal, R (2016). Silencing of PROS1 induces apoptosis and inhibits migration and invasion of glioblastoma multiforme cells. Int J Oncol 49, 2359–2366.

Chen, AC, Kim, S, Shepardson, N, Patel, S, Hong, S, and Selkoe, DJ (2015). Physical and functional interaction between the α- and γ-secretases: A new model of regulated intramembrane proteolysis. J Cell Biol 211, 1157–1176.

Chen, C Di, Tung, TY, Liang, J, Zeldich, E, Tucker Zhou, TB, Turk, BE, and Abraham, CR (2014). Identification of cleavage sites leading to the shed form of the anti-aging protein klotho. Biochemistry 53, 5579–5587.

Chen, S, and Mar, JC (2018). Evaluating methods of inferring gene regulatory networks highlights their lack of performance for single cell gene expression data. BMC Bioinformatics 19, 232.

Cheon, H, Borden, EC, and Stark, GR (2014). Interferons and their stimulated genes in the tumor microenvironment. Semin Oncol 41, 156–173.

Cheon, HJ, and Stark, GR (2009). Unphosphorylated STAT1 prolongs the expression of interferon-induced immune regulatory genes. Proc Natl Acad Sci U S A 106, 9373–9378.

ClinicalTrials.gov (2020). Https://ClinicalTrials.gov. U.S. National Library of Medicine. Available at: https://clinicaltrials.gov/. Accessed December 20, 2020.

Cong, L et al. (2013). Multiplex genome engineering using CRISPR/Cas systems. Science 339, 819–823.

Cook, RS et al. (2013). MerTK inhibition in tumor leukocytes decreases tumor growth and metastasis. J Clin Invest 123, 3231–3242.

Craven, RJ, Xu, L, Weiner, TM, Fridell, Y -W, Dent, GA, Srivastava, S, Varnum, B, Liu, ET, and Cance, WG (1995). Receptor tyrosine kinases expressed in metastatic colon cancer. Int J Cancer 60, 791–797.

Degnin, CR, Laederich, MB, and Horton, WA (2011). Ligand activation leads to regulated intramembrane proteolysis of fibroblast growth factor receptor 3. Mol Biol Cell 22, 3861–3873.

Demarest, SJ et al. (2013). Evaluation of Tyro3 expression, Gas6-mediated akt phosphorylation, and the impact of anti-Tyro3 antibodies in melanoma cell lines. Biochemistry 52, 3102–3118.

Ding, J, Soule, G, Overmeyer, JH, and Maltese, WA (2003). Tyrosine phosphorylation of the Rab24 GTPase in cultured mammalian cells. Biochem Biophys Res Commun 312, 670–675.

Dombernowsky, SL et al. (2015). The sorting protein PACS-2 promotes ErbB signalling by regulating recycling of the metalloproteinase ADAM17. Nat Commun 6, 7518.

Dreymueller, D, Uhlig, S, and Ludwig, A (2015). Adam-family metalloproteinases in lung inflammation: Potential therapeutic targets. Am J Physiol - Lung Cell Mol Physiol 308, L325–L343.

Du, Z, and Lovly, CM (2018). Mechanisms of receptor tyrosine kinase activation in cancer. Mol Cancer 17, 1–13.

Düsterhöft, S et al. (2014). A disintegrin and metalloprotease 17 dynamic interaction sequence, the sweet tooth for the human interleukin 6 receptor. J Biol Chem 289, 16336–16348.

Düsterhöft, S, Jung, S, Hung, CW, Tholey, A, Sönnichsen, FD, Grötzinger, J, and Lorenzen, I (2013). Membrane-proximal domain of a disintegrin and metalloprotease-17 represents the putative molecular switch of its shedding activity operated by protein-disulfide isomerase. J Am Chem Soc 135, 5776–5781.

Düsterhöft, S, Michalek, M, Kordowski, F, Oldefest, M, Sommer, A, Röseler, J, Reiss, K, Grötzinger, J, and Lorenzen, I (2015). Extracellular Juxtamembrane Segment of ADAM17 Interacts with Membranes and Is Essential for Its Shedding Activity. Biochemistry 54, 5791–5801.

Evenas, P, Dahlback, B, and Garcia de Frutos, P (2000). The first laminin G-type domain in the SHBG-like region of protein S contains residues essential for activation of the receptor tyrosine kinase sky. Biol Chem 381, 199–209.

Fauvel, B, and Yasri, A (2014). Antibodies directed against receptor tyrosine kinases: Current and future strategies to fight cancer. MAbs 6, 838–851.

Feinmesser, RL, Wicks, SJ, Taverner, CJ, and Chantry, A (1999). Ca2+/calmodulin-dependent kinase II phosphorylates the epidermal growth factor receptor on multiple sites in the cytoplasmic tail and serine 744 within the kinase domain to regulate signal generation. J Biol Chem 274, 16168–16173.

Feuerbach, D et al. (2017). ADAM17 is the main sheddase for the generation of human triggering receptor expressed in myeloid cells (hTREM2) ectodomain and cleaves TREM2 after Histidine 157. Neurosci Lett 660, 109–114.

FICAN West (2020). GeneCa - Oncogenomic Database. Available at: https://www.geneca.fi. Accessed December 20, 2020.

Foveau, B, Ancot, F, Leroy, C, Petrelli, A, Reiss, K, Vingtdeux, V, Giordano, S, Fafeur, V, and Tulasne, D (2009). Down-regulation of the met receptor tyrosine kinase by presenilin-dependent regulated intramembrane proteolysis. Mol Biol Cell 20, 2495–2507.

Fukumori, A, Feilen, LP, and Steiner, H (2020). Substrate recruitment by γ-secretase. Semin Cell Dev Biol 105, 54–63.

Fukumori, A, and Steiner, H (2016). Substrate recruitment of γ-secretase and mechanism of clinical presenilin mutations revealed by photoaffinity mapping. EMBO J 35, 1628–1643.

Funamoto, S et al. (2013). Substrate ectodomain is critical for substrate preference and inhibition of γ-secretase. Nat Commun 4, 2529.

Gandino, L, Longati, P, Medico, E, Prat, M, and Comoglio, PM (1994). Phosphorylation of serine 985 negatively regulates the hepatocyte growth factor receptor kinase. J Biol Chem 269, 1815–1820.

Georgescu, M-M, Kirsch, KH, Shishido, T, Zong, C, and Hanafusa, H (1999). Biological Effects of c-Mer Receptor Tyrosine Kinase in Hematopoietic Cells Depend on the Grb2 Binding Site in the Receptor and Activation of NF-κB. Mol Cell Biol 19, 1171–1181.

Gjerdrum, C et al. (2010). Axl is an essential epithelial-to-mesenchymal transition-induced regulator of breast cancer metastasis and patient survival. Proc Natl Acad Sci U S A 107, 1124–1129.

Glenn, G, and van der Geer, P (2007). CSF-1 and TPA stimulate independent pathways leading to lysosomal degradation or regulated intramembrane proteolysis of the CSF-1 receptor. FEBS Lett 581, 5377–5381.

Glenn, G, and van der Geer, P (2008). Toll-like receptors stimulate regulated intramembrane proteolysis of the CSF-1 receptor through Erk activation. FEBS Lett 582, 911–915.

Golde, TE, Koo, EH, Felsenstein, KM, Osborne, B a, and Miele, L (2013). γ-Secretase inhibitors and modulators. Biochim Biophys Acta 1828, 2898–2907.

Gooz, P, Dang, Y, Higashiyama, S, Twal, WO, Haycraft, CJ, and Gooz, M (2012). A disintegrin and metalloenzyme (ADAM) 17 activation is regulated by α5β1 integrin in kidney mesangial cells. PLoS One 7, 1–9.

Goruppi, S, Ruaro, E, Varnum, B, and Schneider, C (1997). Requirement of phosphatidylinositol 3-kinase-dependent pathway and Src for Gas6-Axl mitogenic and survival activities in NIH 3T3 fibroblasts. Mol Cell Biol 17, 4442–4453.

Goth, CK, Halim, A, Khetarpal, SA, Rader, DJ, Clausen, H, and Schjoldager, KT-BGT-BG (2015). A systematic study of modulation of ADAM-mediated ectodomain shedding by site-specific O-glycosylation. Proc Natl Acad Sci U S A 112, 14623–14628.

Graham, DK et al. (2006). Ectopic expression of the proto-oncogene Mer in pediatric T-cell acute lymphoblastic leukemia. Clin Cancer Res 12, 2662–2669.

Graham, DK, Dawson, TL, Mullaney, DL, Snodgrass, HR, and Earp, HS (1994). Cloning and mRNA expression analysis of a novel human protooncogene, c-mer. Cell Growth Differ 5, 647–657.

Graham, DK, DeRyckere, D, Davies, KD, and Earp, HS (2014). The TAM family: Phosphatidylserine-sensing receptor tyrosine kinases gone awry in cancer. Nat Rev Cancer 14, 769–785.

Grieve, AG, Xu, H, Künzel, U, Bambrough, P, Sieber, B, and Freeman, M (2017). Phosphorylation of iRhom2 at the plasma membrane controls mammalian TACE-dependent inflammatory and growth factor signalling. Elife 6, 1–22.

Grötzinger, J, Lorenzen, I, and Düsterhöft, S (2017). Molecular insights into the multilayered regulation of ADAM17: The role of the extracellular region. Biochim Biophys Acta - Mol Cell Res 1864, 2088–2095.

Guaiquil, VH, Swendeman, S, Zhou, W, Guaiquil, P, Weskamp, G, Bartsch, JW, and Blobel, CP (2010). ADAM8 is a negative regulator of retinal neovascularization and of the growth of heterotopically injected tumor cells in mice. J Mol Med 88, 497–505.

Güner, G, and Lichtenthaler, SF (2020). The substrate repertoire of γ-secretase/presenilin. Semin Cell Dev Biol 105, 27–42.

Haghverdi L, Lun ATL, Morgan MD & Marioni JC (2018) Batch effects in single-cell RNA-sequencing data are corrected by matching mutual nearest neighbors. Nat Biotechnol 36: 421–427.

Halford, MM, Macheda, ML, Parish, CL, Takano, EA, Fox, S, Layton, D, Nice, E, and Stacker, SA (2013). A fully human inhibitory monoclonal antibody to the Wnt receptor RYK. PLoS One 8, e75447.

Hansel, TT, Kropshofer, H, Singer, T, Mitchell, JA, and George, AJT (2010). The safety and side effects of monoclonal antibodies. Nat Rev Drug Discov 9, 325–338.

Haryuni, RD, Watabe, S, Yamaguchi, A, Fukushi, Y, Tanaka, T, Kawasaki, Y, Zhou, Y, Yokoyama, S, and Sakurai, H (2019). Negative feedback regulation of ErbB4 tyrosine kinase activity by ERK-mediated non-canonical phosphorylation. Biochem Biophys Res Commun 514, 456–461.

Heiring, C, Dahlbäck, B, and Muller, YA (2004). Ligand recognition and homophilic interactions in Tyro3: Structural insights into the Axl/Tyro3 receptor tyrosine kinase family. J Biol Chem 279, 6952–6958.

Hemming, ML, Elias, JE, Gygi, SP, and Selkoe, DJ (2008). Proteomic Profiling of γ-Secretase Substrates and Mapping of Substrate Requirements. PLoS Biol 6, e257.

Hoeing, K, Zscheppang, K, Mujahid, S, Murray, S, Volpe, MA V., Dammann, CEL, and Nielsen, HC (2011). Presenilin-1 processing of ErbB4 in fetal type II cells is necessary for control of fetal lung maturation. Biochim Biophys Acta - Mol Cell Res 1813, 480–491.

Hollmén, M et al. (2012). Proteolytic processing of ErbB4 in breast cancer. PLoS One 7, e39413.

Hollmén, M, Määttä, J a, Bald, L, Sliwkowski, MX, and Elenius, K (2009). Suppression of breast cancer cell growth by a monoclonal antibody targeting cleavable ErbB4 isoforms. Oncogene 28, 1309–1319.

Holtzhausen, A et al. (2019). TAM family receptor kinase inhibition reverses MDSC-mediated suppression and augments anti–PD-1 therapy in melanoma. Cancer Immunol Res 7, 1672–1686.

Hong, CC, Lay, JD, Huang, JS, Cheng, AL, Tang, JL, Lin, MT, Lai, GM, and Chuang, SE (2008). Receptor tyrosine kinase AXL is induced by chemotherapy drugs and overexpression of AXL confers drug resistance in acute myeloid leukemia. Cancer Lett 268, 314–324.

Hornbeck, P V., Kornhauser, JM, Latham, V, Murray, B, Nandhikonda, V, Nord, A, Skrzypek, E, Wheeler, T, Zhang, B, and Gnad, F (2019). 15 years of PhosphoSitePlus ®: Integrating post-translationally modified sites, disease variants and isoforms. Nucleic Acids Res 47, D433–D441.

Houri, N, Huang, KC, and Nalbantoglu, J (2013). The Coxsackievirus and Adenovirus Receptor (CAR) Undergoes Ectodomain Shedding and Regulated Intramembrane Proteolysis (RIP). PLoS One 8, 1–18.

Huang, M, Rigby, AC, Morelli, X, Grant, MA, Huang, G, Furiel, B, Seaton, B, and Furie, BC (2003). Structural basis of membrane binding by Gla domains of vitamin K-dependent proteins. Nat Struct Biol 10, 751–756.

Hubbard, SR, and Till, JH (2000). Protein Tyrosine Kinase Structure and Function. Annu Rev Biochem 69, 373–398.

Huovila, A-PJ, Turner, AJ, Pelto-Huikko, M, Kärkkäinen, I, and Ortiz, RM (2005). Shedding light on ADAM metalloproteinases. Trends Biochem Sci 30, 413–422.

Hutagalung AH & Novick PJ (2011) Role of Rab GTPases in membrane traffic and cell physiology. *Physiol Rev* 91: 119–149

Hutterer, M et al. (2008). Axl and growth arrest-specific gene 6 are frequently overexpressed in human gliomas and predict poor prognosis in patients with glioblastoma multiforme. Clin Cancer Res 14, 130–138.

Inoue, E, Deguchi-Tawarada, M, Togawa, A, Matsui, C, Arita, K, Katahira-Tayama, S, Sato, T, Yamauchi, E, Oda, Y, and Takai, Y (2009). Synaptic activity prompts gamma-secretase-mediated cleavage of EphA4 and dendritic spine formation. J Cell Biol 185, 551–564.

Javier-Torrent, M, Marco, S, Rocandio, D, Pons-Vizcarra, M, Janes, PW, Lackmann, M, Egea, J, and Saura, CA (2019). Presenilin/γ-secretase-dependent EphA3 processing mediates axon elongation through non-muscle myosin IIA. Elife 8, 1–26.

Ji, R, Tian, S, Lu, HJ, Lu, Q, Zheng, Y, Wang, X, Ding, J, Li, Q, and Lu, Q (2013). TAM Receptors Affect Adult Brain Neurogenesis by Negative Regulation of Microglial Cell Activation. J Immunol 191, 6165–6177.

Johnson, WE, Li, C, and Rabinovic, A (2007). Adjusting batch effects in microarray expression data using empirical Bayes methods. Biostatistics 8, 118–127.

Junttila, TT, Sundvall, M, Lundin, M, Lundin, J, Tanner, M, Härkönen, P, Joensuu, H, Isola, J, and Elenius, K (2005). Cleavable ErbB4 Isoform in Estrogen Receptor–Regulated Growth of Breast Cancer Cells. Cancer Res 65, 1384–1393.

Kamp, F, Winkler, E, Trambauer, J, Ebke, A, Fluhrer, R, and Steiner, H (2015). Intramembrane proteolysis of β-amyloid precursor protein by γ-secretase is an unusually slow process. Biophys J 108, 1229–1237.

Karayel, Ö et al. (2020). Integrative proteomics reveals principles of dynamic phosphosignaling networks in human erythropoiesis. Mol Syst Biol 16, 1–22.

Kasikara, C et al. (2017). Phosphatidylserine sensing by TAM receptors regulates AKT-dependent chemoresistance and PD-L1 expression. Mol Cancer Res 15, 753–764.

Kasikara, C et al. (2019). Pan-TAM tyrosine kinase inhibitor BMS-777607 Enhances Anti-PD-1 mAb efficacy in a murine model of triple-negative breast cancer. Cancer Res 79, 2669–2683.

Kasuga, K, Kaneko, H, Nishizawa, M, Onodera, O, and Ikeuchi, T (2007). Generation of intracellular domain of insulin receptor tyrosine kinase by γ-secretase. Biochem Biophys Res Commun 360, 90–96.

Keating, AK et al. (2010). Inhibition of Mer and Axl receptor tyrosine kinases in astrocytoma cells leads to increased apoptosis and improved chemosensitivity. Mol Cancer Ther 9, 1298–1307.

Keenan AB, Torre D, Lachmann A, Leong AK, Wojciechowicz ML, Utti V, Jagodnik KM, Kropiwnicki E, Wang Z & Ma'ayan A (2019) ChEA3: transcription factor enrichment analysis by orthogonal omics integration. Nucleic Acids Res 47: W212–W224.

Kelly, GM, Buckley, DA, Kiely, PA, Adams, DR, and O'Connor, R (2012). Serine Phosphorylation of the Insulin-like Growth Factor I (IGF-1) Receptor C-terminal Tail Restrains Kinase Activity and Cell Growth. J Biol Chem 287, 28180–28194.

Knittle, AM, Helkkula, M, Johnson, MS, Sundvall, M, and Elenius, K (2017). SUMOylation regulates nuclear accumulation and signaling activity of the soluble intracellular domain of the ErbB4 receptor tyrosine kinase. J Biol Chem 292, 19890–19904.

Kong, Y et al. (2015). Probing polypeptide GalNAc-transferase isoform substrate specificities by in vitro analysis. Glycobiology 25, 55–65.

Koorstra, JBM, Karikari, CA, Feldmann, G, Bisht, S, Rojas, PL, Offerhaus, GJA, Alvarez, H, and Maitra, A (2009). The Axl receptor tyrosine kinase confers an adverse prognostic influence in pancreatic cancer and represents a new therapeutic target. Cancer Biol Ther 8, 618–626.

Kopan, R, and Ilagan, MXG (2009). The Canonical Notch Signaling Pathway: Unfolding the Activation Mechanism. Cell 137, 216–233.

Kurppa, KJ et al. (2020). Treatment-Induced Tumor Dormancy through YAP-Mediated Transcriptional Reprogramming of the Apoptotic Pathway. Cancer Cell 37, 104-122.e12

Köksal, AS et al. (2018). Synthesizing Signaling Pathways from Temporal Phosphoproteomic Data. Cell Rep 24, 3607–3618.

Lachmann, A, Torre, D, Keenan, AB, Jagodnik, KM, Lee, HJ, Wang, L, Silverstein, MC, and Ma'ayan, A (2018). Massive mining of publicly available RNA-seq data from human and mouse. Nat Commun 9, 1366.

Lai, C, and Feng, L (2004). Implication of γ-secretase in neuregulin-induced maturation of oligodendrocytes. Biochem Biophys Res Commun 314, 535–542.

Lai, C, Gore, M, and Lemke, G (1994). Structure, expression, and activity of Tyro 3, a neural adhesion-related receptor tyrosine kinase. Oncogene 9, 2567–2578.

Lai, C, and Lemke, G (1991). An extended family of protein-tyrosine kinase genes differentially expressed in the vertebrate nervous system. Neuron 6, 691–704.

Langosch, D, Scharnagl, C, Steiner, H, and Lemberg, MK (2015). Understanding intramembrane proteolysis: from protein dynamics to reaction kinetics. Trends Biochem Sci 40, 318–327.

Langfelder, P, and Horvath, S (2008). WGCNA: An R package for weighted correlation network analysis. BMC Bioinformatics 9, 559.

Laurent, SA et al. (2015). γ-secretase directly sheds the survival receptor BCMA from plasma cells. Nat Commun 6, 7333.

Lee-Sherick, AB et al. (2013). Aberrant Mer receptor tyrosine kinase expression contributes to leukemogenesis in acute myeloid leukemia. Oncogene 32, 5359–5368.

Lee-Sherick, AB et al. (2018). MERTK inhibition alters the PD-1 axis and promotes anti-leukemia immunity. JCI Insight 3.

Lemke, G (2013). Biology of the TAM receptors. Cold Spring Harb Perspect Biol 5, 1–17.

Lemke, G, and Burstyn-Cohen, T (2010). TAM receptors and the clearance of apoptotic cells. Ann N Y Acad Sci 1209, 23–29.

Lemke, G, and Rothlin, C V (2008). Immunobiology of the TAM receptors. Nat Rev Immunol 8, 327–336.

Lemmon, M a, and Schlessinger, J (2010). Cell signaling by receptor tyrosine kinases. Cell 141, 1117–1134.

Lew, ED, Oh, J, Burrola, PG, Lax, I, Zagórska, A, Través, PG, Schlessinger, J, and Lemke, G (2014). Differential TAM receptor–ligand–phospholipid interactions delimit differential TAM bioactivities. Elife 3, 1–23.

Lewis, RE, Volle, DJ, and Sanderson, SD (1994). Phorbol ester stimulates phosphorylation on serine 1327 of the human insulin receptor. J Biol Chem 269, 26259–26266.

Li, T, Chang, CY, Jin, DY, Lin, PJ, Khvorova, A, and Stafford, DW (2004). Identification of the gene for vitamin K epoxide reductase. Nature 427, 541–544.

Li, X et al. (2015). iRhoms 1 and 2 are essential upstream regulators of ADAM17-dependent EGFR signaling. Proc Natl Acad Sci 112, 6080–6085.

Liberzon A, Subramanian A, Pinchback R, Thorvaldsdóttir H, Tamayo P & Mesirov JP (2011) Molecular signatures database (MSigDB) 3.0. Bioinformatics 27: 1739–1740.

Lichtenthaler, SF, Lemberg, MK, and Fluhrer, R (2018). Proteolytic ectodomain shedding of membrane proteins in mammals—hardware, concepts, and recent developments. EMBO J 37, 1–24.

Lijnen, HR, Christiaens, V, and Scroyen, L (2011). Growth arrest-specific protein 6 receptor antagonism impairs adipocyte differentiation and adipose tissue development in mice. J Pharmacol Exp Ther 337, 457–464.

Lin, X, Zhang, J, Chen, L, Chen, Y, Xu, X, Hong, W, and Wang, T (2017). Tyrosine phosphorylation of Rab7 by Src kinase. Cell Signal 35, 84–94.

Ling, L, Templeton, D, and Kung, HJ (1996). Identification of the major autophosphorylation sites of Nyk/Mer, an NCAM-related receptor tyrosine kinase. J Biol Chem 271, 18355–18362.

Linger, RMA et al. (2013). Mer or Axl receptor tyrosine kinase inhibition promotes apoptosis, blocks growth and enhances chemosensitivity of human non-small cell lung cancer. Oncogene 32, 3420–3431.

Linger, RMA, Keating, AK, Earp, HS, and Graham, DK (2008). TAM Receptor Tyrosine Kinases: Biologic Functions, Signaling, and Potential Therapeutic Targeting in Human Cancer. Adv Cancer Res 100, 35–83.

Litterst, C, Georgakopoulos, A, Shioi, J, Ghersi, E, Wisniewski, T, Wang, R, Ludwig, A, and Robakis, NK (2007). Ligand binding and calcium influx induce distinct ectodomain/gamma-secretase-processing pathways of EphB2 receptor. J Biol Chem 282, 16155–16163.

Liu, D, Zha, L, Liu, Y, Zhao, X, Xu, X, Liu, S, Ma, W, Zheng, J, and Shi, M (2020). β2-AR activation promotes cleavage and nuclear translocation of Her2 and metastatic potential of cancer cells. Cancer Sci 111, 4417–4428.

Loges, S et al. (2010). Malignant cells fuel tumor growth by educating infiltrating leukocytes to produce the mitogen Gas6. Blood 115, 2264–2273.

Lomize, AL, Lomize, MA, Krolicki, SR, and Pogozheva, ID (2017). Membranome: A database for proteome-wide analysis of single-pass membrane proteins. Nucleic Acids Res 45, D250–D255.

Lorenzen, I, Lokau, J, Korpys, Y, Oldefest, M, Flynn, CM, Künzel, U, Garbers, C, Freeman, M, Grötzinger, J, and Düsterhöft, S (2016). Control of ADAM17 activity by regulation of its cellular localisation. Sci Rep 6, 35067.

Love MI, Huber W & Anders S (2014) Moderated estimation of fold change and dispersion for RNA-seq data with DESeq2. Genome Biol 15: 550.

Lu, Q et al. (1999). Tyro-3 family receptors are essential regulators of mammalian spermatogenesis. Nature 398, 723–728.

Lu, Q, and Lemke, G (2001). Homeostatic regulation of the immune system by receptor tyrosine kinases of the Tyro 3 family. Science (80-) 293, 306–311.

Lu, Y, Wan, J, Yang, Z, Lei, X, Niu, Q, Jiang, L, Passtoors, WM, Zang, A, Fraering, PC, and Wu, F (2017). Regulated intramembrane proteolysis of the AXL receptor kinase generates an intracellular domain that localizes in the nucleus of cancer cells. FASEB J 31, 1382–1397.

Luskin, MR, Murakami, MA, Manalis, SR, and Weinstock, DM (2018). Targeting minimal residual disease: A path to cure? Nat Rev Cancer 18, 255–263.

Lyu, J, Yamamoto, V, and Lu, W (2008). Cleavage of the Wnt Receptor Ryk Regulates Neuronal Differentiation during Cortical Neurogenesis. Dev Cell 15, 773–780.

Lähdesmäki, H, Rust, AG, and Shmulevich, I (2008). Probabilistic inference of transcription factor binding from multiple data sources. PLoS One 3, 1820.

Ma, J, Shojaie, A, and Michailidis, G (2019). A comparative study of topology-based pathway enrichment analysis methods. BMC Bioinformatics 20, 546.

Mahadevan, D et al. (2007). A novel tyrosine kinase switch is a mechanism of imatinib resistance in gastrointestinal stromal tumors. Oncogene 26, 3909–3919.

Mahajan, NP, Whang, YE, Mohler, JL, and Earp, HS (2005). Activated tyrosine kinase Ack1 promotes prostate tumorigenesis: Role of Ack1 in polyubiquitination of tumor suppressor Wwox. Cancer Res 65, 10514–10523.

Manders, EMM, Stap, J, Brakenhoff, GJ, Van Driel, R, and Aten, JA (1992). Dynamics of three-dimensional replication patterns during the S-phase, analysed by double labelling of DNA and confocal microscopy. J Cell Sci 103, 857–862.

Manfioletti, G, Brancolini, C, Avanzi, G, and Schneider, C (1993). The protein encoded by a growth arrest-specific gene (gas6) is a new member of the vitamin K-dependent proteins related to protein S, a negative coregulator in the blood coagulation cascade. Mol Cell Biol 13, 4976–4985.

Manning, G, Whyte, DB, Martinez, R, Hunter, T, and Sudarsanam, S (2002). The protein kinase complement of the human genome. Science (80-) 298, 1912–1934.

Maretzky, T, McIlwain, DR, Issuree, PDA, Li, X, Malapeira, J, Amin, S, Lang, PA, Mak, TW, and Blobel, CP (2013). iRhom2 controls the substrate selectivity of stimulated ADAM17-dependent ectodomain shedding. Proc Natl Acad Sci 110, 11433–11438.

Mark, MR, Chen, J, Glenn Hammonds, R, Sadick, M, and Godowsk, PJ (1996). Characterization of Gas6, a member of the superfamily of G domain-containing proteins, as a ligand for Rse and Axl. J Biol Chem 271, 9785–9789.

Marron, MB, Singh, H, Tahir, TA, Kavumkal, J, Kim, H-Z, Koh, GY, and Brindle, NPJ (2007). Regulated proteolytic processing of Tie1 modulates ligand responsiveness of the receptor-tyrosine kinase Tie2. J Biol Chem 282, 30509–30517.

Maskos, K et al. (1998). Crystal structure of the catalytic domain of human tumor necrosis factor-α-converting enzyme. Proc Natl Acad Sci U S A 95, 3408–3412.

McCaw, TR, Inga, E, Chen, H, Jaskula-Sztul, R, Dudeja, V, Bibb, JA, Ren, B, and Rose, JB (2020). Gamma Secretase Inhibitors in Cancer: A Current Perspective on Clinical Performance. Oncologist, 1–14.

McElroy, B, Powell, JC, and McCarthy, J V (2007). The insulin-like growth factor 1 (IGF-1) receptor is a substrate for gamma-secretase-mediated intramembrane proteolysis. Biochem Biophys Res Commun 358, 1136–1141.

Meckler, X, and Checler, F (2016). Presenilin 1 and Presenilin 2 Target γ-Secretase Complexes to Distinct Cellular Compartments. J Biol Chem 291, 12821–12837.

Van Meer, G, Voelker, DR, and Feigenson, GW (2008). Membrane lipids: Where they are and how they behave. Nat Rev Mol Cell Biol 9, 112–124.

Merilahti, JAM, and Elenius, K (2019). Gamma-secretase-dependent signaling of receptor tyrosine kinases. Oncogene 38, 151–163.

Merilahti, JAM, Ojala, VK, Knittle, AM, Pulliainen, AT, and Elenius, K (2017). Genome-wide screen of gamma-secretase–mediated intramembrane cleavage of receptor tyrosine kinases. Mol Biol Cell 28, 3123–3131.

Migdall-Wilson, J, Bates, C, Schlegel, J, Brandão, L, Linger, RMA, DeRyckere, D, and Graham, DK (2012). Prolonged exposure to a Mer ligand in leukemia: Gas6 favors expression of a partial Mer glycoform and reveals a novel role for Mer in the nucleus. PLoS One 7.

Miller, MA et al. (2016). Reduced Proteolytic Shedding of Receptor Tyrosine Kinases Is a Post-Translational Mechanism of Kinase Inhibitor Resistance. Cancer Discov 6, 382–399.

Miller, MA, Sullivan, RJ, and Lauffenburger, DA (2017). Molecular Pathways: Receptor Ectodomain Shedding in Treatment, Resistance, and Monitoring of Cancer. Clin Cancer Res 23, 623–629.

Millikin, RJ, Solntsev, SK, Shortreed, MR, and Smith, LM (2018). Ultrafast Peptide Label-Free Quantification with FlashLFQ. J Proteome Res 17, 386–391.

Mirea, MA, Eckensperger, S, Hengstschläger, M, and Mikula, M (2020). Insights into differentiation of melanocytes from human stem cells and their relevance for melanoma treatment. Cancers (Basel) 12, 1–19.

Müller, J et al. (2014). Low MITF/AXL ratio predicts early resistance to multiple targeted drugs in melanoma. Nat Commun 5.

Muraoka-Cook, RS, Sandahl, M, Husted, C, Hunter, D, Miraglia, L, Feng, S, Elenius, K, and Earp, HS (2006). The Intracellular Domain of ErbB4 Induces Differentiation of Mammary Epithelial Cells. Mol Biol Cell 17, 4118–4129.

Murphy, G (2008). The ADAMs: signalling scissors in the tumour microenvironment. Nat Rev Cancer 8, 929–941.

Murphy, G (2009). Regulation of the proteolytic disintegrin metalloproteinases, the 'Sheddases.' Semin Cell Dev Biol 20, 138–145.

Murphy, G (2011). Tissue inhibitors of metalloproteinases. Genome Biol 12, 233.

Myers, K V., Amend, SR, and Pienta, KJ (2019). Targeting Tyro3, Axl and MerTK (TAM receptors): Implications for macrophages in the tumor microenvironment. Mol Cancer 18, 1–14.

Määttä, JA, Sundvall, M, Junttila, TT, Peri, L, Laine, VJO, Isola, J, Egeblad, M, and Elenius, K (2006). Proteolytic Cleavage and Phosphorylation of a Tumor-associated ErbB4 Isoform Promote Ligand-independent Survival and Cancer Cell Growth. Mol Biol Cell 17, 67–79.

Na, H-W, Shin, W-S, Ludwig, A, and Lee, S-T (2012). The cytosolic domain of protein-tyrosine kinase 7 (PTK7), generated from sequential cleavage by a disintegrin and metalloprotease 17 (ADAM17) and γ-secretase, enhances cell proliferation and migration in colon cancer cells. J Biol Chem 287, 25001–25009.

Nagata, K, Ohashi, K, Nakano, T, Arita, H, Zong, C, Hanafusa, H, and Mizuno, K (1996). Identification of the Product of Growth Arrest-specific Gene 6 as a Common Ligand for Axl, Sky, and Mer Receptor Tyrosine Kinases. J Biol Chem 271, 30022–30027.

Naresh, A, Long, W, Vidal, GA, Wimley, WC, Marrero, L, Sartor, CI, Tovey, S, Cooke, TG, Bartlett, JMS, and Jones, FE (2006). The ERBB4/HER4 intracellular domain 4ICD is a BH3-only protein promoting apoptosis of breast cancer cells. Cancer Res 66, 6412–6420.

Nguyen, KQN et al. (2014). Overexpression of MERTK receptor tyrosine kinase in epithelial cancer cells drives efferocytosis in a gain-of-function capacity. J Biol Chem 289, 25737–25749.

Ni, CY, Murphy, MP, Golde, TE, and Carpenter, G (2001). gamma -Secretase cleavage and nuclear localization of ErbB-4 receptor tyrosine kinase. Science 294, 2179–2181.

Nyberg, P, He, X, Härdig, Y, Dahlbäck, B, and García De Frutos, P (1997). Stimulation of Sy tyrosine phosphorylation by bovine protein s domains involved in the receptor-ligand interaction. Eur J Biochem 246, 147–154.

O'Bryan, JP, Frye, RA, Cogswell, PC, Neubauer, A, Kitch, B, Prokop, C, Espinosa, R, Le Beau, MM, Earp, HS, and Liu, ET (1991). axl, a transforming gene isolated from primary human myeloid leukemia cells, encodes a novel receptor tyrosine kinase. Mol Cell Biol 11, 5016–5031.

Ohashi, K, Nagata, K, Toshima, J, Nakano, T, Arita, H, Tsuda, H, Suzuki, K, and Mizuno, K (1995). Stimulation of Sky Receptor Tyrosine Kinase by the Product of Growth Arrest-specific Gene 6. J Biol Chem 270, 22681–22684.

Onken, J, Vajkoczy, P, Torka, R, Hempt, C, Patsouris, V, Heppner, FL, and Radke, J (2017). Phospho-AXL is widely expressed in glioblastoma and associated with significant shorter overall survival. Oncotarget 8, 50403–50414.

Orme, JJ et al. (2016). Heightened cleavage of Axl receptor tyrosine kinase by ADAM metalloproteases may contribute to disease pathogenesis in SLE. Clin Immunol 169, 58–68.

Osenkowski, P, Ye, W, Wang, R, Wolfe, MS, and Selkoe, DJ (2008). Direct and potent regulation of γ-secretase by its lipid microenvironment. J Biol Chem 283, 22529–22540.

Ou, WB, Corson, JM, Flynn, DL, Lu, WP, Wise, SC, Bueno, R, Sugarbaker, DJ, and Fletcher, JA (2011). AXL regulates mesothelioma proliferation and invasiveness. Oncogene 30, 1643–1652.

Paatero, I, Jokilammi, A, Heikkinen, PT, Iljin, K, Kallioniemi, O-P, Jones, FE, Jaakkola, PM, and Elenius, K (2012). Interaction with ErbB4 promotes hypoxia-inducible factor-1α signaling. J Biol Chem 287, 9659–9671.

Paatero, I, Seagroves, TN, Vaparanta, K, Han, W, Jones, FE, Johnson, RS, and Elenius, K (2014). Hypoxia-inducible factor-1α induces ErbB4 signaling in the differentiating mammary gland. J Biol Chem 289, 22459–22469.

Pandiella, A (1999). Cleavage of the TrkA neurotrophin receptor by multiple metalloproteases generates signalling-competent truncated forms. Eur J Neurosci 11, 1421–1430.

Paoletti, P, Bellone, C, and Zhou, Q (2013). NMDA receptor subunit diversity: Impact on receptor properties, synaptic plasticity and disease. Nat Rev Neurosci 14, 383–400.

Paolino, M et al. (2014). The E3 ligase Cbl-b and TAM receptors regulate cancer metastasis via natural killer cells. Nature 507, 508–512.

Paolino, M, and Penninger, JM (2016). The role of TAM family receptors in immune cell function: Implications for cancer therapy. Cancers (Basel) 8.

Peeters, MJW et al. (2019). MERTK Acts as a costimulatory receptor on human cd8 t cells. Cancer Immunol Res 7, 1472–1484.

Prasad, D, Rothlin, CV, Burrola, P, Burstyn-Cohen, T, Lu, Q, Garcia de Frutos, P, and Lemke, G (2006). TAM receptor function in the retinal pigment epithelium. Mol Cell Neurosci 33, 96–108.

Pratapa, A, Jalihal, AP, Law, JN, Bharadwaj, A, and Murali, TM (2020). Benchmarking algorithms for gene regulatory network inference from single-cell transcriptomic data. Nat Methods 17, 147–154.

Quail, DF, and Joyce, JA (2013). Microenvironmental regulation of tumor progression and metastasis. Nat Med 19, 1423–1437.

Rahimi, N, Golde, TE, and Meyer, RD (2009). Identification of ligand-induced proteolytic cleavage and ectodomain shedding of VEGFR-1/FLT1 in leukemic cancer cells. Cancer Res 69, 2607–2614.

Raikwar, NS, Liu, KZ, and Thomas, CP (2014). N-Terminal Cleavage and Release of the Ectodomain of Flt1 Is Mediated via ADAM10 and ADAM 17 and Regulated by VEGFR2 and the Flt1 Intracellular Domain. PLoS One 9, e112794.

Ramirez, M et al. (2016). Diverse drug-resistance mechanisms can emerge from drug-tolerant cancer persister cells. Nat Commun 7, 1–8.

Ran, S, Downes, A, and Thorpe, PE (2002). Increased exposure of anionic phospholipids on the surface of tumor blood vessels. Cancer Res 62, 6132–6140.

Rankin, EB et al. (2014). Direct regulation of GAS6/AXL signaling by HIF promotes renal metastasis through SRC and MET. Proc Natl Acad Sci 111, 13373–13378.

Ravichandran, KS (2010). Find-me and eat-me signals in apoptotic cell clearance: Progress and conundrums. J Exp Med 207, 1807–1817.

Reiss, K, and Saftig, P (2009). The "A Disintegrin And Metalloprotease" (ADAM) family of sheddases: Physiological and cellular functions. Semin Cell Dev Biol 20, 126–137.

Reusch, P, Barleon, B, Weindel, K, Martiny-Baron, G, Gödde, A, Siemeister, G, and Marmé, D (2001). Identification of a soluble form of the angiopoietin receptor TIE-2 released from endothelial cells and present in human blood. Angiogenesis 4, 123–131.

Rhee, SG (2001). Regulation of Phosphoinositide-Specific Phospholipase C. Annu Rev Biochem 70, 281–312.

Riethmueller, S, Ehlers, JC, Lokau, J, Düsterhöft, S, Knittler, K, Dombrowsky, G, Grötzinger, J, Rabe, B, Rose-John, S, and Garbers, C (2016). Cleavage Site Localization Differentially Controls Interleukin-6 Receptor Proteolysis by ADAM10 and ADAM17. Sci Rep 6, 25550.

Rio, C, Buxbaum, JD, Peschon, JJ, and Corfas, G (2000). Tumor necrosis factor-alpha-converting enzyme is required for cleavage of erbB4/HER4. J Biol Chem 275, 10379–10387.

Roberts, DM, Kearney, JB, Johnson, JH, Rosenberg, MP, Kumar, R, and Bautch, VL (2004). The Vascular Endothelial Growth Factor (VEGF) Receptor Flt-1 (VEGFR-1) Modulates Flk-1 (VEGFR-2) Signaling during Blood Vessel Formation. Am J Pathol 164, 1531–1535.

Roskoski, R (2019). Properties of FDA-approved small molecule protein kinase inhibitors. Pharmacol Res 144, 19–50.

Roskoski, R (2020). Properties of FDA-approved small molecule protein kinase inhibitors: A 2020 update. Pharmacol Res 152, 104609.

Rothlin, C V., Ghosh, S, Zuniga, EI, Oldstone, MBA, and Lemke, G (2007). TAM Receptors Are Pleiotropic Inhibitors of the Innate Immune Response. Cell 131, 1124–1136.

Rovida, E, Paccagnini, A, Del Rosso, M, Peschon, J, and Dello Sbarba, P (2001). TNF-alpha-converting enzyme cleaves the macrophage colony-stimulating factor receptor in macrophages undergoing activation. J Immunol 166, 1583–1589.

Sadahiro, H et al. (2018). Activation of the receptor tyrosine kinase AXL regulates the immune microenvironment in glioblastoma. Cancer Res 78, 3002–3013.

Sainaghi, PP, Castello, L, Bergamasco, L, Galletti, M, Bellosta, P, and Avanzi, GC (2005). Gas6 induces proliferation in prostate carcinoma cell lines expressing the Axl receptor. J Cell Physiol 204, 36–44.

Salter, MW, and Kalia, L V. (2004). SRC kinases: A hub for NMDA receptor regulation. Nat Rev Neurosci 5, 317–328.

Sannerud, R et al. (2016). Restricted Location of PSEN2/γ-Secretase Determines Substrate Specificity and Generates an Intracellular Aβ Pool. Cell 166, 193–208.

Sarbassov, DD, Guertin, DA, Ali, SM, and Sabatini, DM (2005). Phosphorylation and regulation of Akt/PKB by the rictor-mTOR complex. Science (80-) 307, 1098–1101.

Sardi, SP, Murtie, J, Koirala, S, Patten, BA, and Corfas, G (2006). Presenilin-dependent ErbB4 nuclear signaling regulates the timing of astrogenesis in the developing brain. Cell 127, 185–197.

Sasaki, T, Knyazev, PG, Cheburkin, Y, Göhring, W, Tisi, D, Ullrich, A, Timpl, R, and Hohenester, E (2002). Crystal structure of a C-terminal fragment of growth arrest-specific protein Gas6: Receptor tyrosine kinase activation by laminin G-like domains. J Biol Chem 277, 44164–44170.

Sasaki, T, Knyazev, PG, Clout, NJ, Cheburkin, Y, Göhring, W, Ullrich, A, Timpl, R, and Hohenester, E (2006). Structural basis for Gas6-Axl signalling. EMBO J 25, 80–87.

Sather, S, Kenyon, KD, Lefkowitz, JB, Liang, X, Varnum, BC, Henson, PM, and Graham, DK (2007). A soluble form of the Mer receptor tyrosine kinase inhibits macrophage clearance of apoptotic cells and platelet aggregation. Blood 109, 1026–1033.

Van Schaeybroeck, S et al. (2014). ADAM17-dependent c-MET-STAT3 signaling mediates resistance to MEK inhibitors in KRAS mutant colorectal cancer. Cell Rep 7, 1940–1955.

Schauenburg, L, Liebsch, F, Eravci, M, Mayer, MC, Weise, C, and Multhaup, G (2018). APLP1 is endoproteolytically cleaved by γ-secretase without previous ectodomain shedding. Sci Rep 8, 1–12.

Schelter, F, Kobuch, J, Moss, ML, Becherer, JD, Comoglio, PM, Boccaccio, C, and Krüger, A (2010). A Disintegrin and Metalloproteinase-10 (ADAM-10) Mediates DN30 Antibody-induced Shedding of the Met Surface Receptor. J Biol Chem 285, 26335–26340.

Schlegel, J et al. (2013). MERTK receptor tyrosine kinase is a therapeutic target in melanoma. J Clin Invest 123, 2257–2267.

Schmieder R & Edwards R (2011) Quality control and preprocessing of metagenomic datasets. Bioinformatics 27: 863–864.

Schulze, WX, Deng, L, and Mann, M (2005). Phosphotyrosine interactome of the ErbB-receptor kinase family. Mol Syst Biol 1, 2005.0008.

Seegar, TCM et al. (2017). Structural Basis for Regulated Proteolysis by the α-Secretase ADAM10. Cell 171, 1638-1648.e7.

Segawa, K, Kurata, S, Yanagihashi, Y, Brummelkamp, TR, Matsuda, F, and Nagata, S (2014). Caspase-mediated cleavage of phospholipid flippase for apoptotic phosphatidylserine exposure. Science (80-) 344, 1164–1168.

Seitz, HM, Camenisch, TD, Lemke, G, Earp, HS, and Matsushima, GK (2007). Macrophages and Dendritic Cells Use Different Axl/Mertk/Tyro3 Receptors in Clearance of Apoptotic Cells. J Immunol 178, 5635–5642.

Shao, H, Lauffenburger, D, and Wells, A (2017). Tyro3 carboxyl terminal region confers stability and contains the autophosphorylation sites. Biochem Biophys Res Commun 490, 1074–1079.

Shao H, Wang A, Lauffenburger D & Wells A (2018) Tyro3-mediated phosphorylation of ACTN4 at tyrosines is FAK-dependent and decreases susceptibility to cleavage by m-Calpain. Int J Biochem Cell Biol 95: 73–84

Sharma, S V. et al. (2010). A Chromatin-Mediated Reversible Drug-Tolerant State in Cancer Cell Subpopulations. Cell 141, 69–80.

Skinner, HD et al. (2017). Integrative analysis identifies a novel AXL-PI3 kinase-PD-L1 signaling axis associated with radiation resistance in head and neck cancer. Clin Cancer Res 23, 2713–2722.

Solntsev, SK, Shortreed, MR, Frey, BL, and Smith, LM (2018). Enhanced Global Post-translational Modification Discovery with MetaMorpheus. J Proteome Res 17, 1844–1851.

Sommer, A et al. (2016). Phosphatidylserine exposure is required for ADAM17 sheddase function. Nat Commun 7, 11523.

Son, BK, Kozaki, K, Iijima, K, Eto, M, Nakano, T, Akishita, M, and Ouchi, Y (2007). Gas6/Axl-PI3K/Akt pathway plays a central role in the effect of statins on inorganic phosphate-induced calcification of vascular smooth muscle cells. Eur J Pharmacol 556, 1–8.

Song, X, Wang, H, Logsdon, CD, Rashid, A, Fleming, JB, Abbruzzese, JL, Gomez, HF, Evans, DB, and Wang, H (2011). Overexpression of receptor tyrosine kinase Axl promotes tumor cell invasion and survival in pancreatic ductal adenocarcinoma. Cancer 117, 734–743.

Srinivasan, R, Gillett, CE, Barnes, DM, and Gullick, WJ (2000). Nuclear expression of the c-erbB-4/HER-4 growth factor receptor in invasive breast cancers. Cancer Res 60, 1483–1487.

Stauffer, W, Sheng, H, and Lim, HN (2018). EzColocalization: An ImageJ plugin for visualizing and measuring colocalization in cells and organisms. Sci Rep 8, 1–13.

Stitt, TN et al. (1995). The anticoagulation factor protein S and its relative, Gas6, are ligands for the Tyro 3/Axl family of receptor tyrosine kinases. Cell 80, 661–670.

Subramanian, A et al. (2005). Gene set enrichment analysis: A knowledge-based approach for interpreting genome-wide expression profiles. Proc Natl Acad Sci U S A 102, 15545–15550.

Sugiyama N, Imamura H & Ishihama Y (2019) Large-scale Discovery of Substrates of the Human Kinome. Sci Rep 9: 1–12

De Strooper, B et al. (1999). A presenilin-1-dependent γ-secretase-like protease mediates release of Notch intracellular domain. Nature 398, 518–522.

De Strooper, B (2003). Aph-1, Pen-2, and Nicastrin with Presenilin Generate an Active γ-Secretase Complex. Neuron 38, 9–12.

De Strooper, B, Saftig, P, Craessaerts, K, Vanderstichele, H, Guhde, G, Annaert, W, Von Figura, K, and Van Leuven, F (1998). Deficiency of presenilin-1 inhibits the normal cleavage of amyloid precursor protein. Nature 391, 387–390.

Sugiyama, N, Gucciardo, E, Tatti, O, Varjosalo, M, Hyytiäinen, M, Gstaiger, M, and Lehti, K (2013). Epha2 cleavage by MT1-MMP triggers single cancer cell invasion via homotypic cell repulsion. J Cell Biol 201, 467–484.

Sun, L et al. (2018). Rab34 regulates adhesion, migration, and invasion of breast cancer cells. Oncogene 37, 3698–3714.

Sun, L, Zhao, L, Yang, G, Yan, C, Zhou, R, Zhou, X, Xie, T, and Zhao, Y (2015). Structural basis of human γ -secretase assembly. Proc Natl Acad Sci U S A 112, 6003–6008.

Sun, W, Fujimoto, J, and Tamaya, T (2004). Coexpression of Gas6/Axl in human ovarian cancers. Oncology 66, 450–457.

Sun, WS, Fujimoto, J, and Tamaya, T (2003). Coexpression of growth arrest-specific gene 6 and receptor tyrosine kinases Axl and Sky in human uterine endometrial cancers. Ann Oncol 14, 898–906.

Sundvall, M, Korhonen, A, Vaparanta, K, Anckar, J, Halkilahti, K, Salah, Z, Aqeilan, RI, Palvimo, JJ, Sistonen, L, and Elenius, K (2012). Protein Inhibitor of Activated STAT3 (PIAS3) Protein Promotes SUMOylation and Nuclear Sequestration of the Intracellular Domain of ErbB4 Protein. J Biol Chem 287, 23216–23226.

Sundvall, M, Veikkolainen, V, Kurppa, K, Salah, Z, Tvorogov, D, van Zoelen, EJ, Aqeilan, R, and Elenius, K (2010). Cell Death or Survival Promoted by Alternative Isoforms of ErbB4. Mol Biol Cell 21, 4275–4286.

Suzuki, J, Fujii, T, Imao, T, Ishihara, K, Kuba, H, and Nagata, S (2013). Calcium-dependent phospholipid scramblase activity of TMEM 16 protein family members. J Biol Chem 288, 13305–13316.

Swendeman, S, Mendelson, K, Weskamp, G, Horiuchi, K, Deutsch, U, Scherle, P, Hooper, A, Rafii, S, and Blobel, CP (2008). VEGF-a stimulates ADAM17-dependent shedding of VEGFR2 and crosstalk between vegfr2 and ERK signaling. Circ Res 103, 916–918.

Swoboda, A et al. (2020). STAT3 promotes melanoma metastasis by CEBP-induced repression of the MITF pathway. Oncogene, 1091–1105.

Szklarczyk, D et al. (2019). STRING v11: Protein-protein association networks with increased coverage, supporting functional discovery in genome-wide experimental datasets. Nucleic Acids Res 47, D607–D613.

Tanabe, K, Nagata, K, Ohashi, K, Nakano, T, Arita, H, and Mizuno, K (1997). Roles of γ-carboxylation and a sex hormone-binding globulin-like domain in receptor-binding and in biological activities of Gas6. FEBS Lett 408, 306–310.

Tejeda, GS, Ayuso-Dolado, S, Arbeteta, R, Esteban-Ortega, GM, Vidaurre, OG, and Díaz-Guerra, M (2016). Brain ischaemia induces shedding of a BDNF-scavenger ectodomain from TrkB receptors by excitotoxicity activation of metalloproteinases and γ-secretases. J Pathol 238, 627–640.

Thor, AD, Edgerton, SM, and Jones, FE (2009). Subcellular localization of the HER4 intracellular domain, 4ICD, identifies distinct prognostic outcomes for breast cancer patients. Am J Pathol 175, 1802–1809.

Thorp, E, Vaisar, T, Subramanian, M, Mautner, L, Blobel, C, and Tabas, I (2011). Shedding of the Mer tyrosine kinase receptor is mediated by ADAM17 protein through a pathway involving reactive oxygen species, protein kinase Cδ, and p38 mitogen-activated protein kinase (MAPK). J Biol Chem 286, 33335–33344.

Tibrewal, N, Wu, Y, D'Mello, V, Akakura, R, George, TC, Varnum, B, and Birge, RB (2008). Autophosphorylation docking site Tyr-867 in Mer receptor tyrosine kinase allows for dissociation of multiple signaling pathways for phagocytosis of apoptotic cells and down-modulation of lipopolysaccharide-inducible NF-κB transcriptional activation. J Biol Chem 283, 3618–3627.

Tsai, CL, Chang, JS, Yu, MC, Lee, CH, Chen, TC, Chuang, WY, Kuo, WL, Lin, CC, Lin, SM, and Hsieh, SY (2020). Functional genomics identifies hepatitis-induced STAT3-TyrO3-STAT3 signaling as a potential therapeutic target of hepatoma. Clin Cancer Res 26, 1185–1197.

Tsou, W-I, Nguyen, K-QN, Calarese, DA, Garforth, SJ, Antes, AL, Smirnov, S V., Almo, SC, Birge, RB, and Kotenko, S V. (2014). Receptor tyrosine kinases, TYRO3, AXL, and MER, demonstrate distinct patterns and complex regulation of ligand-induced activation. J Biol Chem 289, 25750–25763.

Tsukita, Y et al. (2019). Axl kinase drives immune checkpoint and chemokine signalling pathways in lung adenocarcinomas. Mol Cancer 18, 1–6.

Tucher, J, Linke, D, Koudelka, T, Cassidy, L, Tredup, C, Wichert, R, Pietrzik, C, Becker-Pauly, C, and Tholey, A (2014). LC–MS Based Cleavage Site Profiling of the Proteases ADAM10 and ADAM17 Using Proteome-Derived Peptide Libraries. J Proteome Res 13, 2205–2214.

Tworkoski, KA, Platt, JT, Bacchiocchi, A, Bosenberg, M, Boggon, TJ, and Stern, DF (2013). MERTK controls melanoma cell migration and survival and differentially regulates cell behavior relative to AXL. Pigment Cell Melanoma Res 26, 527–541.

Tworkoski, KA, Singhal, G, Szpakowski, S, Zito, CI, Bacchiocchi, A, Muthusamy, V, Bosenberg, M, Krauthammer, M, Halaban, R, and Stern, DF (2011). Phosphoproteomic Screen Identifies Potential Therapeutic Targets in Melanoma. Mol Cancer Res 9, 801–812.

Ubil, E, Story, C, Earp, HS, Ubil, E, Caskey, L, Holtzhausen, A, Hunter, D, Story, C, and Earp, HS (2018). Tumor-secreted Pros1 inhibits macrophage M1 polarization to reduce antitumor immune response. J Clin Invest 128, 2356–2369.

Uehara, H, and Shacter, E (2008). Auto-Oxidation and Oligomerization of Protein S on the Apoptotic Cell Surface Is Required for Mer Tyrosine Kinase-Mediated Phagocytosis of Apoptotic Cells. J Immunol 180, 2522–2530.

Uhlen, M et al. (2017). A pathology atlas of the human cancer transcriptome. Science (80-) 357.

Urano, Y, Hayashi, I, Isoo, N, Reid, PC, Shibasaki, Y, Noguchi, N, Tomita, T, Iwatsubo, T, Hamakubo, T, and Kodama, T (2005). Association of active γ-secretase complex with lipid rafts. J Lipid Res 46, 904–912.

Urban, S, and Moin, SM (2014). A subset of membrane-altering agents and γ-secretase modulators provoke nonsubstrate cleavage by rhomboid proteases. Cell Rep 8, 1241–1247.

Vasaikar, S V., Straub, P, Wang, J, and Zhang, B (2018). LinkedOmics: Analyzing multi-omics data within and across 32 cancer types. Nucleic Acids Res 46, D956–D963.

Vetrivel, KS, Cheng, H, Lin, W, Sakurai, T, Li, T, Nukina, N, Wong, PC, Xu, H, Chem, JB, and Thinakaran, G (2004). Association of gamma-secretase with lipid rafts in post-Golgi and endosome membranes. J Biol Chem 279, 44945–44954.

Vidal, GA, Naresh, A, Marrero, L, and Jones, FE (2005). Presenilin-dependent γ-Secretase Processing Regulates Multiple ERBB4/HER4 Activities. J Biol Chem 280, 19777–19783.

Vogel, WH, and Jennifer, P (2016). Management Strategies for Adverse Events Associated With EGFR TKIs in Non-Small Cell Lung Cancer. J Adv Pract Oncol 7, 723–735.

Vuoriluoto, K, Haugen, H, Kiviluoto, S, Mpindi, J-P, Nevo, J, Gjerdrum, C, Tiron, C, Lorens, JB, and Ivaska, J (2011). Vimentin regulates EMT induction by Slug and oncogenic H-Ras and migration by governing Axl expression in breast cancer. Oncogene 30, 1436–1448.

Wakabayashi, T et al. (2009). Analysis of the γ-secretase interactome and validation of its association with tetraspanin-enriched microdomains. Nat Cell Biol 11, 1340–1346.

Wali, VB, Gilmore-Hebert, M, Mamillapalli, R, Haskins, JW, Kurppa, KJ, Elenius, K, Booth, CJ, and Stern, DF (2014). Overexpression of ERBB4 JM-a CYT-1 and CYT-2 isoforms in transgenic mice reveals isoformspecific roles in mammary gland development and carcinogenesis. Breast Cancer Res 16, 1–15.

Waschbüsch, D, and Khan, AR (2020). Phosphorylation of Rab GTPases in the regulation of membrane trafficking. Traffic 21, 712–719.

Weber, S, and Saftig, P (2012). Ectodomain shedding and ADAMs in development. Development 139, 3693–3709.

Weinger, JG, Gohari, P, Yan, Y, Backer, JM, Varnum, B, and Shafit-Zagardo, B (2008). In brain, Axl recruits Grb2 and the p85 regulatory subunit of PI3 kinase; in vitro mutagenesis defines the requisite binding sites for downstream Akt activation. J Neurochem 106, 134–146.

Wen, MC, Murao, K, Imachi, H, Sato, M, Nakano, T, Kodama, T, Sasaguri, Y, Wong, NCW, Takahara, J, and Ishida, T (2001). Phosphatidylinositol 3-OH kinase-Akt/protein kinase B pathway mediates Gas6 induction of scavenger receptor A in immortalized human vascular smooth muscle cell line. Arterioscler Thromb Vasc Biol 21, 1592–1597.

Wesoly, J, Szweykowska-Kulinska, Z, and Bluyssen, HAR (2007). STAT activation and differential complex formation dictate selectivity of interferon responses. Acta Biochim Pol 54, 27–38.

Wheeler, DL, and Yarden, Y (eds.. (2015). Receptor Tyrosine Kinases: Family and Subfamilies, Cham: Springer International Publishing.

Wilhelmsen, K, and van der Geer, P (2004). Phorbol 12-myristate 13-acetate-induced release of the colony-stimulating factor 1 receptor cytoplasmic domain into the cytosol involves two separate cleavage events. Mol Cell Biol 24, 454–464.

Williams, CC, Allison, JG, Vidal, GA, Burow, ME, Beckman, BS, Marrero, L, and Jones, FE (2004). The ERBB4/HER4 receptor tyrosine kinase regulates gene expression by functioning as a STAT5A nuclear chaperone. J Cell Biol 167, 469–478.

Wolfe, MS (2020). Unraveling the complexity of γ-secretase. Semin Cell Dev Biol 105, 3–11.
Wu, G, Ma, Z, Cheng, Y, Hu, W, Deng, C, Jiang, S, Li, T, Chen, F, and Yang, Y (2018). Targeting Gas6/TAM in cancer cells and tumor microenvironment. Mol Cancer 17, 1–10.
Wu, YM, Robinson, DR, and Kung, HJ (2004). Signal pathways in up-regulation of chemokines by tyrosine kinase MER/NYK in prostate cancer cells. Cancer Res 64, 7311–7320.
Xu, J, Litterst, C, Georgakopoulos, A, Zaganas, I, and Robakis, NK (2009). Peptide EphB2/CTF2 generated by the gamma-secretase processing of EphB2 receptor promotes tyrosine phosphorylation and cell surface localization of N-methyl-D-aspartate receptors. J Biol Chem 284, 27220–27228.
Xu, L, Hu, F, Zhu, H, Liu, X, Shi, L, Li, Y, Zhong, H, and Su, Y (2018). Soluble TAM receptor tyrosine kinases in rheumatoid arthritis: correlation with disease activity and bone destruction. Clin Exp Immunol 192, 95–103.
Xu, P, Liu, J, Sakaki-Yumoto, M, and Derynck, R (2012). TACE Activation by MAPK-Mediated Regulation of Cell Surface Dimerization and TIMP3 Association. Sci Signal 5, ra34–ra34.
Yamaoka, T, Kusumoto, S, Ando, K, Ohba, M, and Ohmori, T (2018). Receptor tyrosine kinase-targeted cancer therapy. Int J Mol Sci 19.
Yanagihashi, Y, Segawa, K, Maeda, R, Nabeshima, Y-I, and Nagata, S (2017). Mouse macrophages show different requirements for phosphatidylserine receptor Tim4 in efferocytosis. Proc Natl Acad Sci U S A 114, 8800–8805.
Yates AD, Achuthan P, Akanni W, Allen J, Allen J, Alvarez-Jarreta J, Amode MR, Armean IM, Azov AG, Bennett R, et al (2020) Ensembl 2020. Nucleic Acids Res 48: D682–D688.
Yokoyama, Y et al. (2019). Immuno-oncological Efficacy of RXDX-106, a Novel TAM (TYRO3, AXL, MER) Family Small-Molecule Kinase Inhibitor. Cancer Res 79, 1996–2008.
Yumoto, N, Wakatsuki, S, Kurisaki, T, Hara, Y, Osumi, N, Frisén, J, and Sehara-Fujisawa, A (2008). Meltrin beta/ADAM19 interacting with EphA4 in developing neural cells participates in formation of the neuromuscular junction. PLoS One 3, e3322.
Zhong, Z, Wang, Y, Guo, H, Sagare, A, Fernández, JA, Bell, RD, Barrett, TM, Griffin, JH, Freeman, RS, and Zlokovic, B V. (2010). Protein S protects neurons from excitotoxic injury by activating the TAM receptor tyro3-phosphatidylinositol 3-kinase-Akt pathway through its sex hormone-binding globulin-like region. J Neurosci 30, 15521–15534.
Zhou, R, Yang, G, Guo, X, Zhou, Q, Lei, J, and Shi, Y (2019). Recognition of the amyloid precursor protein by human γ-secretase. Science (80-) 363, eaaw0930.
Zhu, S et al. (2009). A genomic screen identifies TYRO3 as a MITF regulator in melanoma. Proc Natl Acad Sci 106, 17025–17030.
Zhu, Y, Sullivan, LL, Nair, SS, Williams, CC, Pandey, AK, Marrero, L, Vadlamudi, RK, and Jones, FE (2006). Coregulation of estrogen receptor by ERBB4/HER4 establishes a growth-promoting autocrine signal in breast tumor cells. Cancer Res 66, 7991–7998.
Zong, C, Yan, R, August, A, Darnell, JE, and Hanafusa, H (1996). Unique signal transduction of Eyk: Constitutive stimulation of the JAK-STAT pathway by an oncogenic receptor-type tyrosine kinase. EMBO J 15, 4515–4525.
Zscheppang, K, Dörk, T, Schmiedl, A, Jones, FE, and Dammann, CEL (2011a). Neuregulin receptor ErbB4 functions as a transcriptional cofactor for the expression of surfactant protein B in the fetal lung. Am J Respir Cell Mol Biol 45, 761–767.
Zscheppang, K, Konrad, M, Zischka, M, Huhn, V, and Dammann, CEL (2011b). Estrogen-induced upregulation of Sftpb requires transcriptional control of neuregulin receptor ErbB4 in mouse lung type II epithelial cells. Biochim Biophys Acta - Mol Cell Res 1813, 1717–1727.
Zwick, E, Bange, J, and Ullrich, A (2002). Receptor tyrosine kinases as targets for anticancer drugs. Trends Mol Med 8, 17–23.

TURUN
YLIOPISTO
UNIVERSITY
OF TURKU

Painosalama Oy, Turku, Finland 2021

ISBN 978-951-29-8488-6 (PRINT)
ISBN 978-951-29-8489-3 (PDF)
ISSN 0355-9483 (Print)
ISSN 2343-3213 (Online)